ELECTRONIC STRUCTURE OF DISORDERED ALLOYS

A Thesis Submitted
in Partial Fulfilment of the Requirements
for the Degree of
DOCTOR OF PHILOSOPHY

by

VIJAI KUMAR SRIVASTAVA

to the
DEPARTMENT OF PHYSICS
INDIAN INSTITUTE OF TECHNOLOGY KANPUR
MAY, 1982

To

My Mother

PHY – 1982 – D – SRI – ELE

CERTIFICATE

This is to certify that the work reported in this thesis entitled, 'ELECTRONIC STRUCTURE OF DISORDERED ALLOYS' has been carried out by Vijai Kumar Srivastava under my supervision.

No part of this work has been submitted elsewhere for a degree.

May 3, 1982.

Abhijit Mookerjee

(Abhijit Mookerjee)
Assistant Professor
Department of Physics
Indian Institute of Technology
Kanpur, India.

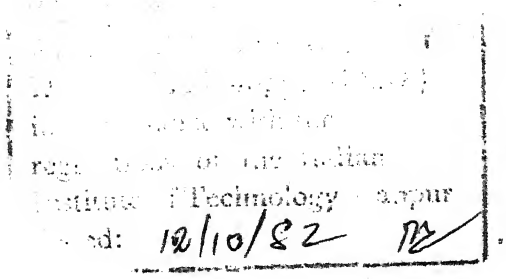

ACKNOWLEDGEMENTS

I am grateful to Dr. Abhijit Mookerjee for suggesting the problem and for his kind help even otherwise during the course of my Ph.D. programme. His deep interest and ready assistance at all times have contributed greatly to this work.

I am grateful to Dr. M. Yussouff for many helpful discussions at various stages of this work.

I am thankful to my colleagues, Mr. Pankaj Joshi, Mrs. Vasundhra Choudhry and Mr. R.P. Singh for many useful discussions.

It is a pleasure to thank my dear friend Mr. P.K. Srivastav for his kind help in proof reading.

I am grateful to the University Grants Commission and Christ Church College, Kanpur for financial support in the form of a Teacher Fellowship under Faculty Improvement Programme.

Thanks are due to Mr. S.K. Tewari for the patience and enthusiasm which he showed during the preparation of the manuscript.

Lastly I thank Mr. H.K. Panda and Mr. Lallu Singh for satisfactory duplication work.

Vijai Kumar Srivastava

CONTENTS

LIST OF FIGURES

LIST OF TABLES

SYNOPSIS

Thesis entitled 'ELECTRONIC STRUCTURE OF DISORDERED ALLOYS' submitted by VIJAI KUMAR SRIVASTAVA to the Department of Physics, Indian Institute of Technology Kanpur, in partial fulfilment of the requirements of the Ph.D. degree.

Coherent-potential approximation (CPA), during the past two decades, has been one of the main theoretical developments in the area of study of electronic structure of disordered alloys. The simplest case for which most of the CPA calculations have been done, is that of a random binary alloy A_cB_{1-c} where c is the concentration of A in B. Here the site energies are taken to be random (diagonal disorder) and the overlap-integrals are assumed to be non-random, i.e. there is no off-diagonal disorder. Also, it is further assumed that correlated scattering from two or more sites is ignored. This is known as single site coherent-potential approximation (1CPA). There are several equivalent approaches to 1CPA (reviewed in the chapter II of the thesis) all of which lead to the same results.

The need to go beyond 1CPA has been felt for a long time. Several suggestions have been put forward about the ways of generalising the 1CPA and ways of incorporating off-diagonal disorder and short-range order (SRO). Calculations based on these suggestions suffer from two main drawbacks. Firstly,

for any exactly solvable realistic model, which involves more than one orbital per site, the corresponding algebraic equations become tediously unwieldy, particularly on a three-dimensional lattice. Secondly, any tractable or further simplified approximation always leads to the unphysical averaged Green's function in the strong scattering regime. The essential Herglotz property of the Green's function is violated.

The correct Herglotz property of Green's function is preserved in the augmented-space formalism introduced by Mookerjee (1973). This formalism is discussed in detail in chapter III. The present work which is based on augmented-space formalism offers an unambiguous, tractable, self-consistent cluster generalisation (CCPA) of 1CPA, which retains the Herglotz property at all energies for all ranges of disorder. Off-diagonal disorder and short-range order have also been incorporated. The general formalism of the CCPA is also discussed in chapter III. A graphical method coupled with the recursion technique of Haydock (1972) enables us to work on a realistic three-dimensional lattice.

The most important contribution of this work is the generation of a self-consistent self-energy. This reproduces the density of states near the band edges more accurately than that produced by non self-consistent cluster embedding approaches tried earlier (Choudhary, V. 1981). The embedding

in a non self-consistent medium produces spurious structure near the band edges, which is completely absent here.

The results of a self-consistent cluster calculation of a single orbital model on the diamond and b.c.c. lattices have been reported. The most instructive feature of the results is that here the band width is larger than that in 1CPA. Clustering features appear in the minority (impurity) band and effects of off-diagonal disorder and SRO are easily identified.

In the chapter IV, it is shown that how our cluster-CPA formalism can be applied for the calculation of electronic density of states of valence bands of ternary, random III-V semiconducting alloys e.g. $Ga_c\ In_{1-c}\ As$ where $0 < C < 1$. In these alloys each atomic site provides four sp^3 hybridised orbitals for bonding. These materials form tetrahedrally cordinated, covalently bonded solids in a zinc-blende structure. In these alloys one f.c.c. sublattice of the common ion is non-random while that of the other ion is randomly occupied by the constituent atoms.

Chen and Sher (1978) have applied single-site, self-consistent CPA to the III-V semiconducting alloys. They used a bond orbital model (BOM) and parameterized Hamiltonian fitted to experimental data. This approach is extremely instructive but completely ignores the effect

of clusters and cannot adequately deal with off-diagonal disorder. They have treated the diagonal-disorder in 1CPA but off-diagonal disorder in virtual-crystal approximation (VCA). This is not a consistent procedure. Here an attempt has been made to improve upon this drawback. The coherent-potential medium is made self-consistent and off-diagonal disorder is taken into account. A calculation of this type has been done for $Ga_{0.5}In_{0.5}As$. The interaction between adjacent bonds with an anion in common has been taken into account exactly. The result is that there is an improvement in the band-edges and structure near them, particularly in the p-like part of the density of states.

In the concluding chapter V, the possible extensions and future usefulness of the cluster-CPA have been discussed.

CHAPTER I

INTRODUCTION

1.1 Disordered Solids: Classification and Problems

Ever since the enunciation of the Bloch's theorem in 1928 and the emergence of the band picture, considerable successful effort has gone into the understanding of electronic properties of crystalline, periodic systems. Concerted and extensive effort began into the study of disordered systems only in the late sixties. However the following decade has seen extensive development in what was then termed a 'frontier area' of research. Experimental as well as theoretical understanding has undergone such a seachange, that disordered systems are no longer considered 'exotic'.

Disordered solids encompass a rather extensive class. Broadly, they can be grouped into following classes:

(1) Compositionally disordered solids as in the case of random alloys both substitutional (CuZn, $Ga_c\ In_{1-c}As$ etc.) and interstitial (PdH).

(2) Structurally disordered solids as in the case of amorphous materials like a-Si, a-Se, a-GaAs and glasses etc.

(3) Magnetic alloys with compositional disorder (spin-

glasses, AuFe, CuMn, Fe_cNi_{1-c}, Fe-Ni-Mn) and structural disorder(e.g. amorphous magnets like metal glasses).

(4) Amorphous alloys e.g. a-$Ga_cIn_{1-c}As$, a-Si(H).

(5) Polymers.

The kind of problems one encounters when one turns to random systems are also multifarious. For example,

(1) The understanding of various disorder linked transitions, magnetic transitions, order-disorder transitions.

(2) The theoretical understanding of various electronic properties like density of states, optical properties, photo-emission, conductivity, dielectric response and electron related magnetic properties.

(3) The understanding and description of the nature of disorder-driven localization-transition of the excitations in random systems.

(4) The understanding of other elementary excitations in random systems such as phonons, magnons, polarons etc.

In the following work we shall concentrate on compositionally disordered crystalline alloys. Further we shall address ourselves exclusively to the understanding of density of electronic states. Although the various techniques we shall introduce, may with a little modification also be applied to other classes of systems and certainly to other electronic, phononic, magnonic etc. properties. We shall

not touch upon phase-transitions of any kind nor investigate the 'Localization' problem.

1.2 Theoretical Approach

The structure and properties of various crystalline materials can be very well understood by the application of Bloch's theorem. The idea of bands and band gaps came out of this. But, the long-range order that Bloch's theorem assumes, is not essential for the existence of bands and gaps between them. The well defined bonding and antibonding energy levels in isolated atoms spread into bands as the atom themselves bond to form the solid state. This has been the view point of chemists. In fact all the band structure calculations of density of states take account only of interactions between near neighbours. Long-range order is not necessary. The local bonding behaviour is sufficient to determine the energy bands and properties arising from these. This fact suggests that a theory based on local-chemistry of bonding may be attempted.

The usual starting point is Schrödinger equation:

$$\underline{H}\ \psi_n = E_n \psi_n \qquad (1.1)$$

However the eigenfunctions ψ_n are inappropriate for the discussion of large systems with consequent high degeneracy because any physically measurable quantity involves summation over $N \sim 10^{23}$ electrons with a loss of

physical insight and anything related to the eigenfunction ψ_n. Also the eigenstates are unstable under small perturbations which are insignificant beyond some distance from perturbation. The $\vec{k}$-space, which relates to the individual eigenstates ψ_n (which are inappropriate for our purpose), needs to be ''thrown out'' (Heine, Solid state physics, vol. 35, p. 5). This can be achieved by taking recourse to what is called 'local density' of states defined as:

$$n(E,\vec{r}) = n(E)\ |\psi_E(\vec{r})|^2 \qquad (1.2)$$

where $n(E)$ is the total density of states of the system, that is modulated by $|\psi|^2$ for a typical state of energy E. Integrated upto Fermi-energy E_F, this gives the total electron density. In an alloy or compound it tells which bands are more or less weighted on which atoms.

Alternatively, for each spin direction one can write:

$$n(E) = \sum_n \delta(E-E_n) \qquad (1.3)$$

$$n(E,\vec{r}) = \sum_n |\psi_n(\vec{r})|^2\ \delta(E-E_n) \qquad (1.4)$$

Here the summation is over all the eigenstates of $\underline{H}$. Equation (1.4) defines the local density of states interms of extended eigenstate ψ_n of the whole system and its determination via the determination of ψ_n and E_n (i.e. band structure) helps us in no better way. But fortunately $n(E,\vec{r})$ is related to the imaginary part of

of the Green's function by the relation (see appendix B),

$$n(E,\vec{r}) = -\frac{1}{\pi}\,\mathrm{Im}\,G(\vec{r},\vec{r},E) \qquad (1.5)$$

and the Green's function can be obtained directly without the knowledge of ψ_n. The Green's function formalism provides one of the most powerful methods, since ~~most of~~ all the electronic properties and their response to perturbations caused by externally applied forces are related to the single or many-particle Green's functions.

We shall adopt a tight-binding approach as most suitable for a local environment view-point. We may express eigen-states as a linear-combination of atomic orbitals (LCAO):

$$\psi_n(\vec{r}) = \sum_{\alpha\ell} a_{n,\alpha\ell}\,\phi_{\alpha\ell}(\vec{r}) \qquad (1.6)$$

Here ℓ is the site index for some atomic site and α indicates the type of orbital. The orbitals $\phi_{\alpha\ell}(\vec{r})$ are localised along the atomic site ℓ (but this has no bearing on the fact that ψ_n are extended). In view of equation (1.6) $\underline{H}$ can be written as a matrix with elements $\langle\alpha\ell|\underline{H}|\alpha'\ell'\rangle$ (in Dirac notation) representing the hopping integrals of the electron from orbital $\alpha\ell$ to $\alpha'\ell'$ for $\alpha'\ell' \neq \alpha\ell$ and the energy of the orbital $\alpha\ell$ for $\alpha'\ell' = \alpha\ell$.

The principal difficulty with the old LCAO methods was the non-orthogonality of basis i.e.

$$\langle\alpha\ell|\alpha'\ell'\rangle = S^{\alpha\alpha'}_{\ell\ell'} \neq \delta_{\ell\ell'},\ \delta_{\alpha\alpha'}.$$

This leads to computational difficulties. There have been various attempts at methods which 'ignore' the non-orthogonality and assume $S^{\alpha\alpha'}_{\ell\ell'} = \delta_{\ell\ell'}\,\delta_{\alpha\alpha'}$ and take into account the effect of non-orthogonality in different, not very satisfactory, ways. Other efforts change the basis from $|\alpha\ell\rangle$ to $\underline{U}|\alpha\ell\rangle$ such that $\underline{U}^{\dagger}\underline{S}\underline{U} = \underline{I}$. This new basis is orthogonal and may be used directly. (Anderson, 1969).

An old approach resuscitated in recent years has provided a real break-through in making the LCAO method feasible and eventually as good as any k-space methods-this is the ''chemical pseudo-potential'' method. (Bullett, Heine, Solid State Physics, Vol. 35). The basic idea of the method is the use of a new pseudo-basis $|\bar{\Phi}_{\alpha\ell}\rangle$, and a new effective Hamiltonian $\tilde{H} = \underline{S}^{-1}\underline{H}$, both of which may be obtained from the atomic wavefunctions and potentials (Hermann and Skillmann, 1963). Here $\tilde{H}$ is non-symmetric but that in no way creates difficulties in the procedure we shall subsequently follow.

In some of the older books LCAO is described as ultimately unfeasible because to use it effectively the computational effort becomes intractable. With the introduction of chemical pseudo-potential method, various recursion techniques (Haydock, Heine, Kelly, Solid State Physics Vol. 35) and fast computers, this drawback no longer exists. LCAO or modification thereof, has had a renaissance (Bullett, Solid State Physics Vol. 35. p. 129).

The resurgence of the tight-binding, local environment methods is a great boon to us - as in disordered systems the lack of periodicity invalidates all k-space approaches.

Assuming now that basis-orbitals are orthogonal, it can be easily shown that the local density of states is given by

$$n_{\alpha\ell}(E) = -\frac{1}{\pi} \operatorname{Im} \langle \alpha\ell | \underline{G}(E) | \alpha\ell \rangle \qquad (1.7)$$

where $\underline{G}(E) = \lim_{Z \to E} (Z\underline{I} - \underline{H})^{-1}$ (see appendix B)

Here the Green's function $\underline{G}(E)$ is a matrix which can be transformed according to different basis functions. The important point to note is that for determination of $n_{\alpha\ell}(E)$ we need only one matrix element of $\underline{G}(E)$. The same is true for equation (1.5): we need to know only $r = r'$ part of $\underline{G}(E)$ which simplifies the problem enormously. We are able to express measurable quantities in terms of some appropriate small parts of $\underline{G}(E)$ that can be solved for and computed seperately from all the unwanted remainder of $\underline{G}(E)$.

Local orbitals viz. the atomic site orbitals or the bond-orbitals in case of covalently bonded atoms and their interaction between near neighbours only, have been used as a basis for small as well as large systems to explain the observed phenomena. In alloys also, affinities are known to affect essentially the near neighbour configurations. This is a pointer to a valid local-theory and is welcome because of its implication that considering configurations of local environments i.e. small clusters, may be sufficient.

1.3 Configuration Averaging

In the absence of disorder, once the Hamiltonian model is set up, the solution of quantum-mechanical problem is essentially the solution of Schrodinger equation. However, with the introduction of disorder we face a new problem i.e. the lack of sufficient information about the sample. For example, in a random, binary alloy, the configuration of individual atoms on the lattice sites is different for different samples and an experimentalist at the outset has no knowledge of the particular configuration of his sample. Nor is such a knowledge of much use. Evidently, every different sample of the alloy will give experimental information having different micro-structure according to the particular configuration it has. The experimentalist, on the other hand, is primarily interested in the overall statistical trends of his results which he interprets as the physical 'properties' of the random alloy. A theorist too can generate a number of results depending upon the particular configuration he chooses for his random parameters. This again is not very useful. One could try to theoretically derive properties of the most probable configuration and propose that these properties are highly likely. But again the number of different configurations as probable as the most likely and those of comparable likelihoods of occurrence, are intractably numerous. Therefore, we have to evolve a statistical description of the system.

The most basic of these descriptions is the averaging over all possible configurations. It was pointed out by Anderson in 1972 that the type of statistical description essentially depends on what we are trying to describe. He warned that only experimentally observable physical quantities related to the response of a physical system to a probe must be averaged. This warning was given to explain source of controversies that arose over non-physical results obtained because non-physical quantities like self-energy, the wave-functions etc. were averaged. The Green's function corresponding to any spectrum like that of the electrons, phonons etc., can be configurationally averaged since its imaginary part is directly proportional to the density of states, a measurable quantity. Other physical quantities may be derived from it and compared with experiments. This is an additional pointer towards a local theory.

In fact, the study of configurationally averaged single-particle Green's function forms the substance of our thesis.

1.4 The Model

The full many-body electronic problem in the disordered system is beyond the scope of present work. We shall consider an equivalent one-electron problem. The one-electron potentials will be chosen in such a way as to incorporate the maximum possible many-body effects.

Firstly, the Born-Oppenheimer approximation helps us to seperate the nuclear and electronic parts of the wave-function describing the many-particle system consisting of nuclei and electrons in the alloy. The Schrodinger equation is still a many electron wave equation describing the motion of electrons in a field of nuclei. The Hartree-Fock scheme then yields a one-electron equation for stationary states in the presence of nuclei and an average potential due to all other electrons. The effects of exchange and correlation can also be taken into account by Slater's method.

In case of a random, binary alloy of the type A_cB_{1-c}, the Hamiltonian in a Hilbert space $\mathcal{H}$ can be written as:

$$\underline{H} = \sum_{i,n} e_{in}\, \underline{P}_{in} + \sum_{i \neq j} \sum_{n} \sum_{m} V_{in,jm}\, \underline{T}_{in,jm} \qquad (1.8)$$

Here $\underline{P}$ and $\underline{T}$ are projection and transfer operators, i and j are nearest neighbour site indices and n and m are band or orbital indices. Here both $\{e_{in}\}$ and $\{V_{in,jm}\}$ can be random variables. The disorder due to randomness of e_{in}, the atomic potential at the site i, is called diagonal disorder whereas the disorder due to randomness of $V_{in,jm}$, the overlap-term, is called off-diagonal disorder. Here e_{in} can take two possible values e^A_{in} or e^B_{in} depending on whether the i-th site is occupied by A-type or B-type constituent. The dependence of e_{in}, on the configuration around the i-th site is to be ignored.

The occupancies of each site are assumed to be statistically independent. Short-range order due to chemical affinities is not taken into account. The probabilities of finding an A-type or B-type constituent at any site are then directly proportional to their concentrations. Here $V_{in,jm}$ can take three possible values V_{nm}^{AA}, V_{nm}^{BB} or V_{nm}^{AB}.

The main idea is to get a configurationally averaged Green's function i.e. $\langle G(E) \rangle$, incorporating the effect of clusters. In view of this, we have first reviewed in Chapter II, the older methods (i.e. single-site coherent-potential approximation methods) of calculating $\langle G(E) \rangle$. We have pointed out the drawbacks and discussed possible lines of generalisations. In Chapter III, we have developed a self-consistent cluster-coherent-potential approximation (CCPA) based on augmented space formalism of Mookerjee (1973). This formalism (CCPA) has been applied to three-dimensional diamond and b.c.c. lattices (Chapter III) choosing arbitrary values of atomic potentials and overlap-integrals. The results are quite encouraging. The CCPA formalism has been applied to III-V semiconductors and their alloys using bond-orbital model (Chapter IV). These semiconductors and their alloys are covalently bonded with a four-fold co-ordination and the alloys fall in the category of substitutionally disordered solids.

In the concluding Chapter V, we have discussed the main achievements of the CCPA formalism and its various possible applications.

CHAPTER II

OLDER FORMALISMS AND THEIR DRAWBACKS

2.1 Introduction :

In this chapter we shall review the existing methods for calculation of the electronic density of states in disordered solids. The aim will be to examine these methods in detail with a view to point out the approximations involved in them and particularly the shortcomings that these approximations entail in the results. Such an examination will indicate a way of generalising the methods so as to overcome the shortcomings and formulate a method that is feasible and yields physically valid results in a realistic situation.

There are several approaches available to us of increasing degree of sophistication such as Rigid-Band approximation, Virtual-Crystal approximation, Minimum-Polarity approximation, Virtual Bound State approximation and the Coherent-Potential approximation.

Except for the single site coherent-potential approximation (1CPA) and virtual-crystal approximation (VCA), all other approaches mentioned above have very limited success and are suited for some specific system and fail in others. We shall review these two in turn.

2.2 Virtual-Crystal Approximation :

In this model the actual random alloy potential is replaced by an average, periodic potential

$$\bar{V} = cV_A + (1-c)\ V_B$$

where V_A and V_B are the potentials of the constituents A and B present in the atomic concentrations c and (1-c) respectively. The VCA does not reveal any features characteristic of disorder other than the crude averages. In case the potentials of constituents are very similar, the VCA is not a bad approximation. Because the effective potential is periodic, the standard methods available to crystalline systems are valid here. The VCA often serves as the starting point of more sophisticated iterative self-consistent approximations.

2.3 Coherent Potential Approximation (CPA) :

The single site CPA had remained till late, the main theoretical development in the study of electronic structure of random systems. It maintains the analytic features of the exact Green's function and interpolates correctly between several individual limiting cases e.g. virtual-crystal, atomic and dilute limits , in the case of random, binary alloys.

The literature on 1CPA can be classified into three categories : (1) Diagrammatic approaches using propagator or locator formalisms (2) The effective-medium approach (3) Multiple-scattering approaches. All different approaches yield the same

final result within this approximation. A detailed account of all the three approaches is given here.

2.3.1 The Diagrammatic Approach :

This approach was introduced by Yonezawa and Matsubara (1966), Yonezawa (1968) and Leath (1968,70) using propagator formalism. We shall illustrate the approach through tight-binding Anderson model (1958) including diagonal-disorder only. The Hamiltonian can be written as :

$$\underline{H} = \underline{H}_o + \underline{V} \qquad (2.1)$$

Here $\underline{H}_o$ is the non-random translationally invariant part $\sum_{ij} V_{ij}\underline{T}_{ij}$ while $\underline{V} = \sum_i \underline{v}_i = \sum_i e_i\underline{P}_i$ is the random part of $\underline{H}$. e_i is a random variable which can take values e_A or e_B where e_A and e_B are the atomic potentials of the constituents A and B respectively $\underline{P}_i$ and $\underline{T}_{ij}$ are projection and transfer operators. The unperturbed propagator is $\underline{G}_o = (Z\underline{I} - \underline{H}_o)^{-1}$. The Dyson equation relating the perturbed propagator $\underline{G}$ to $\underline{G}_o$ is

$$\underline{G} = \underline{G}_o + \underline{G}_o \underline{V} \underline{G}$$

$$= \underline{G}_o + \underline{G}_o \underline{V} \underline{G}_o + \underline{G}_o \underline{V} \underline{G}_o \underline{V} \underline{G}_o + \ldots \qquad (2.2)$$

On configuration averaging either side with respect to variables $\{e_i\}$ we have

$$\langle\underline{G}\rangle = \underline{G}_o + \sum_i \underline{G}_o \langle\underline{v}_i\rangle \underline{G}_o + \sum_{i,j} \underline{G}_o \langle\underline{v}_i \underline{G}_o \underline{v}_j\rangle \underline{G}_o + \ldots \qquad (2.3)$$

Here $\langle\underline{G}\rangle$ represents configuration average of $\underline{G}$. Equation (2.3) forms the basis of diagrammatic approach. For the generation

of diagrams, for every propagator $\underline{G}_o$ a horizontal line is assigned. For every $\langle \underline{G} \rangle$ we assign a double horizontal line and for each $\underline{v}_i$ within the averaging, we assign a vertical dashed 'scattering-line', together with an 'interaction vertex' labelled i (see fig. 2.1). Terms like $\underline{G}_o \langle \underline{v}_i \underline{G}_o \underline{v}_i \rangle \underline{G}_o$ are represented by

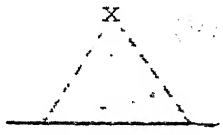

The diagrammatic representation of equation (2.3) is shown in fig. 2.2

We call a diagram 'irreducible' if it cannot be broken into two by rupturing along a propagator. An irreducible diagram is called an 'skeleton' diagram if it does not consist of units enclosed within one another, so that the enclosed units could be considered as insertions on the internal propagators. In fig. 2.2 diagrams (a), (b), (d), (h) and (i) are irreducible of which (h) is not a skeleton diagram

In order to sum the contributions of various diagrams a set of rules, similar to Feynman rules, is evolved. We shall take the specific case of a random, binary alloy for illustration. The equation (2.3) is rewritten as follows :

$$\langle \underline{G} \rangle = \underline{G}_o + \sum_i \underline{G}_o \langle \underline{v}_i \rangle \underline{G}_o + \sum_{j \neq i} \underline{G}_o \langle \underline{v}_i \underline{G}_o \underline{v}_j \rangle \underline{G}_o + \sum_i \underline{G}_o \langle \underline{v}_i \underline{G}_o \underline{v}_i \rangle \underline{G}_o + \cdots \qquad (2.4)$$

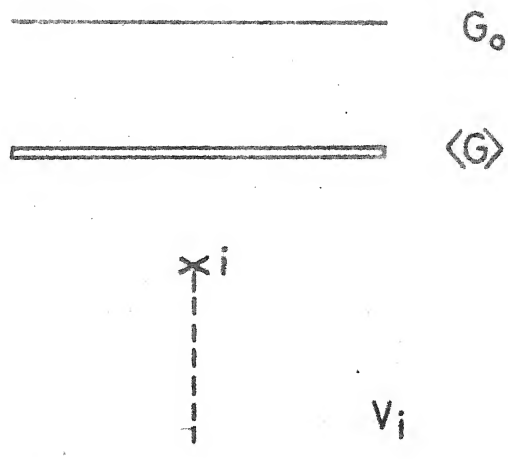

Fig.2·1 Translation to diagrammatic language

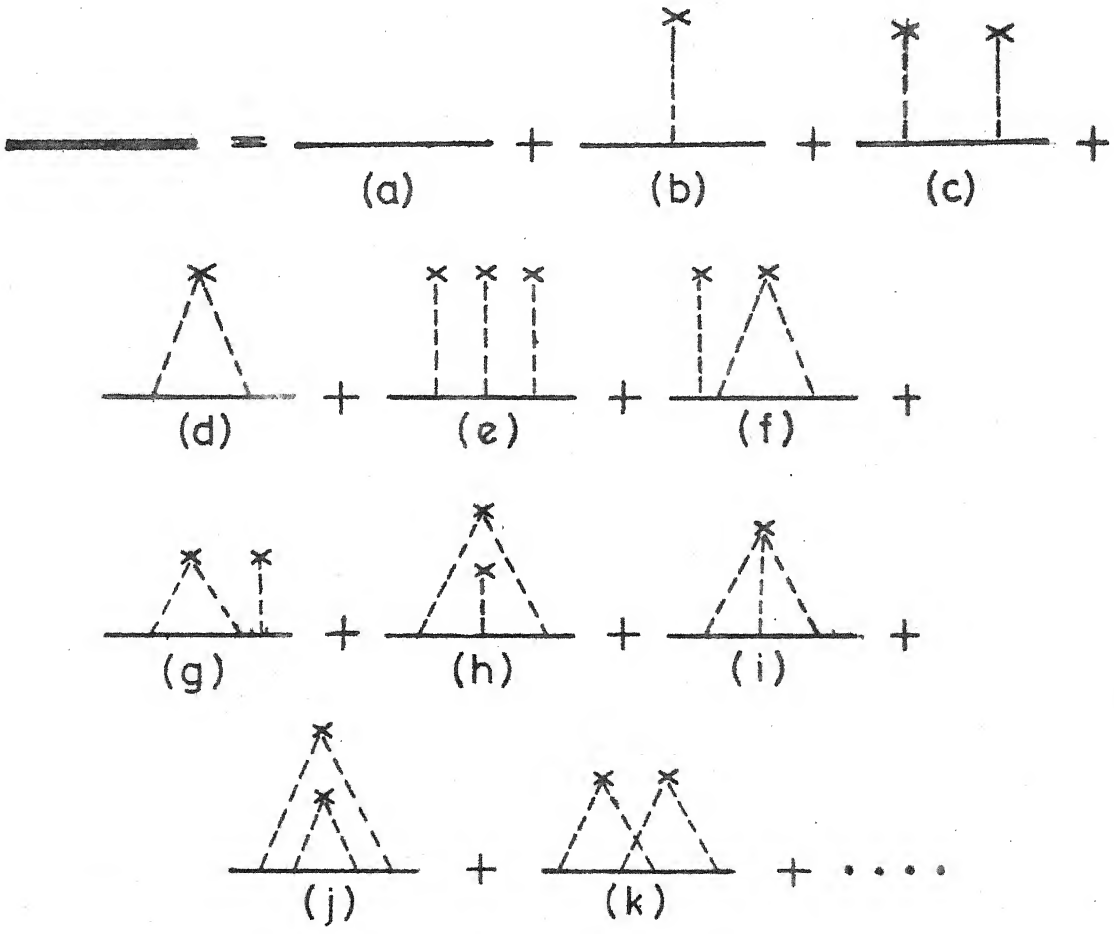

Fig.2·2 Equation (2·3) in diagrammatic language

Now we introduce the following contribution rules :

(i) With each horizontal oropagator we associate a factor $\underline{G}_o = (Z\underline{I} - \underline{H}_o)^{-1}$ where

$$\underline{H}_o = \sum_i e_B \underline{P}_i + \sum_{ij} \underline{V}_{ij} \underline{T}_{ij}$$

With each scattering line we associate a factor W and with each interaction vertex a factor c, the concentration of A component. These factors arise from

$$\langle \underline{v}_i \rangle = \langle (e_i - e_B)\ \underline{P}_i \rangle = c\ W\ \underline{P}_i, \text{ here } W = (e_A - e_B)$$

is the difference in atomic potentials of the two constituents.

(ii) All internal vertices are summed over without restrictions. The latter rule necessitates multiple occupancy corrections. To understand this, let us use the two rules on the diagrammatic expansion of fig. 2.2.We get

$$\langle \underline{G} \rangle = \underline{G}_o + cW \sum_i \underline{G}_o \underline{P}_i \underline{G}_o + c^2 W^2 \sum_{ij} \underline{G}_o \underline{P}_i \underline{G}_c \underline{P}_j \underline{G}_o + c^2 W^2 \sum_i \underline{G}_o \underline{P}_i \underline{G}_o \underline{P}_i \underline{G}_o + \cdots\cdots \quad (2.5)$$

Now using the independence of various e_i we have

$$\langle \underline{v}_i \underline{G}_o \underline{v}_j \rangle = \langle \underline{v}_i \rangle \underline{G}_o \langle \underline{v}_j \rangle \text{ if } i \neq j, \text{ and the}$$

above equation may be written as

$$\langle \underline{G} \rangle = \underline{G}_o + \sum_i \underline{G}_o \langle \underline{v}_i \rangle \underline{G}_o + \sum_{ij} \underline{G}_o \langle \underline{v}_i \underline{G}_o \underline{v}_j \rangle \underline{G}_o + \sum_i \underline{G}_o \langle \underline{v}_i \underline{G}_o \underline{v}_i \rangle \underline{G}_o + \cdots \quad (2.6)$$

Comparison of equations (2.4) and (2.6) reveals the fact that the multiple-scattering occupancy corrections arise because of the summation restrictions in equation (2.4). We may rewrite equation (2.4) removing these restrictions, to get

$$\langle \underline{G} \rangle = \underline{G}_o + \sum_i \underline{G}_o \langle \underline{v}_i \rangle \underline{G}_o + \sum_{ij} \underline{G}_o \langle \underline{v}_i \underline{G}_o \underline{v}_j \rangle \underline{G}_o + \sum_i \{ \underline{G}_o \langle \underline{v}_i \underline{G}_o \underline{v}_i \rangle \underline{G}_o - \underline{G}_o \langle \underline{v}_i \rangle \underline{G}_o \langle \underline{v}_i \rangle \underline{G}_o \} + \ldots \quad (2.7)$$

The subtracted term corresponds to the contribution of a diagram as shown in fig. 2.3a. This diagram is obtained from a diagram shown in fig. 2.3b by breaking away the scattering lines from the interaction vertex. If we look at a higher order term

$$\sum_i \{ \underline{G}_o \langle \underline{v}_i \underline{G}_o \underline{v}_i \underline{G}_o \underline{v}_i \rangle \underline{G}_o - 3\underline{G}_o \langle \underline{v}_i \rangle \underline{G}_o \langle \underline{v}_i \underline{G}_o \underline{v}_i \rangle \underline{G}_o - \underline{G}_o \langle \underline{v}_i \rangle \underline{G}_o \langle \underline{v}_i \rangle \underline{G}_o \langle \underline{v}_i \rangle \underline{G}_o \}$$

the subtracted terms again correspond to contributions from diagrams formed by breaking away the scattering lines from the interaction vertex in every possible way.

Now the diagrams may be summed according to the rules :

(i) All skeleton diagrams are drawn and from these skeleton diagrams derived diagrams are generated by breaking away the scattering lines from the interaction vertices in every possible way and giving diagrams already explicitly included.

(ii) With every rightmost and internal propagator a contribution $\underline{G}$ is associated and with leftmost propagator a contribution $\underline{G}_o$. For a binary alloy, W is associated with every scattering line and a factor c with every interaction vertex. An overall negative sign is associated to every derived diagram. Fig. 2.4 illustrates the diagrams generated according to new rules.

We have now obtained a Dyson equation connecting $\underline{G}$ to $\underline{G}_o$ given by

$$\underline{G} = \underline{G}_o + \underline{G}_o \underline{\Sigma} \underline{G} \qquad (2.8)$$

This is not a trivial result. Although the Dyson equation exists for the unaveraged $\underline{G}$, a priori it cannot be said to have existed after averaging. This is because different 'self-energy' parts of a diagram for a perturbation expansion for $\underline{\Sigma}$ connected only by the propagator cannot contribute independent matrix factors on averaging. The Dyson equation has been derived by laborious resummation and regrouping of terms.

We are now in a position to make approximations. The single-site CPA corresponds to choosing only those skeleton diagrams which involve just one site. Diagrams such as shown in fig. 2.5 involving pairs and triplets etc. are rejected. However for self-consistency diagrams such as shown in fig. 2.5a are included.

The diagrams are now tabulated as shown in fig. 2.6. The first column includes all skeleton diagrams, each row having a diagram of one order. The derived diagrams from it occupy the

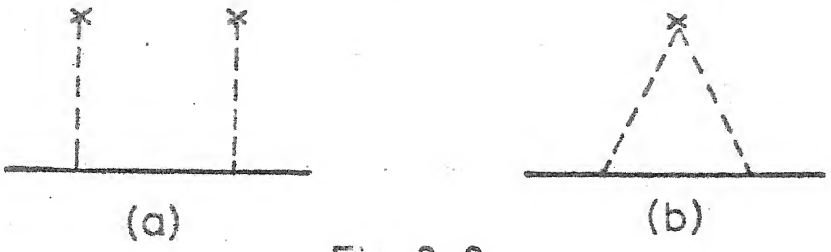

(a) (b)

Fig. 2·3

(a)

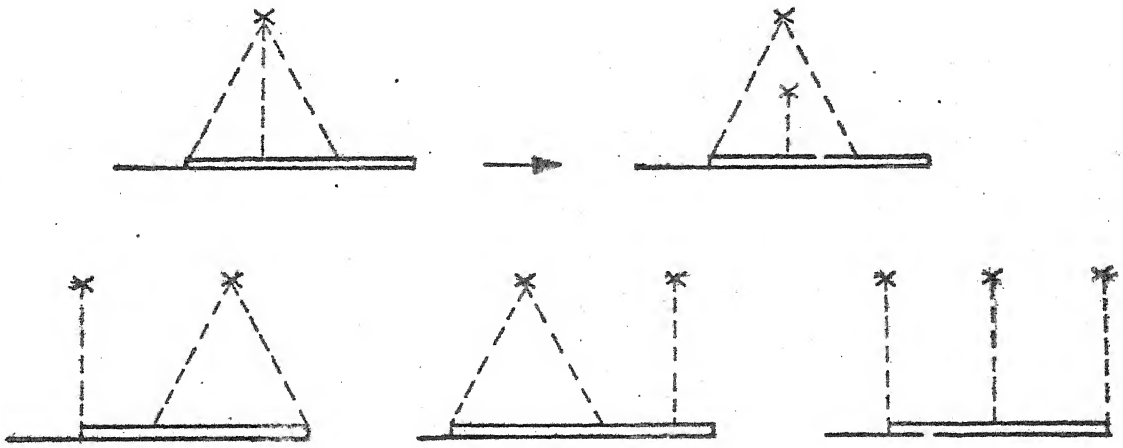

(b)

Fig. 2·4
Construction of derived diagrams

(a) (b)

Fig. 2·5

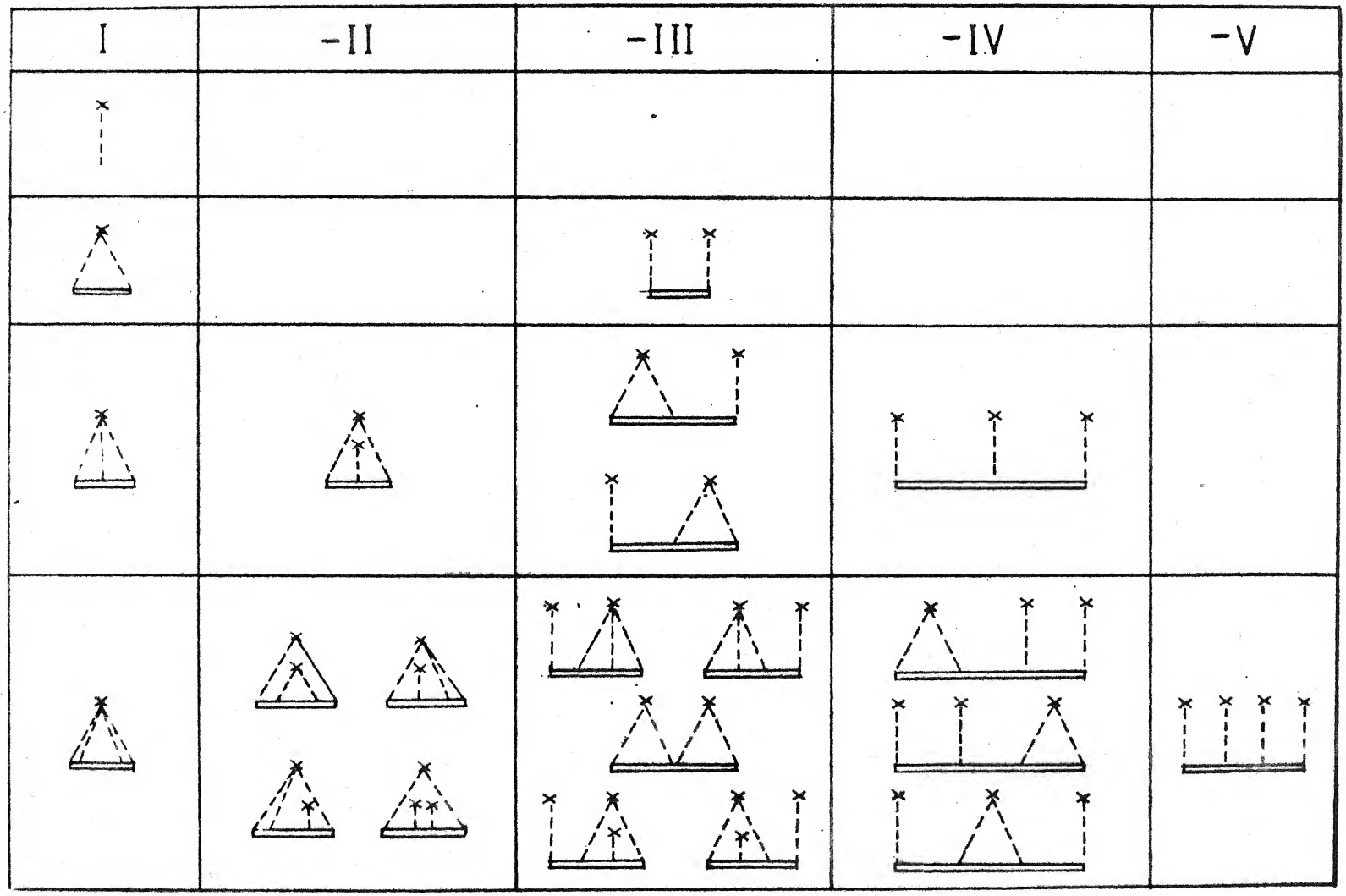

Fig. 2·6 Diagrammatic calculation of self-energy by Leath's method

same row. The second column contains all irreducible derived diagrams and subsequent columns contain derived reducible diagrams that break up into two, three etc. irreducible parts. We may now add up columnwise.

In 1CPA the self-energy $\underline{\Sigma}$ is site diagonal i.e. $\underline{\Sigma} = \underline{\Sigma}\,\underline{I}$. The sum of the first column is

$$(\text{bare}) = cW + c\,W\,\bar{\underline{G}}\,W + c\,W(\bar{\underline{G}}\,W)^2 + \ldots$$

$$= \frac{cW}{1-\bar{\underline{G}}W}\,, \quad \bar{\underline{G}} = \langle \underline{G} \rangle_{ii}$$

Now $\underline{\Sigma}\,(\bar{\underline{G}}) = \underline{\Sigma}\,(\text{bare}) - \{\underline{\Sigma}\,(\tau) - \underline{\Sigma}\,(\bar{\underline{G}})\} - \underline{\Sigma}\,(\tau)\,\bar{\underline{G}}\,\underline{\Sigma}\,(\tau) - \ldots$

where $\tau = \bar{\underline{G}}/(1-\underline{\Sigma}(\tau)\,\bar{\underline{G}})$ takes into account internal insertions in the derived diagrams. The self energy is a function of $\bar{\underline{G}}$. A little algebra immediately gives

$$\underline{\Sigma}(\bar{\underline{G}}) = cW/\{1-(W-\underline{\Sigma})\,\bar{\underline{G}}\} \qquad (2.9)$$

Equations (2.8) and (2.9) are sufficient for the determination of $\underline{\Sigma}$ and $\underline{G}$. $\underline{\Sigma}$ being site diagonal we have from equation (2.8) $\underline{G} = \underline{G}_o(Z-\underline{\Sigma})$. Equation (2.9) is solved by iteration techniques, starting from, say, the VCA (Brouers et al 1973, Ducastelle 1972).

This process for diagram summation is quite general. For glassy disorders we have different contributions for the interaction vertices and scattering lines.

In equation (2.1) the alternative choice of $\underline{V}$ as the unperturbed Hamiltonian leads to the locator formalism, where the perturbation expansion is in terms of localised states (Matsubara and Toyozawa 1962, Matsubara and Kaneyoshi 1966, Ziman 1969).

In the propagator formalism we start off with Bloch-like extended electronic states in a periodic system. We then introduce the diagonal disorder as a perturbation and study the effect on electronic states. In locator formalism we begin with atomistically localised electronic states, introduce the overlap term and study the resulting change.

For the single-site CPA both the propagator and locator formalisms give identical results.

2.3.2 Mean-Field Approach :

The idea of mean-field or effective medium (Soven 1967) gives perhaps a simpler physical insight into the CPA. Here we define an effective Hamiltonian $\underline{H}_{eff}$ such that the Green's function corresponding to it is equal to the configurationally averaged Green's function of the actual Hamiltonian $\underline{H}$ under consideration.

Let our actual Hamiltonian in the tight-binding basis be

$$\underline{H} = \sum_i e_i \underline{P}_i + \sum_{ij} V_{ij} \underline{T}_{ij} \qquad (2.10)$$

where $\underline{P}_i$ and $\underline{T}_{ij}$ are projection and transfer operators respectively Here both e_i, the site energies and V_{ij}, the nearest neighbour overlaps may be random.

Within a single-site approximation it is not very profitable to include effects of off-diagonal disorder. Conceptually random V_{ij}, involve two sites. Intuition expects the lowest order approximation to be a pair-CPA (2CPA).

In the presence of off-diagonal disorder, the 1CPA density of states is correct only to three moments rather than eight (as in the case of diagonal disorder only) whereas a consistent 2CPA is correct upto fifteen moments, whether we have pure diagonal disorder, pure off-diagonal disorder or both.

In 1CPA, V_{ij}'s are supposed to be non-random and we set $V_{ij} = \bar{V}$, where $\bar{V}$ is some mean potential.

Now we define our effective Hemiltonian

$$\underline{H}_{eff} = \sum_i \Sigma_i(E)\, \underline{P}_i + \sum_{ij} \Sigma_{ij}\,(|\vec{r}_i - \vec{r}_j|, E)\, \underline{T}_{ij} \qquad (2.11)$$

Again in 1CPA the self-energy Σ_i is same for all the sites i.e. $\Sigma_i(E) = \Sigma_o(E)$ and $\Sigma_{ij} = \bar{V}$. So we write finally

$$\underline{H}_{eff} = \sum_i \Sigma_o(E)\, \underline{P}_i + \bar{V} \sum_{ij} \underline{T}_{ij} \qquad (2.12)$$

The idea is to find out those $\Sigma_o(E)$ which yield

$$\underline{G}_{eff}(Z) = \langle \underline{G} \rangle \qquad (2.13)$$

$\langle \underline{G} \rangle$ indicates configuration average of $\underline{G}$

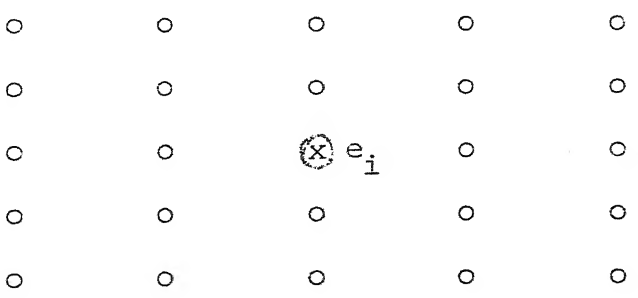

Fig. 2.7

Now in order to determine $\underline{H}_{eff}$ self-consistently for 1CPA, we embed an exact potential e_i at the site i within the effective medium in such a way that we do not produce any extra scattering on the average (Fig. 2.7). In mathematical terms we have

$$\langle \underline{G}^{(i)} \rangle = \underline{G}_{eff} \tag{2.14}$$

where $\underline{G}^{(i)} = (Z\underline{I} - \underline{H}_{eff}^{(i)})^{-1}$

and $\underline{H}_{eff}^{(i)} = \underline{H}_{eff} + \sum_i (e_i - \Sigma_o)\underline{P}_i = \underline{H}_{eff} + \underline{h}$

Now we may write

$$\underline{G}^{(i)} = (Z\underline{I} - \underline{H}_{eff} - \underline{h})^{-1} = (\underline{I} - \underline{G}_{eff}\underline{h})^{-1}\, \underline{G}_{eff}$$

Let us define an operator $\underline{T}$ such that

$$\underline{G}^{(i)} = \underline{G}_{eff} + \underline{G}_{eff}\, \underline{T}\, \underline{G}_{eff} \tag{2-15}$$

then $$\underline{T} = (\underline{I} - \underline{h}\underline{G}_{eff})^{-1}\underline{h} = \sum_i \frac{\ell_i \underline{P}_i}{1 - \ell_i \underline{G}_{eff}} = \sum_i \underline{t}_i$$

Here $$\ell_i = (e_i - \Sigma_o(E)).$$

From equation (2.15) we can write

$$\langle \underline{G}^{(i)} \rangle = \underline{G}_{eff} + \underline{G}_{eff} \langle \underline{T} \rangle \underline{G}_{eff} .$$

Now in order to satisfy equation (2.14) we write

$$\langle \underline{t}_i \rangle = 0 \tag{2.16}$$

or $$\left\langle \frac{e_i - \Sigma_o(E)}{1 - [e_i - \Sigma_o(E)]\, g(Z - \Sigma_o)} \right\rangle = 0 \tag{2.17}$$

which is identical to equation (2.9). So we conclude that in single-site CPA mean-field or effective-medium approach is equivalent to the diagammatic approach.

2.3.3 Multiple-Scattering Approach

The calculation of $\langle \underline{G} \rangle$ is carried outeasily within the framework of multiple-scattering theory. We express single-particle Hamiltonian of equation (2.10) as

$$\underline{H} = \underline{H}_a + \underline{W} \tag{2.18}$$

where $\underline{H}_a$ is some suitably chosen reference Hamiltonian. The difference $\underline{W}$ is the perturbation causing scattering. The basic requirement of the multiple scattering theory (Anderson and Mcmillan 1967) is that the perturbation term $\underline{W}$ can be decomposed as a sum of contributions from each site i.e.

$$\underline{W} = \underline{H} - \underline{H}_a = \sum_n w_n \underline{P}_n, \qquad w_n = e_n - \Sigma(E) \tag{2.19}$$

As defined earlier

$$\underline{T} = \underline{W} + \underline{W}\,\underline{G}_a\,\underline{T} \tag{2.20}$$

This relates $\underline{G}_a = (Z\underline{I} - \underline{H}_a)^{-1}$ to $\underline{G}$ by

$$\underline{G} = \underline{G}_a + \underline{G}_a\,\underline{T}\,\underline{G}_a \tag{2.21}$$

In order to express $\underline{T}$ interms of single-site operators we use the relation (2.19) to obtain

$$\underline{T} = \sum_n w_n(\underline{I} + \underline{G}_a\,\underline{T})\,\underline{P}_n = \sum_n \underline{t}_n \text{ (say)} \tag{2.22}$$

which gives

$$\underline{T} = \sum_n w_n \underline{P}_n + \sum_n w_n \underline{P}_n \underline{G}_a \sum_m w_m \underline{P}_m + \cdots \tag{2.23}$$

equations (2.22) and (2.23) yield

$$\begin{aligned} t_n &= w_n \underline{P}_n \left(\underline{I} + \underline{G}_a t_n + \sum_{m\neq n} \underline{G}_a t_m\right) \\ &= \left(\underline{I} - w_n \underline{P}_n \underline{G}_a\right)^{-1} w_n \underline{P}_n \left(\underline{I} + G_a \sum_{m\neq n} t_m\right) \\ &= \tau_n \left(\underline{I} + \underline{G}_a \sum_{m\neq n} t_m\right) \end{aligned} \tag{2.24}$$

where $\underline{\tau}_n = \left(\underline{I} - w_n \underline{P}_n \underline{G}_a\right)^{-1} w_n \underline{P}_n$ is the atomic t-matrix representing complete scattering from n-th site.

Iteration of equation (2.24) leads to the usual multiple scattering expansion

$$\underline{t}_n = \tau_n + \underline{\tau}_n \underline{G}_a \sum_{m\neq n} \underline{\tau}_m + \underline{\tau}_n \underline{G}_a \sum_{m\neq n} \underline{\tau}_m \underline{G}_a \sum_{p\neq m} \underline{\tau}_p + \cdots$$

which reveals the fact that $\underline{t}_n$ is actually dependent on all sites. From equation (2.21) on averaging both sides, we get:

$$\langle \underline{G} \rangle = \underline{G}_a + \underline{G}_a \langle T \rangle \underline{G}_a \tag{2.25}$$

The single site CPA can now be introduced by averaging (2.24),

$$\begin{aligned} \langle \underline{t}_n \rangle &= \langle \underline{\tau}_n \left(\underline{I} + \underline{G}_a \sum_{m\neq n} \underline{t}_m\right) \rangle \\ &= \langle \underline{\tau}_n \rangle \left(\underline{I} + \underline{G}_a \sum_{m\neq n} \langle \underline{t}_m \rangle\right) \\ &+ \langle \left(\underline{\tau}_n - \langle \underline{\tau}_n \rangle\right) \underline{G}_a \sum_{m\neq n} \left(\underline{t}_m - \langle \underline{t}_m \rangle\right) \rangle \end{aligned} \tag{2.26}$$

The first term in equation (2.26) may be thought of as representing the scattering of an isolated site i immersed in an average medium, while the second term describes fluctuations around this average behaviour. In single-site approximation we neglect the second term. The electronic properties of the alloy are then determined from the closed set of equations:

$$\langle \underline{t}_n \rangle = \langle \underline{\tau}_n \rangle \left(\underline{I} + \underline{G}_a \sum_{m \neq n} \langle \underline{t}_m \rangle \right) \qquad (2.27)$$

The self-consistent solution of $\underline{H}_a$ follows from $\langle T \rangle = 0$ which implies $\langle \underline{G} \rangle = \underline{G}_a$. The 1CPA equation for determining self-energy now becomes

$$\langle \underline{\tau}_n \rangle = 0$$

or

$$\left\langle \frac{(e_n - \underline{\Sigma}(E))}{1-[e_n - \underline{\Sigma}(E)]\, g(Z-\underline{\Sigma})} \right\rangle = 0 \qquad (2.28)$$

which is a result which we have aready obtained in diagrammatic and mean field approaches.

These three are the principal viewpoints, basically equivalent, though the formal mathematics appears different. The final results therefore, not surprisingly, are the same in all cases. The reason why we review all three in detail, is that we wish to examine an avenue of generalising the single-site CPA's to include cluster effects without sacrificing the Herglotz property essential for physically meaningful results.

2.4 Failure of 1CPA

The 1CPA provides a reasonably good description of an alloy over a wide range of parameters. It works well when W, the difference in orbital energies of the two components of a binary alloy, is small and becomes inadequate when $\delta = \frac{|W|}{|Z_1 V_{BB}|}$ is large (Here Z_1 is number of nearest neighbours).

Since 1CPA is a single-site approximation it cannot take correctly into account the effects due to two or more sites. Firstly, it cannot correctly account for the randomness in the hopping-integrals involving two or more sites. In binary alloys the shape of the electronic density of states function as well as the band-widths depend on relative values of various interactions between neighbouring atoms. These numbers can be very different for the two constituents of an alloy even though their atomic potentials are similar. Secondly, short-range order due to chemical clustering cannot be taken into account. Finally the effect of statistical clustering which is particularly important in the impurity bands, is totally absent. The impurity band shows some fine structure (Payton and Visscher 1967, Dean 1972, Alben et al 1975) which is lost in 1CPA. This is a serious drawback because many physical quantities like conductivity, electronic specific heat, paramagnetic susceptibility etc. may be greatly affected by the structure in the impurity band (Vander Rest et al 1975).

The 1CPA fails to give correct band-widths, even in the absence of off-diagonal disorder, the 1CPA band width is considerably smaller than the true band-width. It is pertinent to quote here the 'union theorem' which states that if (E_{B_1}, E_{B_2}) and (E'_{B_1}, E'_{B_2}) are the lower and upper band-edges of the two constituents A and B of the alloy, then the band-edges of any alloy A_cB_{1-c} are $(\bar{E}_1, \bar{E}_2)$ where $\bar{E}_1 = \min (E_{B_1}, E'_{B_1})$ and $\bar{E}_2 = \max (E_{B_2}, E'_{B_2})$. From the theorem it follows directly that if E_1 and E_2 are sets representing the energy spectra of A and B, then the spectrum of any alloy A_c, B_{1-c} is $E_1 \cup E_2$.

The experiments on the magnetic properties of Cu-Ni alloys at large Cu-concentrations indicate that local-environment strongly affects the magnetic susceptibility of an individual Ni atom in the alloy (Kumar and Joshi 1978). In this regime the 1CPA which ignores all environmental effect, does not give satisfactory results. The failure of 1CPA for large W can be understood from the fact that for large W the electron mean-free path is small and in order to obtain a good estimate of the configurationally averaged Green's function we must consider scattering due to pairs, triplets etc. in a self-consistent manner. This is completely ignored in 1CPA.

The general conclusion is that 1CPA gives a good qualitative agreement with experimental data, certainly far-

superior to other earlier approximations. But in cases where local environmental effects are important, we must take into account the cluster effects, for a good quantitative agreement.

2.5 Generalisations of 1CPA

From time to time suggestions have been put forward about ways of generalising the 1CPA to take into account the effect of clusters, off-diagonal disorder and SRO. Extensive work has been done in this direction (Aiyer et al 1969, Soven 1967, Capek 1971, Cyrot-Lackmann and Ducastelle 1971, Freed and Cohen 1971, Nickel and Krummhansal 1971, Schwartz and Siggia1972, Srivastava and Joshi 1973).

Attempts to generalise 1CPA, in the diagrammatic approaches have failed because of the enormous number of terms or diagrams to be summed. In the diagrammetic approach if we retain skeleton diagrams which involve only the sites within a cluster of size n and reject all skeleton digrams which involve sites outside the cluster, we generate a cluster-CPA (CCPA) of a cluster of n-sites. Leath (1972) and Nickel and Krummhansal (1971a, 1971b) have given the procedure for pair-CPA (2CPA). In the Fig. 2.8 we have shown the cumbersome diagrammatic summation reproduced from the paper of Leath (1972). The complexity of the procedure is apparent. Any slight error in inclusion of any class of diagrams yields approximations that are non-Herglotz (Nickel and Krummhansal 1971a, 1971b). Any contemplation of applying

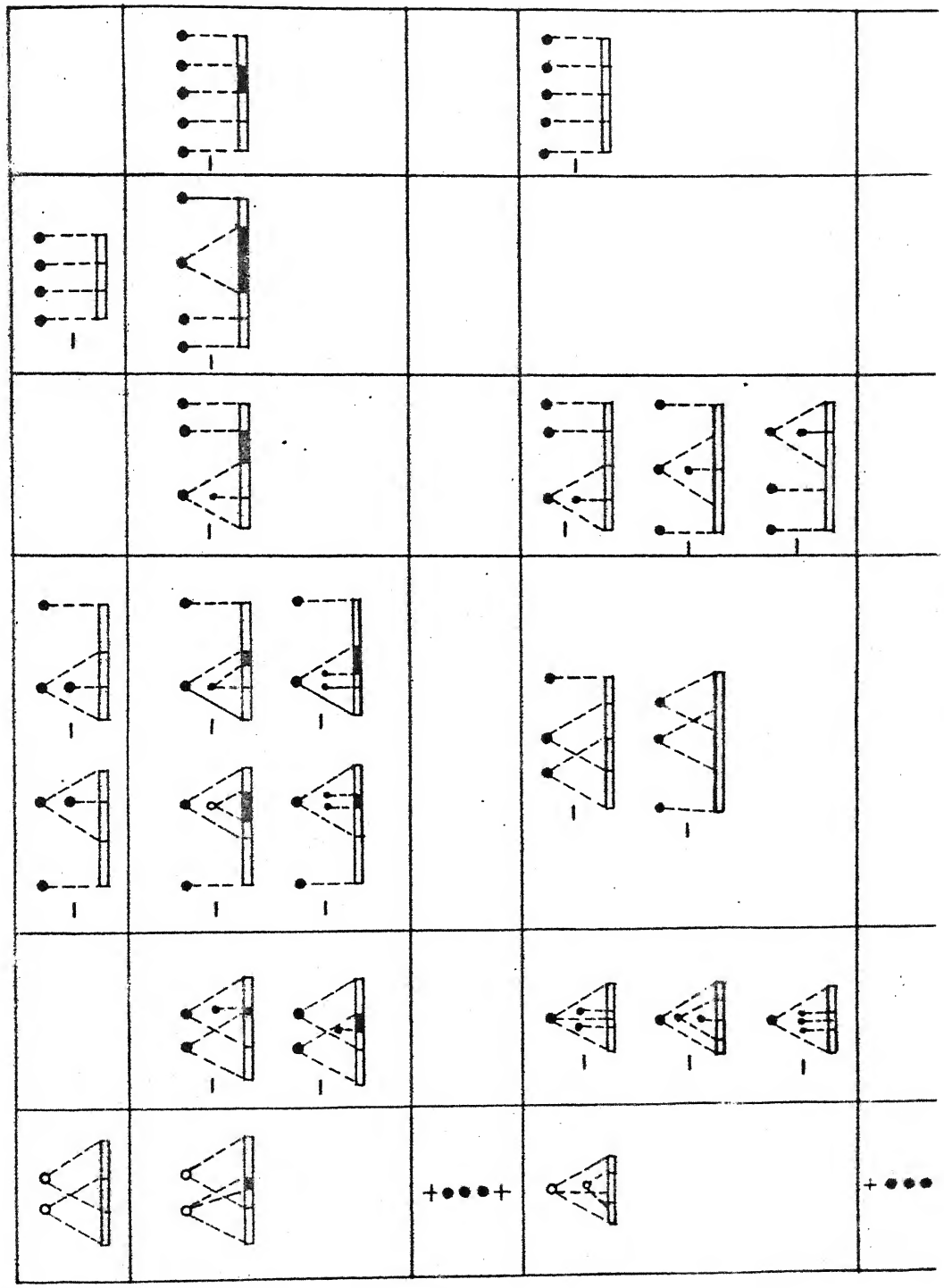

Fig. 2·8a

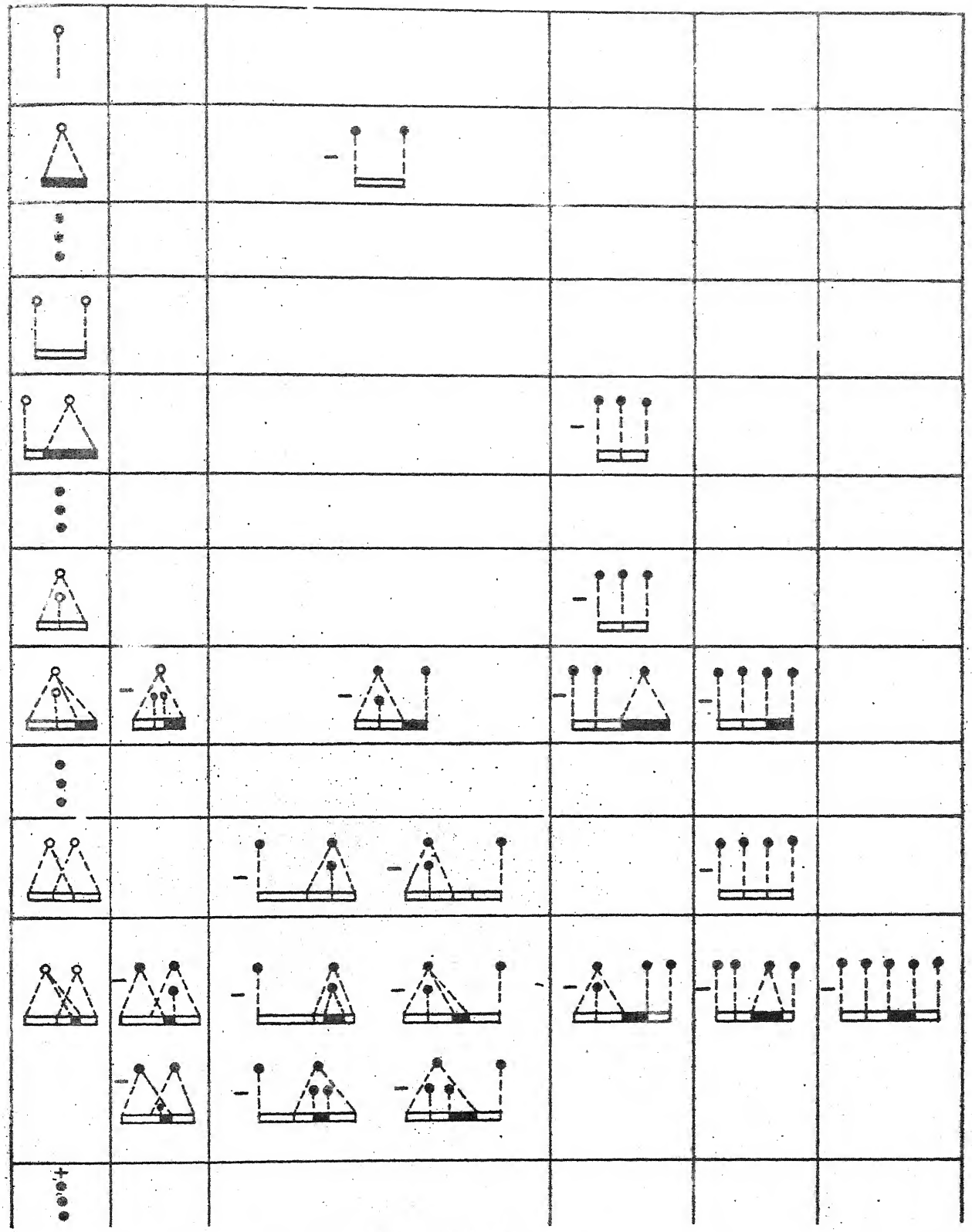

Fig. 2·8b

Repeat of Fig. (2.8a) for the case of those diagrams (column 1) which would appear in the t matrix for scattering by an isolated pair of defects.

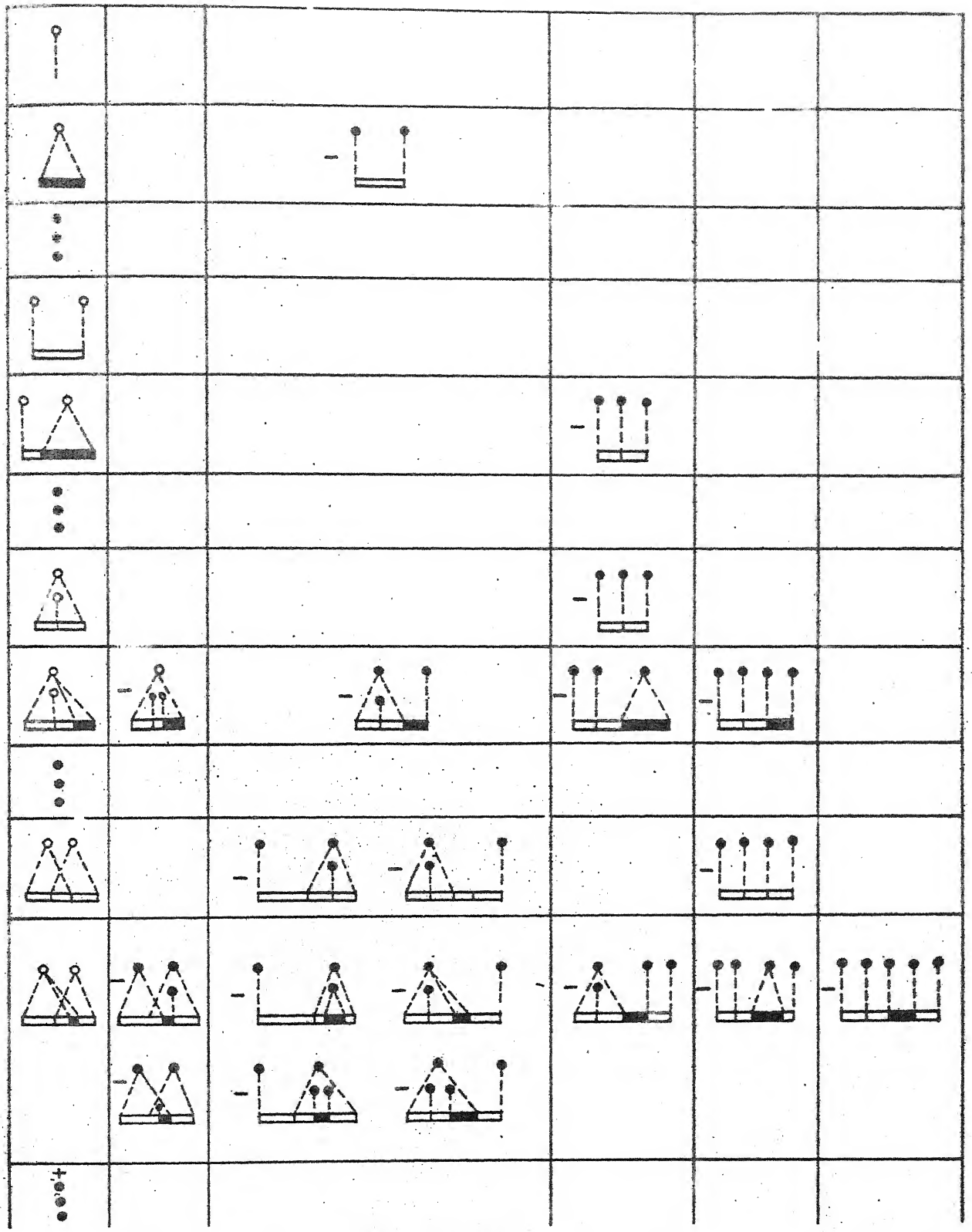

Fig. 2·8b

Repeat of Fig. (2.8a) for the case of those diagrams (column 1) which would appear in the t matrix for scattering by an isolated pair of defects.

such a diagrammatic summation to bigger clusters in three -dimensional lattices, appears intractable.

In the multiple scattering approach the system is partitioned into clusters, each containing n-sites (Tsukda 1972) and clusters are labelled as $C_1, C_2 \ldots C_j \ldots$ just as individual sites are labelled as $\vec{R}_1, \vec{R}_2 \ldots \vec{R}_j \ldots$. Let the vector $(<R_{nj+1}| \ldots <R_{nj+n}|)$ be denoted by $\{C_j|$ and diagonal matrix with $e_{nj+1} \ldots e_{nj+n}$ down the diagonals, by e_j then

$$\underline{V} = \sum_j e_j \underline{P}_j = \sum_j v_j \qquad (2.29)$$

where $\underline{P}_j$ projects the j-th element in the n-cluster subspace.

In the multiple-scattering picture, initally the electronic wavefunction evolves according to an unperturbed Hamiltonian $\underline{H}_o$. The scattering potential $\underline{W} = \underline{V} - \underline{\Sigma}$ is then switched on. If we assume that $\underline{\Sigma}$ is cluster diagonal then electron suffers multiple scattering from clusters and scattering events from different clusters are represented. The $\underline{T}$ matrix relates the emergent electronic wave function, modified due to scattering, to the unperturbed incident wavefunction. As before (see equations 2.22 and 2.24)

$$\underline{T} = \sum_j \underline{t}_j \quad \text{and} \quad \underline{t}_j = \underline{\tau}_j \left(\underline{I} + \bar{\underline{G}}_j \sum_{k \neq j} \underline{t}_k\right)$$

$\bar{\underline{G}}_j$ is an (nxn) matrix and

$$\underline{\tau}_j = (\underline{v}_j - \underline{\Sigma}_j)\left[\underline{I} - \bar{\underline{G}}_j (\underline{v}_j - \underline{\Sigma}_j)\right]^{-1}$$

The CCPA equation then reads

$$\langle \underline{\tau}_j \rangle = 0 \qquad (2.30)$$

The self-consistency condition (2.30) may be written interms of the matrix elements of the configurationally averaged Green's-function, if we observe that the Green's function for the system with the averaged medium everywhere, except the cluster (or cell) j can be written as:

$$\underline{G}_j = \langle \underline{G} \rangle + \langle \underline{G} \rangle \quad \underline{\tau}_j \langle \underline{G} \rangle \qquad (2.31)$$

Therefore the condition (2.30) becomes

$$\langle \underline{G}_j \rangle = \langle \underline{G} \rangle \qquad (2.32)$$

which is similar to the 1CPA condition.

This equation when applied to simple model of random , binary alloy on a linear chain, with diagonal-disorder only, yields satisfactory results. The band-edges are produced more accurately than in 1CPA. Ducastelle has shown that for CCPA with cluster-diagonal self-energy the approximate Green's function retains the Herglotz property of the exact Green's function which is a very favourable point, for the generalisation in this form. But when we apply CCPA equations to realistic situations the calculations become infeasible (Tsukda 1972). For this reason several other simplifications have been suggested.

2.5.1 Central-Site Approximation

Equation (2.30) and (2.32) are (nxn) matrix equations and require solutions of n^2 non-linear simultaneous equations in n^2 unknown matrix elements of the cluster-diagonal self-energy. To simplify the calculation of CCPA people have approximated the form of cluster diagonal self-energy. If we assume $\underline{\Sigma}$ to be site-diagonal within the cluster there will be only one adjustable parameter in the effective Hamiltonian making it impossible to satisfy all the n^2-relations (2.30) or (2.32). Within these limitations the first approximation known as 'self-consistent central-site approximation'(SCCSA) was due to Butler (1972). In this approximation equation (2.32) is replaced by a single equation,

$$\langle \vec{R}_o | \langle \underline{G}_j \rangle | \vec{R}_o \rangle = \langle \vec{R}_o | \langle \underline{G} \rangle | \vec{R}_o \rangle \qquad (2.33)$$

where $|\vec{R}_o\rangle$ is the orbital on the site at the centre of the cluster Equation (2.33) is equivalent to choosing a $\underline{\Sigma}$ in such a way that the averaged density of states per site at the centre of the cluster is consistent with the external medium. This prescription though entirely adhoc gives good results in the weak scattering limit (Butler 1972, Brouers et al 1973a, 1973b). When applied to strong scattering region this approximation begins to fail. At some energy region within tje band $\underline{G}(Z)$ loses its Herglotz property. The density of states becomes many-valued and the sum-rule for the integrated density of states is violated

(nickel and Butler 1973). These difficulties arise for simple cubic (Butler 1973) and diamond (Kumar and Joshi 1975) lattices for a 50-50 alloy with $\delta = 1$ where δ is the modified relative separation in the well depths. In order to remove these difficulties Butler (1973) suggested a self-consistent boundary-site approximation (SCBSA) which is discussed in the next section.

2.5.2 Boundary-Site Approximation

In this approximation the consistency is required between the averaged diagonal element of the Green's function at the boundary site $\langle \bar{R}_b | \langle \underline{G}_j \rangle | \bar{R}_b \rangle$ (where b is a boundary-site in the cluster) and a diagonal element of the Green's function for the averaged medium i.e.

$$\langle \bar{R}_b | \langle G_j \rangle | \bar{R}_b \rangle = \langle \bar{R}_b | \langle \underline{G} \rangle | \bar{R}_b \rangle \qquad (2.34)$$

For a linear chain Butler (1973) has shown that the SCBSA is exactly equivalent to CCPA. This is a surprising result, since the SCBSA also, like SCCSA, employs a scalar self-energy. But this equivalence does not carry over to two or three dimensions. Kumar and Joshi (1975) have applied SCBSA to a 50-50 alloy with $\delta = 1$, on a diamond lattice. It does not seem to show any analytic trouble. In a detailed SCBSA calculation Kumar and Joshi (1978) have found that in the extreme split band case, some of the partial density of states do become negative in a small energy region. Thus yielding unphysical results.

So far, we have discussed the situations where only diagonal-disorder was present. Several attempts have been made to include randomness in the hopping-integrals (Blackmann et al 1971, Shiba 1971, Foo et al 1973, Niizeki 1975, Kumar et al 1975). Here it is assumed that the diagonal term of the Hamiltonian can have either of the two values e_A and e_B, and hopping integrals may have values V_{AA}, V_{BB} or V_{AB} depending on the configuration of the nearest-neighbour pairs. Even this model fails to produce more than simply an S-wave scattering (Elliot et al 1974).

2.6 Cluster-Embedding

In addition to various approaches for cluster generalisations discussed in the previous section, people have tried to embed large size clusters in some non-self-consistent effective (or average) medium e.g. immersion of a large size cluster in 1CPA or VCA medium (Diehl and Leath 1979a, Choudhry 1981). Here once the effective medium (1CPA or VCA) is obtained, one can write an exact Hamiltonian for a culster of n-sites as

$$\underline{H}_c^{(n)} = \underline{H}_{eff}^{(n)} + \underline{h} \qquad (2.35)$$

where $\underline{H}_{eff}^{(n)}$ is the Hamiltonian corresponding to a n-cluster effective medium and $\underline{h} = \underline{H}_c^{(n)} - \underline{H}_{eff}^{(n)}$ is the difference Hamiltonian finite only over the cluster.

The Green's function corresponding to $\underline{H}_c^{(n)}$ is,

$$\underline{G}_c^{(n)} = (Z\underline{I} - \underline{H}_c^{(n)})^{-1}$$

$$= (Z\underline{I} - \underline{H}_{eff}^{(n)} - \underline{h})^{-1}$$

$$= (\underline{I} - \underline{G}_{eff}^{(n)}\,\underline{h})^{-1}\,\underline{G}_{eff}^{(n)} \qquad (2.36)$$

where $\underline{G}_{eff}^{(n)} = (Z\underline{I} - \underline{H}_{eff}^{(n)})^{-1}$

each of $\underline{H}_c^{(n)}$, $\underline{G}_c^{(n)}$, $\underline{h}$ and $\underline{H}_{eff}^{(n)}$ is (nxn) square matrix. The inversion of $(\underline{I} - \underline{G}_{eff}^{(n)}\,\underline{h})$ is that of a finite matrix, because $\underline{h}$ has non-zero elements only in the cluster subspace. Here $\underline{H}_c^{(n)}$ includes exact details of the interactions over the cluster while it sees the rest of the medium effectively. Consequently, by choosing clusters of larger sizes, details of environment implanted can be gradually increased. If we choose a central site and its neighbours, the density of states at the central site obtained from the corresponding number on the diagonal of $\underline{G}_c^{(n)}$ is closer to the true Hamiltonian than the effective medium (VCA or 1CPA).

For each possible configuration over a cluster, we can determine the density of states at the central site and also the configurationally averaged Green's function. Particular features in the density of state curve can be attributed to specific clusters.

But this kind of cluster embedding often gives rise to two kinds of difficulties: (1) the band-width remains incorrect

and (2) because the density of states still integrates to unity (one electron per site), this has the effect of distorting the structure specially near the band-edges to preserve normalisation. Thus spurious structure may be obtained where there should be none.

So, from the discussion of the previous few sections, it is obvious that none of the proposed cluster generalisations are satisfactory. We therefore, turn to an altogether different viewpoint of configuration-averaging, namely the augmented space formalism (Mookerjee 1973, Mookerjee and Bishop 1974, Haydock and Mookerjee 1974, Mookerjee 1975a, 1975b, Kaplan and Gray 1976-1977, Kaplan et al 1980, Kumar, Mookerjee and Srivastava 1982). Basing ourselves on this formalism, we shall develop an unambiguous, tractable generalisation of the 1CPA which retains the Herglotz property at all energies for all ranges of disorder (Kumar, Mookerjee and Srivastava 1982). Off-diagonal disorder and short-range order shall also be incorporated.

Recently in a series of papers(Kaplan and Gray (1976,77) and Diehl and Leath (1979a, 1979b))the authors have examined augmented space formalism and have generated self-consistent results, with off-diagonal disorder on linear chains in particular (Kaplan et al 1980). There is a close and exact relationship of their algebraic equations to the graphical

method that has been adopted in our work. The graphical method has the added advantage that it is ideally suited in conjunction with the 'Recursion' technique (Appendix A) of Haydock et al (1972, 1975) for the application to realistic models on three-dimensional lattices. The equivalent algebraic equations soon become tediously unwieldy as soon as the cluster size increases, particularly on a three-dimensional lattice. This is the principal contribution of this work and an indication of its future usefulness.

CHAPTER III

AUGMENTED-SPACE FORMALISM AND CLUSTER COHERENT-POTENTIAL APPROXIMATION

3.1 Augmented-Space Method

In this section we shall introduce a different approach to the problem of configuration averaging: namely, the augmented-space formalism, first introduced by Mookerjee (1973) and subsequently developed in various aspects by other workers (see Chapter II). We shall describe here the construction of the augmented space and shall define the notation to be used throughout the remainder of the thesis.

We start with the assumption that the lattice sites are randomly occupied by the atoms of the type A,B,C etc. The random variable e_i then takes on the values e_A, e_B or e_C etc. corresponding to the occupation of the site i. A set of values taken up by the random variables $\{e_i\}$ is called a configuration. A certain probability density $P(\{e_i\})$ is associated with various different configurations. Assuming that different e_i are statistically independent,

$$P(\{e_i\}) = \prod_i p_i(e_i) \qquad (3.1)$$

where $p_i(e_i)$ is the probability density of the individual variables. This assumption ignores short-range order due to chemical clustering effect, which invariably leads to

statistical correlation between the $\{e_i\}$. The more general case of dependent variables has been considered by Kaplan and Gray (1976-1977).

Haydock (1972) noted the fact that the probability density $p_i(e_i)$ satisfies the properties

$$p_i(e_i) \geq 0 \quad \text{and} \quad \int_{-\infty}^{\infty} p_i(e_i)\, de_i = 1$$

These properties are specific to the imaginary part of a Herglotz function e.g. the resolvent of a self-adjoint operator in a certain Hilbert space. Taking clue from this Mookerjee (1973) suggested that a Hilbert space ϕ_i and a basis $\{|f_n^i\rangle\}$ may be introduced such that $p_i(e_i)$ corresponds to the imaginary part of the resolvent of a suitably chosen operator $\underline{M}_i$ in ϕ_i. If $|f_o^i\rangle$ is a specially chosen member of the orthonormal basis $\{|f_n^i\rangle\}$ in ϕ_i then,

$$p_i(e_i) = -\frac{1}{\pi} \operatorname{Im} \langle f_o^i | (e\underline{I} - \underline{M}_i)^{-1} | f_o^i \rangle \qquad (3.2)$$

$$\text{where} \quad e \to e_i + i\varepsilon^+$$

A prescription for construction of a suitable $\underline{M}$ for a given $p(e)$ is as follows:

For a given $p(e)$, if one could find a convergent continued fraction of the kind,

$$\cfrac{1}{e - a_1 - \cfrac{b_1^2}{e - a_2 - \cfrac{b_2^2}{e - a_3 - \cfrac{b_3^2}{\ddots}}}}$$

Then a representation of the operator $\underline{M}$ is the tridiagonal matrix with a_1, a_2, a_3..., etc. along the diagonal and b_1, b_2,..., etc. along the off-diagonal positions i.e.,

$$\begin{vmatrix} a_1 & b_1 & 0 & 0 & 0 & 0 & 0 & . \\ b_1 & a_2 & b_2 & 0 & 0 & 0 & 0 & . \\ 0 & b_2 & a_3 & b_3 & 0 & 0 & 0 & . \\ . & . & . & . & . & . & . & . \end{vmatrix}$$

in some basis $\{|f_n>\}$. Of course, we have to restrict ourselves to probability distributions all of whose moments are finite, otherwise a convergent continued fraction is not possible. Most of the physically valid probability distributions are of this kind, the only exception being the Lorentzian. The procedure involved in Haydock's (1972) method of recursion for determining matrix elements of Green's operator is the inverse of this.

For a binary alloy case with diagonal disorder only, e.g. A_cB_{1-c}, e represents the diagonal element of the Hamiltonian in a tight binding (or atomic orbital) basis. The diagonal terms $\{e_i\}$ form a set of random variables described by

$$e_i = e^A N_i + e^B (1-N_i)$$

where $\{N_i\}$ are a set of random occupation variables for the solute A in the solvent B. In the absence of short- range order the various N_i's are independent random variables with probability densities

$$p(N_i) = c\,\delta(N_i-1) + (1-c)\,\delta(N_i) \qquad (3.3)$$

$$= \frac{1}{\pi} \operatorname*{Im}_{\eta\to 0} \left\{\frac{c}{N_i+i\eta-1} + \frac{(1-c)}{N_i+\eta i}\right\}$$

$$= -\frac{1}{\pi} \operatorname*{Im}_{\eta\to 0^+} + \left\{\frac{c}{N'-1} + \frac{(1-c)}{N'}\right\} \quad \text{where } N'=N_i+i\eta$$

$$= -\frac{1}{\pi} \operatorname*{Im}_{\eta\to 0^+} \left\{\frac{1}{N'-a_1 - \dfrac{c(1-c)}{N'-(1-c)}}\right\}$$

$$= -\frac{1}{\pi} \operatorname*{Im}_{\eta\to 0^+} \left\{\frac{1}{N'- a_1 - \dfrac{b_1^2}{N'-a_2}}\right\}$$

where $a_1 = c$, $a_2 = (1-c)$ and $b_1^2 = c(1-c)$. A representation of the matrix $\underline{M}$ is thus a 2 x 2 matrix

$$\begin{bmatrix} c & \sqrt{c(1-c)} \\ \sqrt{c(1-c)} & (1-c) \end{bmatrix} \qquad (3.4)$$

with eigenvalues 0 and 1. Its eigenstates $|f_1\rangle$ and $|f_2\rangle$ describe occupancies corresponding to these eigenvalues.

We now introduce the ''disorder-field''. To each variable N_i we have associated a vector space ϕ_i and a representation of a self adjoint operator $\underline{M}_i$ corresponding to the bimodal probability density of that variable in some basis $\{|f_n^i\rangle\}$. If we had taken the set of eigenvectors $\{|h_n^i\rangle\}$ of $\underline{M}_i$ as our basis, then each $|h_n^i\rangle$ in ϕ_i would correspond to one particular value taken by the variable e_i. In general any element in ϕ_i is a linear combination of the $\{|h_n^i\rangle\}$. ϕ_i with its basis and operator $\underline{M}_i$ thus contains

all possible information about the configurations of the variable e_i.

The product space $\Phi = \prod_i \otimes \phi_i$ can now be constructed which contains all possible states of the set $\{e_i\}$ i.e. all configurations of the disordered system. The basis in the product space is

$$|f\rangle = \{|f_i^1\rangle\} \otimes \{|f_i^2\rangle\} \otimes \ldots \qquad (3.5)$$

and if $g^{(\underline{M}_i)}(Z) = (Z\underline{I} - \underline{M}_i)^{-1}$

then $P(\{e_i\}) = -\frac{1}{\pi} \operatorname{Im} \langle f_o | \underline{G}(Z) | f_o \rangle$

where $|f_o\rangle = |f_o^1\rangle \otimes |f_o^2\rangle \otimes |f_o^3\rangle \otimes \ldots \qquad (3.6)$

and $\underline{G}(Z) = g^{(\underline{M}_1)}(Z) \otimes g^{(\underline{M}_2)}(Z) \otimes g^{(\underline{M}_3)}(Z) \otimes \ldots$

We call Φ the disorder-field. It is clear from the way it is constructed that it contains complete information about the statistical behaviour of the system. The information about probability of configurations is described by the operators $\underline{M}_i$ defined on the field.

We now describe the configuration averaging procedure. Let us first consider a function $f(e)$ of one variable only. Its average is

$$\bar{f} = \int_{-\infty}^{\infty} f(e)\, p(e)\, de$$

$$= \int_{-\infty}^{\infty} f(e) \left\{ -\frac{1}{\pi} \operatorname*{Im}_{Z \to e+i0^+} g_{oo}^{(\underline{M})}(Z) \right\} de$$

where $p(e) = -\frac{1}{\pi} \operatorname{Im}\, g_{oo}^{(\underline{M})}(e+i0^+)$

Assuming now that $f(Z)$ is a function of a complex variable Z and has no singularities on the real axis, in the neighbourhood of the branch cut of the function $\underline{g}^{M}_{oo}(Z)$;

$$\bar{f} = -\frac{1}{2\pi i} \oint f(Z)\, \underline{g}^{M}_{oo}(Z)\, dZ \qquad (3.7)$$

The contour over which the integration is carried out is taken around the branch cut of $\underline{g}^{M}(Z)$ along the real axis and not including any singularities of $f(Z)$. Since $\underline{M}$ is a Hermitian operator on ϕ, we can write

$$\bar{f} = -\frac{1}{2\pi i} \oint f(Z)dZ \, \langle f_o | \int_{-\infty}^{\infty} (Z-h)^{-1} d\underline{p}(h) | f_o \rangle$$

where we have written $\underline{g}^{M}(Z) = \int_{-\infty}^{\infty} (Z-h)^{-1} d\underline{p}(h)$, $\underline{p}(h)$ being the spectral projection operator of $\underline{M}$. Thus

$$\bar{f} = \langle f_o | \int_{-\infty}^{\infty} f(h) d\underline{p}(h) | f_o \rangle$$

$$= \langle f_o | \underline{f}(\underline{M}) | f_o \rangle \qquad (3.8)$$

where $\underline{f}(\underline{M})$ is the same function of $\underline{M}$ as f is of e. The average has been expressed as a representation of a suitably constructed operator.

The generalisation to a function of several variables is straight forward with one $\underline{M}^{(i)}$ associated with each variable e_i. In case $f(e)$ is itself a matrix element of the kind say $\langle \vec{r}_i | \underline{F}(e) | \vec{r}_j \rangle$, $\underline{F} \in \mathcal{H}$ state vectors $|f_o, \vec{r}_i\rangle = |f_o\rangle \otimes |\vec{r}_i\rangle$ are defined on the augmented product

space $\Psi = \mathcal{H} \otimes \prod^{\otimes} \phi_i$ and the average becomes

$$\bar{F} = \langle f_o; \vec{r}_i | \left[\int_{-\infty}^{\infty} \{ \mathrm{Im}\, \underline{G}^{(M)}(h+i0^+) \} \otimes \underline{F}(h)\, dh \right] | f_o; \vec{r}_i \rangle$$

We shall now consider the problem of configuration averaging of the Green's function. For a substitutionally disordered, random, binary alloy A_cB_{1-c}, the Hamiltonian (with nearest neighbour interaction only) in the tight-binding basis can be written as

$$\underline{H} = \sum_i e_i \underline{P}_i + \sum_{ij} V_{ij} \underline{T}_{ij}$$

For a predominant diagonal disorder, we may assume $V_{ij} = \bar{V}$ and write

$$\underline{H} = \sum_i e_i \underline{P}_i + \bar{V} \sum_{ij} \underline{T}_{ij}, \quad \underline{H} \in \mathcal{H} \tag{3.9}$$

where $\bar{V}$ is the weighted average of the overlap-integral. This is valid for cases when the bandwidths of the constituents are roughly similar.

Referring to the Hamiltonian of equation (3.9) with diagonal disorder only, the Green's function can be written as

$$G_{ii}(Z, \{e_i\}) = \langle \vec{r}_i | (Z\underline{I} - \underline{H})^{-1} | \vec{r}_i \rangle$$

The poles of G_{ii} are situated at the eigenvalues of $\underline{H}$. These are distinct from those of $g^{(M)}(Z)$ which are at the values that e_i may take. Using the averaging procedure, therefore, for every single random variable e_i, we have

$$G_{ii}(Z) = \langle f_o;\vec{r}_i | (Z\underline{I}-\tilde{\underline{H}})^{-1} | f_o;\vec{r}_i \rangle \qquad (3.10)$$

where $|f_o;\vec{r}_i\rangle = |f_o\rangle \otimes |\vec{r}_i\rangle$, $|f_o\rangle$ is given by equation (3.6) and

$$\tilde{\underline{H}} = \sum_i \underline{P}_i \otimes \underline{Q}_i + \bar{V} \sum_{ij} \underline{T}_{ij} \otimes \underline{I} \qquad (3.11)$$

where

$$\underline{Q}_i = \underline{I} \otimes \underline{I} \otimes \underline{I} \cdots\cdots \otimes \underline{M}_i \otimes \underline{I} \otimes \cdots \qquad (3.12)$$

The expanded Hamiltonian $\tilde{\underline{H}}$ contains complete information about the system and is defined on the expanded Hilbert space $\Psi = \mathcal{H} \otimes \Phi$ where $\Phi = \prod_i^{\otimes} \phi_i$. Description of the quantum behaviour of the system is in the subspace $\mathcal{H}$, while that of the statistical behaviour is in Φ, the disorder space. The configuration averaged Green's function is a particular representation in this expanded space Ψ. The problem has thus been reduced to the determination of the resolvent of the Hamiltonian $\tilde{\underline{H}}$ in the augmented space Notice that up to this stage of configuration averaging no approximations are involved. Subsequently, in the determination of the resolvent in the augmented space, herglotzicity retaining approximations may now be introduced systematically. In the next section we shall describe a method which will enable us to do just this.

3.2 The Graphical Technique

The graphical method was introduced by Haydock (1972) for calculation of the resolvent. It will be used to generate the cluster-CPA formalism for a general alloy system.

By a graph we shall mean a set of 'vertices' connected by 'links'. Let $\{|i\rangle\}$ be any complete linearly independent basis in which the Hamiltonian is described. The overlap matrix

$$S_{ij} = \langle i|j\rangle$$

is a unit matrix in case the basis is orthonormal. Matrix elements of an operator $\underline{M}$ are given by

$$M_{ij} = \langle i|\underline{M}|j\rangle$$

A graph is associated with every basis $\{|i\rangle\}$. To every element $|i\rangle$ of the basis set $\{|i\rangle\}$ is associated a vertex v_i, and to each distinct pair of elements $(|i\rangle, |j\rangle)$ a link or bond ℓ_{ij} which may be directional (i.e. ℓ_{ij} may not be equal to ℓ_{ji}) or otherwise. To any operator $\underline{M}$ there corresponds a graph consisting of vertices and those links for which $M_{ij} \neq 0$. If we want to invert an operator $\underline{M}$, then the contribution of each vertex v_i, is defined as

$k(v_i) = 1/M_{ii}$ and that of the link ℓ_{ij} as $k(\ell_{ij}) = +M_{ij}$.

A path Q_N of length N is defined as a series of ordered vertices and links i.e.

$$Q_N = \{v_i \ \ell_{ij} \ v_j \cdots \ v_N\}$$

Contribution of a path is defined as

$$k(Q_n) = \prod_{\text{vertices}} k(v_i) \prod_{\text{links}} k(\ell_{ij})$$

A self-avoiding path of length N, $Q_N=\{v_i \ell_{ij} v_j \cdots v_N\}$ is a path such that $v_n \neq v_m$ with the only exception that v_i may be the same as v_N, in which case it is a self-avoiding closed polygonal path.

The renormalised contribution of a vertex v_N in a path Q_N is defined as

$$k(v_N) = \sum_{N=0}^{\infty} \sum_{Q'_N} k(Q'_N) \qquad (3.13)$$

where Q'_N are all polygonal self-avoiding paths from v_n and back, on the graph from which the vertices $v_1 \cdots v_{N-1}$ have been removed. If $\underline{M}^{-1} = \underline{G} = (Z\underline{I}-\underline{H})^{-1}$ then the representation of $\underline{G}$ in the same basis can be expressed (Haydock 1972, Mookerjee 1979) as follows:

$$G_{ij} = \sum_{N=0}^{\infty} \sum_{Q_N} k(Q_N) \qquad (3.14)$$

where Q_N are all self avoiding paths from v_i to v_j.

A use of graphical representation will be made, when approximations like CCPA are generated.

3.3 1CPA in the Augmented Space

The Hamiltonian $\underline{\tilde{H}}$ defined on the extended space $\Psi = \mathcal{H} \otimes \Phi$, can be written in the site-field representation $|nf\rangle$ as

$$\underline{\tilde{H}}_{nf,mf'} = \underline{M}^{n}_{ff'} \delta_{nm} + \underline{V}_{nm} \delta_{ff'} \qquad (3.15)$$

where $\underline{M}^{n}_{ff'}$ is the operator in Φ associated with the probability distribution and $\underline{V}_{nm}$ is the operator in $\mathcal{H}$. The disorder field space states are specified by the set of states $\{|f^{n}_{i}\rangle\}$ occupied in all individual fields ϕ_n, the exact form depending on the probability distribution p(e). In general, one chooses the basis in ϕ_n such that the representation of $\underline{M}_n$ is tridiagonal so that p(e) is given by a continued fraction. For a bimodal density the $\underline{M}^{n}_{ff'}$, for each n is given by equation (3.4) and its graph is a single link chain like

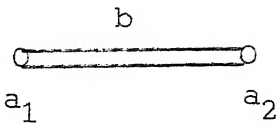

where $a_1 = (1-c)$, $a_2 = c$, $b = \sqrt{c(1-c)}$.

Finally the configuration averaged Green's function is the resolvent corresponding to the Hamiltonian $\underline{\tilde{H}}$.

Until now all equations are exact. Approximations are made while employing the graphical technique. The exact

graph on which the calculation from equation (3.13) is formidable, is replaced by a simpler graph on which the path counting is(simpler and) tractable.

Choosing for $\underline{M}$ in equation (3.13) as $(ZI-\tilde{H})$ the configurationally averaged Green's functions $\bar{G}_{nm}(Z)$ can be determined by considering self avoiding non-intersecting paths in the complete augmented space $\Psi = \mathcal{H} \otimes \Phi$. Walks in the augmented space imply the following. An electron at a site labelled by n and field state $|f\rangle = |f_i^1\rangle \otimes |f_j^2\rangle \otimes \ldots |f_k^n\rangle \ldots$ can be induced by $\underline{H}$ either to make spatial hops to one of the near neighbours of n with the matrix element V, keeping the field state same, or it can remain on the spatial site, while the field at the site n changes according to $\underline{M}_n$, the field at all other spatial sites remaining same. For $|f\rangle = |f_o^1\rangle \otimes |f_o^2\rangle \otimes \ldots$,

$$\bar{G}_{nm}(Z) = \langle nf|(ZI-\tilde{H})^{-1}|mf\rangle \qquad (3.16)$$

In this sense the problem has been reduced to that of an ordered system but at the expense of a much amplified set of eigenfunctions.

Starting from the vertex (Of) the first steps possible (fig. 3.1) are to the near neighbours ℓ_i in the direct space (shown by single lines) or to a different configuration state of the site O labelled by (Of_o) by a disordered field hop (shown by double lines).

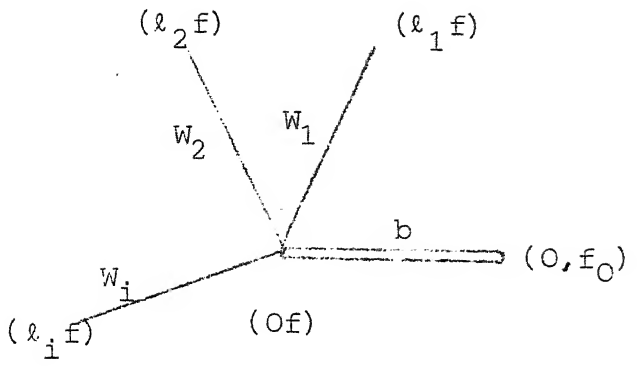

Fig. (3.1)

If $R_o(Z)$ is the contribution of all self-avoiding non-intersecting paths from vertex 0 and back in the space $\mathcal{H}$, then the resolvent in an ordered system would be

$$P_{oo}(Z) = \frac{1}{Z - R_o(Z)} \tag{3.17}$$

In three dimensions this will include the contribution $\sum_i v_i^2 P_{ii}^{(o)}$ where i are various neighbours of '0' and $P_{ii}^{(0)}$ corresponds to the resolvent calculated from a sub-graph in which the vertex '0' has been removed, besides contributions of closed self-avoiding loops in $\mathcal{H}$. In the extended space, the configuration averaged Green's function $\bar{G}(Z)$ can be written as

$$\bar{G}(Z) = \frac{1}{[Z - R(Z) - T(Z)]} \tag{3.18}$$

$R(Z)$ is the contribution of all self-avoiding paths from the vertex 'Of' and back that are either (a) entirely in the spatial part of the augmented space or (b) self-avoiding paths in the augmented space which include field- hops but

do not form closed loops. $T(Z)$ is the contribution of all closed self-avoiding loops from 'Of' and back in the full augmented space, connecting different spatial sites via field hops.

The essential approximation is now made: in the augmented space Ψ, there exist, closed self-avoiding loops which arise not because of any closed loops in the spatial lattice, but because of the field introduced. These paths contribute to $T(Z)$ and our approximation involves delinking all such paths such that $T(Z) = 0$. Once we have done that our graph consists of essentially that in the ordered system together with an extra field hop with the off-diagonal element of $\underline{M}^{(n)}$ in the tridiagonal representation ($b = \sqrt{c(1-c)}$ in the case of binary alloys) as the link function. If starting from a vertex 'nf' we hop to a vertex 'nf_n' then the subgraph with the vertex 'nf' missing is an infinite graph which is exactly similar to the original one. This property did not exist in the undelinked graph. A direct consequence of this property is

$$G^{(Of)}_{Of_O, Of_O} = G_{Of, Of} = \bar{G}_{OO} = G(Z) \qquad (3.19)$$

This will not hold in the absence of the type of delinking adopted above.

Now we shall show that the above delinking procedure (Bishop and Mookerjee 1974) is exactly the 1CPA.

Let $G^{DL}(Z)$ be the resolvent, corresponding to the graph in the augmented space after delinking and let

$$M_{ij} = W_i \delta_{j,i+1}$$

be the tridiagonal representation of the operator $\underline{M}_n$ in each subspace ϕ_n of Φ. Then,

$$G^{DL}(Z) = \frac{1}{[Z-R_o(Z-W_1^2 G_1(Z))-W_1^2 G_1(Z)]}$$

$$= P_{oo}[Z-W_1^2 G_1(Z)] \qquad (3.20)$$

where

$$G_i(Z) = \frac{1}{[Z-R_o(Z-W_1^2 G_1)-W_{i+1}^2 G_{i+1}(Z)]} \qquad (3.21)$$

In the conventional 1CPA formalism a self-energy $\Sigma(Z)$ is defined by

$$G^{CP}(Z) = \frac{1}{[Z-\Sigma(Z)-R_o(Z-\Sigma)]}$$

$$= P_{oo}[Z-\Sigma(Z)] \qquad (3.22)$$

where $G^{CP}(Z)$ is the 1CPA-Green's function. The self-energy $\Sigma(Z)$ is determined self consistently from the 1CPA equation,

$$\int_{-\infty}^{\infty} \frac{X-\Sigma(Z)}{1-G(Z)(X-\Sigma(Z))} p(X)\,dX = 0 \qquad (3.23)$$

so that

$$G^{CP}(Z) = \int_{-\infty}^{\infty} \frac{p(X)\,dX}{A(Z)-X} \tag{3.24}$$

where $$A(Z) = \frac{1+G^{CP}(Z)\Sigma}{G^{CP}} \tag{3.25}$$

Now just as in equation (3.7), $G^{CP}(Z)$ from equation (3.24) can be written as

$$G^{CP}(Z) = \langle f_o | \left[A(Z)\underline{I} - \underline{M}\right]^{-1} | f_o \rangle \tag{3.26}$$

Graphically therefore

$$G^{CP}(Z) = \frac{1}{\left[A(Z) - W_1^2\, G_1^{CP}(Z)\right]} \tag{3.27}$$

where

$$G_i^{CP}(Z) = \frac{1}{\left[A(Z) - W_{i+1}^2\, G_{i+1}^{CP}(Z)\right]} \tag{3.28}$$

But $A(Z)$ from equations (3.26) and (3.27) is the same as $G^{DL}(Z)$ from equations (3.20) and (3.21). This equivalence of two approximations has also been shown by Mookerjee (1974) using multiple-scattering diagrams. It establishes a direct connection with the delinking approximation of the diagrammatic approach to the CPA.

3.4 Cluster CPA(CCPA) in the Augmented Space Method

The essential approximation involved in the 1CPA described in the last section is to delink all closed, self-avoiding paths involving both spatial and field hops in the augmented space. In the cluster - CPA, those self-avoiding, non intersecting paths are included which involve disorder

field hops over the n-sites of the cluster. A self-energy renormalising the interaction between each pair of sites in this cluster can then be defined. The corresponding n x n matrix for $\underline{\Sigma}$ will have less than n^2 independent components, which can be determined in a self-consistent way by an iterative procedure.

The starting Hamiltonian is a tight-binding type:

$$\underline{H}=\sum_i \sum_n e_{in}\, \underline{P}_{in} + \sum_{i\neq j} \sum_n \sum_m V_{in,jm}\, \underline{T}_{in,jm}, \quad \underline{H} \in \mathcal{H} \tag{3.29}$$

where $\underline{P}$ and $\underline{T}$ are projection operators and transfer operators in $\mathcal{H}$; n,m are band or orbital indices. Both the diagonal terms $\{e_{in}\}$ and the off-diagonal terms $\{V_{in,jm}\}$ form a set of random variables described by

$$e_{in} = e^{A}_{in}\, N_i + e^{B}_{in}\, (1-N_i)$$

$$V_{in,jm} = V^{AA}_{nm} N_i N_j + V^{BB}_{nm}(1-N_i)(1-N_j) + V^{AB}_{nm}\{N_i(1-N_j)+N_j(1-N_i)\}, \tag{3.30}$$

where $\{N_i\}$ are a set of random ''occupation'' variables for the solute A in the solvent B. In the absence of short-range order the various N_i's are independent random variables with probability density

$$p(N_i) = c\, \delta(N_i-1) + (1-c)\, \delta(N_i) \tag{3.31}$$

Using (3.30) we may rewrite (3.29) in a more useful form

$$\underline{H} = \underline{H}_B + \sum_i \sum_n e_n N_i \underline{P}_{in} + \sum_{i\neq j} \sum_n \sum_m V^{(1)}_{nm} N_i N_j \underline{T}_{in,jm}$$

$$+ \sum_{i\neq j} \sum_n \sum_m V^{(2)}_{nm} (N_i + N_j) \underline{T}_{in,jm} \qquad (3.32)$$

where $\underline{H}_B$ is the Hamiltonian of the pure solvent, $e_n = e^A_n - e^B_n$ $V^{(1)}_{nm} = V^{AA}_{nm} + V^{BB}_{nm} - 2\,V^{AB}_{nm}$ and $V^{(2)}_{nm} = V^{AB}_{nm} - V^{BB}_{nm}$.

The Hamiltonian is now in a form appropriate for the augmented space formalism. Corresponding to each N_i there is a operator $\underline{M}^{(i)}$ in a two-dimensional vector space $\phi^{(i)}$. A representation of $\underline{M}^{(i)}$ in a basis $\{|v^i_0\rangle, |v^i_1\rangle\}$ is

$$\begin{bmatrix} c & \{c(1-c)\}^{1/2} \\ \{c(1-c)\}^{1/2} & 1-c \end{bmatrix} \quad \text{(Mookerjee 1973)} ,$$

where c is the concentration of the solute A. The augmented space Hamiltonian is

$$\tilde{\underline{H}} = \underline{H}_B \otimes \underline{I} + \sum_n e_n \sum_i \underline{P}_{in} \otimes \underline{M}^{(i)} \otimes \underline{I}^{(i)}$$

$$+ \sum\sum_{nm} V^{(1)}_{nm} \sum_{i\neq j} \underline{T}_{in,jm} \otimes \underline{M}^{(i)} \otimes \underline{M}^{(j)} \otimes \underline{I}^{(ij)}$$

$$+ \sum_{nm} V^{(2)}_{nm} \sum_{i\neq j} \underline{T}_{in,jm} \otimes (\underline{M}^{(i)} \otimes \underline{I}^{(i)}$$

$$+ \underline{M}^{(j)} \otimes \underline{I}^{(j)})$$

$$\tilde{\underline{H}} \in \mathcal{H} \otimes \prod_i \phi^{(i)} \qquad (3.33)$$

$\underline{I}^{(i)}, \underline{I}^{(ij)}$ in the above equation indicate identity operators in all sub-spaces $\phi^{(k)}$ except those superscripted.

The configurationally averaged Green function is then given by

$$\langle G_{in,jm}(Z)\rangle = \langle \vec{r}_i, n, \tau^o | \; (Z\underline{\tilde{I}} - \underline{\tilde{H}})^{-1} \; | \vec{r}_j, m, \tau^o \rangle \qquad (3.34)$$

with $|\tau^o\rangle \equiv \prod_i^{\otimes} |v_o^i\rangle$. Note that to this stage the relations are all exact.

The density of states then follows directly:

$$\langle n(E)\rangle = -(1/\pi) \sum_n \mathrm{Im} \langle G_{in,in}(E+i\eta)\rangle_{\eta \to 0^+} \; . \qquad (3.35)$$

In the language of Kaplan et al. (1980), it is the off-diagonal terms of $\underline{M}^{(i)}$'s which are responsible for the creation of pseudofermions or configuration fluctuations above the augmented space ''ground state'' $|\tau^o\rangle$. In the presence of off-diagonal disorder pseudofermions are simultaneously created at two sites $\vec{r}_i$ and $\vec{r}_j$ by the term $\underline{M}^i \otimes \underline{M}^j$.

Short-range chemical ordering may be described in an elementary way by a Markovian pair type-between neighbouring sites $\vec{r}_i$ and $\vec{r}_j$

$$p(N_j;N_i=1) = \{1-\alpha(1-c)\}\, \delta(N_j-1) + \alpha(1-c)\; \delta(N_j)$$

$$p(N_j;N_i=0) = \alpha c\, \delta(N_j-1) + (1-\alpha c)\; \delta(N_j) \qquad (3.36)$$

The single parameter α then is a measure of short-range ordering. If $\alpha = 1$ then there is no short-range order and the alloy is purely random. If $1 < \alpha < (1-c)^{-1}$, then AB

type of clustering is favoured. The maximum value corresponds to a situation when the alloy is not really random at all, but forms a superlattice of A and B constituents. If $\alpha < 1$, then AA or BB type of clustering is favoured.

This type of description of short-range order may be rather crude. Here we are dealing with a ''quenched'' short-range order, that is, a short-range order that is not governed by thermodynamics and is consequently temperature independent. In more realistic situations one has to go through a more sophisticated formulation involving concentration-concentration fluctuations.

Having formally performed the configuration averaging exactly, we shall now proceed to generate the approximation methodically, keeping in mind the important Herglotz property which must not be violated at any stage. We shall adopt a graphical formulation. It is well known that calculation of Green functions on connected graphs, using the nested path technique always produces Herglotz results (Haydock 1972, thesis). This methodology has been described in great detail by Bishop and Mookerjee (1974) and Mookerjee (1975a,b).

The graphs may be generated by the method described in section (3.2). The essential approximation now involves ignoring or delinking the contribution of possible self-avoiding paths. The relation of these polygonal paths to the CPA has been discussed by Bishop and Mookerjee (1974) and

Mookerjee (1975b) has demonstrated their relation to the multiple scattering diagrams. The philosophy of approximation is as follows.

We consider exactly all paths that involve only the spatial part of the augmented space, i.e. $\mathcal{H}$. Such paths are connected to the lattice structure and must not be approximated or delinked without destroying some of the feature of the underlying lattice. In three and two dimensions the recursion method helps us to deal with this infinite set of paths.

If we want a CCPA with $(\vec{r}_1, \vec{r}_2, \ldots, \vec{r}_N)$ within the cluster, then all polygonal paths that do not completely lie in the subspace $\mathcal{H}$ and involve these vertices and none others must also be exactly accounted for. These are related to the multiple scattering within the cluster.

Larger polygonal paths which involve sites within and without the cluster but which do not completely lie in the subspace $\mathcal{H}$ must be delinked. The type of delinking depends very much on the environment we wish to immerse our cluster in. Immersion in a VCA medium yields the travelling pseudofermion approximation (generalization of the ATA) of Diehl et al (1979a). If we wish to immerse in a 1CPA medium, we simply delink all these larger polygonal paths into a Cayley tree (Bishop and Mookerjee 1974). The result is not self consistent

and in particular the band-width is the same as that of the 1CPA. If we wish to embed our cluster in a self-consistent cluster medium, we partition the lattice in Tsukada type clusters, delink the environment itself into cluster paths and self-consistently calculate the effect. We shall describe this in detail in the next section. It is instructive to note at this point that this graphical technique is ~~exactly~~ similar ~~equivalent~~ to the partitioning idea of Kaplan et al. (1980).

3.4.1 The Self-Consistent Medium

The calculation of the self-consistent medium in the CCPA is of central interest and is the most important contribution of this work. To illustrate the procedure let us first consider a 2CPA. We shall indicate the generalisation of bigger clusters subsequently.

Note first that after the delinking procedure according to the prescription described in the previous section, the resulting graph has the following structure: each bond in the original lattice has, in augmented space, an ''octagon'' decorating it (Fig. 3.2a). The eight vertices of the octagon corresponds to the eight different configurations of the two-site cluster (2×2^2). Because of the cluster delinking, no octagon belonging to a bond has any connection to another, corresponding to another bond, through an augmented space link. This exactly implements the idea that within this

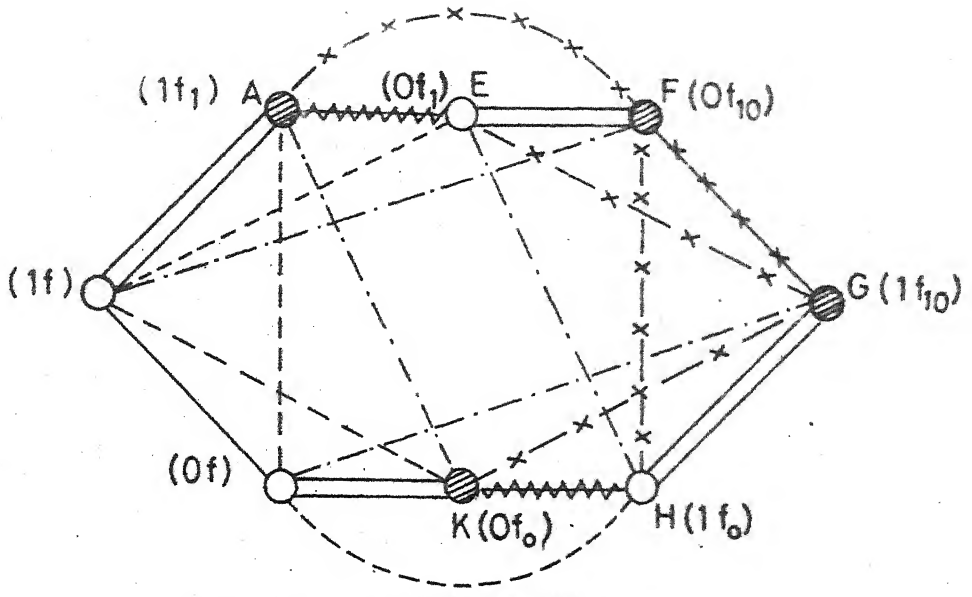

$V_1 = 2CV^{(2)} + C^2 V^{(1)} + V_{BB}$

$V_2 = V^{(2)} + C(1-C)V^{(1)} + V_{BB}$

$V_3 = 2(1-C)V^{(2)} + (1-C)^2 V^{(1)} + V_{BB}$

$\sqrt{C(1-C)}\left[V^{(2)} + (1-C)V^{(1)}\right]$

$\sqrt{C(1-C)}\left[V^{(2)} + CV^{(1)}\right]$

$C(1-C)V^{(1)}$

$\sqrt{C(1-C)}\,e$

$\equiv e_B + Ce$

$\equiv e_B + (1-C)e$

Fig. 3·2a

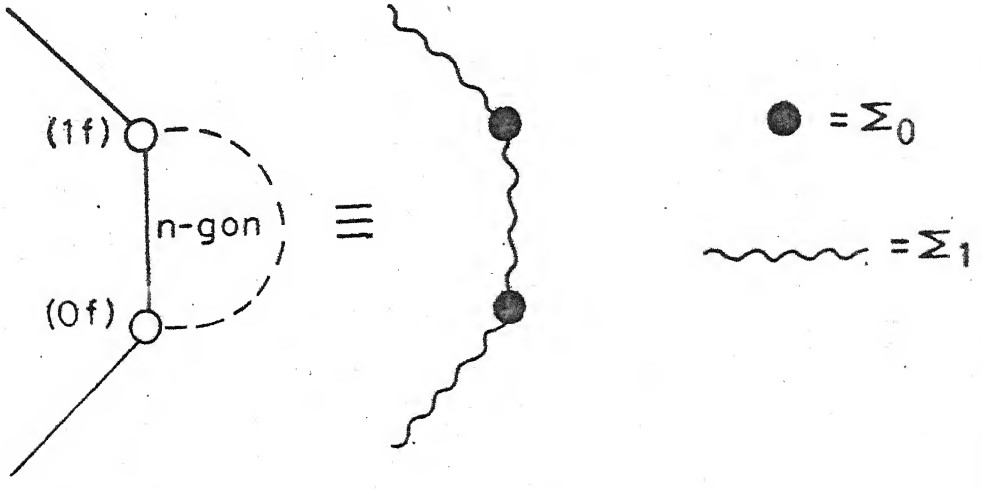

Fig. 3·2b

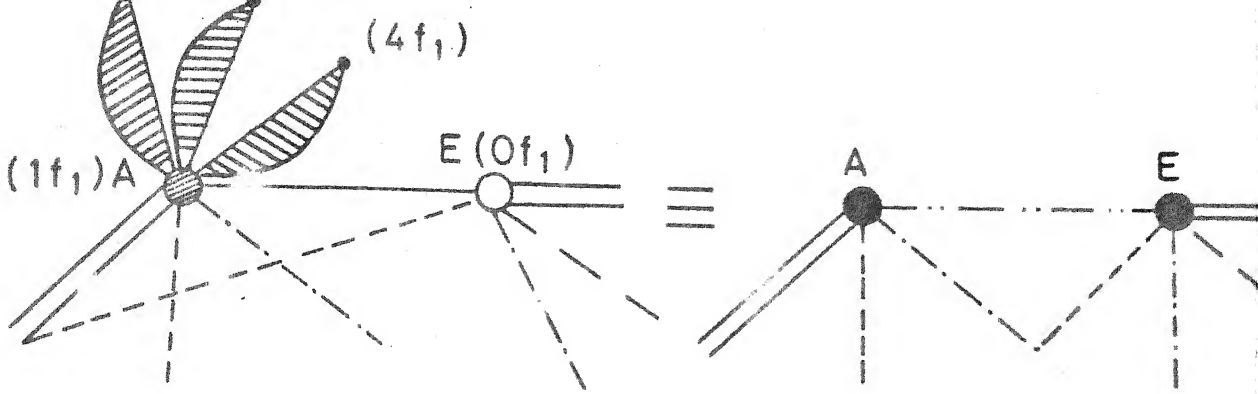

represents an octagonal decoration as in Fig. 3·2a

$= \sigma_0$

$= \sigma_1$

Fig. 3·2c

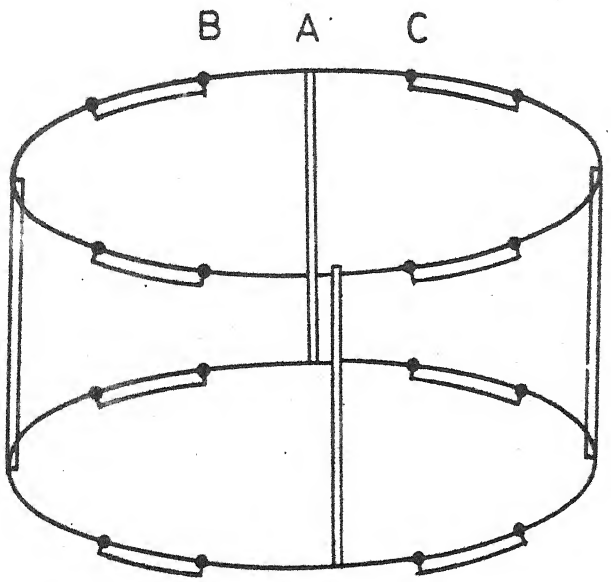

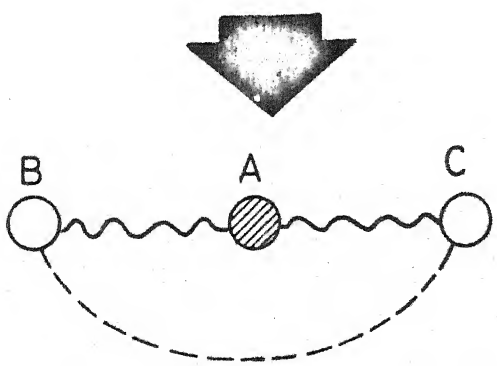

$= \Sigma_0$

$= \Sigma_0'$

$= \Sigma_1$

$= \Sigma_2$

approximation correlated scattering from three or more sites belonging to different bonds is ignored. The final effect is that each bond is renormalized as shown in Fig. 3.2b. This gives rise to a matrix self-energy

$$\underline{\Sigma} = \begin{bmatrix} \Sigma_0 & \Sigma_1 \\ \Sigma_1 & \Sigma_0 \end{bmatrix}$$

The aim is to calculate $\underline{\Sigma}$ self-consistently. It fully describes the self-consistent medium in the 2CPA.

The bond renormalization procedure follows in two steps:

(a) The decorating octagon is not an isolated octagon involving only the two spatial sites (0 and 1). If we look at the vertex A(i.e. $1f_1$ in the notation of Mookerjee 1973), the bond AE ($1f_1$ to $0f_1$) belonging to the octagon is only one of the Z bonds emanating from A to the Z nearest neighbours of 1. The other remaining Z-1 bonds to $2f_1, 3f_1, \ldots$ also hang on to the site A. Moreover these bonds themselves in turn have their own octagons decorating them (Fig.3.2c). Thus the bond AE is itself immersed in a self-consistent medium. The same is true for the bonds FG and HK of the octagon. We may take this into account by saying that the medium renormalizes the bonds AE, FG and HK. Once the renormalization is accounted for, the octagon is effectively isolated. The renormalized vertices $\sigma_0(Z)$ and links $\sigma_1(Z)$ are found as follows. Let us divide the lattice as follows into two

subspaces (1) an unrenormalized bond AE, which we shall call system 1. It has a Hamiltonian $\underline{H}^{(1)} = V_2(\underline{T}_{AE} + \underline{T}_{EA})$. (2) A lattice L, which is the original lattice minus the link AE, and in which all bonds and sites are renormalized by $\underline{\Sigma}$. This has a Hamiltonian

$\underline{H}^{(2)} = \Sigma_o(Z) \sum_{i \neq A,E} \underline{P}_i + \Sigma_1(Z) \sum_{i,j \neq A,E} \underline{T}_{ij}$. (3) A linking Hamiltonian $\underline{H}^{(int)} = \Sigma_1(Z) \sum_i (\underline{T}_{iA} + \underline{T}_{Ai} + \underline{T}_{iE} + \underline{T}_{Ei})$.

If we now use the notation $\underline{X}^{-P_y}$ to denote the inverse of the operator $\underline{X}$ in the subspace y

$$\underline{G}^{(1)} = \underline{P}_1 \underline{G} \underline{P}_1 = [Z\underline{I} - \underline{H}^{(1)} - \underline{H}^{(int)} \underline{G}^{(2)} \underline{H}^{(int)}]^{-} \underline{P}_1 ,$$

where $\underline{G}^{(2)} = [Z\underline{I} - \underline{H}^{(2)}]^{-\underline{P}_2}$

with $\underline{P}_1 + \underline{P}_2 = \underline{I}$. (3.37)

Examination of the eqn. 3.37 immediately indicates that the effect of the rest of the lattice hanging on to the bond AE is to change the Hamiltonian $\underline{H}^{(1)}$ to $\underline{H}^{(1)} + \underline{\sigma}$ where the self-energy $\underline{\sigma}$ is given by

$$\sigma_{AA} = \sigma_{EE} = \sigma_o = \Sigma_1^2(Z) \sum_{k,m \varepsilon \mathcal{N}_A} G^{(2)}_{km}$$

$$\sigma_{AE} = \sigma_{EA} = \sigma_1 = \Sigma_1^2(Z) \sum_{k \varepsilon \mathcal{N}_A} \sum_{m \varepsilon \mathcal{N}_E} G^{(2)}_{km} \qquad (3.38)$$

$\mathcal{N}_A$ denotes a nearest neighbour of A.

(b) Let us now work on the renormalized, isolated octagon.

As before, let us divide the octagon into two subsystems : a bond B (Of,if), the rest of the octagon M.

$$\underline{\tilde{H}}^{B} = \sum\sum_{ij\varepsilon Of,1f} \underline{\tilde{H}}_{ij} \ , \ \underline{\tilde{H}}^{M} = \sum\sum_{ij\neq Of,1f} \underline{\tilde{H}}_{ij}$$

$$\underline{\tilde{H}}^{BM} = \sum_{i\varepsilon B} \sum_{j\varepsilon M} (\underline{\tilde{H}}_{ij} + \underline{\tilde{H}}_{ji}).$$

As before, we have

$$\underline{G}^{B} = \underline{P}_{B} \, \underline{G} \, \underline{P}_{B} = [Z\underline{I} - \underline{\tilde{H}}^{B} - \underline{\tilde{H}}^{BM} \, \underline{G}^{M} \, \underline{\tilde{H}}^{BM}]^{-} \underline{P}_{B}$$

$$\underline{G}^{M} = [Z\underline{I} - \underline{\tilde{H}}^{M}]^{-} \underline{P}_{M} \ .$$

This immediately shows how the octagon renormalizes the bond B. We have

$$\Sigma_{o} = \tilde{H}^{B}_{oo} + \sum_{j\neq O\neq k}\sum \tilde{H}^{BM}_{Oj} \, G^{M}_{jk} \, \tilde{H}^{BM}_{kO}$$

$$\Sigma_{1} = \tilde{H}^{B}_{O1} + \sum_{j\neq O} \sum_{k\neq 1} \tilde{H}^{BM}_{Oj} \, G^{M}_{jk} \, \tilde{H}^{BM}_{kl} \ . \qquad (3.39)$$

Equations (3.38) and (3.39) together provide a self-consistent set of equations for the calculations of the self-energy $\underline{\Sigma}$. The various Green functions involved can be easily calculated on a three-dimensional lattice using the recursion technique of Haydock et al. In the case when we are using energy dependent effective Hamiltonians, the recursion has to be done separately for each value of energy.

The cluster generalization to arbitrary large clusters now follows exactly the same philosophy. Equations (3.38) and

(3.39) remain the same. The only modification is the augmented space unit. For example, in the 3CPA the augmented space unit is the 24-gon (Fig. 3.2d) (Mookerjee 1973) and

$$\underline{\Sigma} = \begin{bmatrix} \Sigma_o & \Sigma_1 & \Sigma_1 \\ \Sigma_1 & \Sigma_o' & \Sigma_2 \\ \Sigma_1 & \Sigma_2 & \Sigma_o' \end{bmatrix}$$

This has four independent components, but note that both (3.38) and (3.39) for this case also yield four equations:

$$\begin{aligned}
\Sigma_o &= \Sigma_{AA} = H^B_{AA} + \sum_{km} H^{BM}_{Ak} G^M_{km} H^{BM}_{mA} \\
\Sigma_o' &= \Sigma_{BB} = H^B_{BB} + \sum_{km} H^{BM}_{Bk} G^M_{km} H^{BM}_{mB} \\
\Sigma_1 &= \Sigma_{AB} = H^B_{AB} + \sum_{km} H^{BM}_{Ak} G^M_{km} H^{BM}_{mB} \\
\Sigma_2 &= \Sigma_{BC} = H^B_{BC} + \sum_{km} H^{BM}_{Bk} G^M_{km} H^{BM}_{mC}
\end{aligned} \qquad (3.40)$$

we shall be interested in the diamond lattice, where the nearest neighbour cluster consists of 5 sites. Here the decorating lattice is a 160-gon (Mookerjee 1974) and the self energy is still four independent members

$$\underline{\Sigma} = \begin{bmatrix} \Sigma_o & \Sigma_1 & \Sigma_1 & \Sigma_1 & \Sigma_1 \\ \Sigma_1 & \Sigma_o' & \Sigma_2 & \Sigma_2 & \Sigma_2 \\ \Sigma_1 & \Sigma_2 & \Sigma_o' & \Sigma_2 & \Sigma_2 \\ \Sigma_1 & \Sigma_2 & \Sigma_2 & \Sigma_o' & \Sigma_2 \\ \Sigma_1 & \Sigma_2 & \Sigma_2 & \Sigma_2 & \Sigma_o \end{bmatrix}$$

As the cluster size increases, the augmented space graph itself becomes large and the augmented space unit which renormalizes the cluster also becomes large. For clusters of size N, this unit is a $(N \times 2^N)$-gon. However, the number of independent members in $\underline{\Sigma}$ still remains relatively small, and the $\underline{G}^M$ can be calculated by the recursion method with great facility even on quite large augmented space units. This fortunate marriage of the above method with the recursion technique reduces the calculation of quite large CCPAs to a tractable problem .

The self-energy $\underline{\Sigma}$, hence the CCPA is cluster diagonal a property essential to preserve Herglotzicity (Butler 1973) The effective Hamiltonian is invariant with respect to cluster translations. However the exact effective Hamiltonian is translationally invariant. In contrast in the CCPA's the self-energy at the cluster-centre and cluster-periphery are indeed different. Unless it is possible to construct clusters in which all the sites are equivalent (as in the 2CPA) this distinction is unavoidable and inherent in any cluster-approximation (Tsukada 1972).

The self-consistent equations (3.38) and (3.39) involve an iterative solution for $\underline{\Sigma}$. We could, for example start with $\underline{\Sigma}_o^o(Z) = \Sigma_{CPA}$, $\Sigma_1^o(Z) = V\text{-in}$, use (3.38) to generate $\underline{\sigma}$, then (3.39) to get $\underline{\Sigma}$ and iterate the procedure. This method will be useful only if this procedure converges. The

calculations were carried out on diamond and b.c.c. lattices with one electron per site and off-diagonal disorder. The procedure converged rapidly, except near band edges, where the convergence is not rapid but nevertheless no more than a hundred iterations were required in any case. The results are discussed in the following section.

(3.5) Results and Discussion

(a) Diamond Lattice

In this section we shall present results for the density of states for a single s-orbital per site model on a diamond lattice. In order to compare our generalisation to the self-consistent cluster CPA with previous 1CPA calculations, we first present these 1CPA results in fig. 3.3.

Figure 3.3a shows the 1CPA density of states per site in units of π^{-1} (-imaginary part of Green's function) for a dilute 90-10 alloy with small and large separations of the well depths of the constituents. As expected, the latter case shows an impurity band. The characteristic feature of the 1CPA is the lack of structure, particularly in the impurity band. The two-peaked structure in the majority band is characteristic of the diamond lattice and not a feature of disorder. Computer experiments, however, indicate peaks in the impurity band associated with clusters. Figure 3.3b presents 1CPA results for a concentrated 50-50 alloy

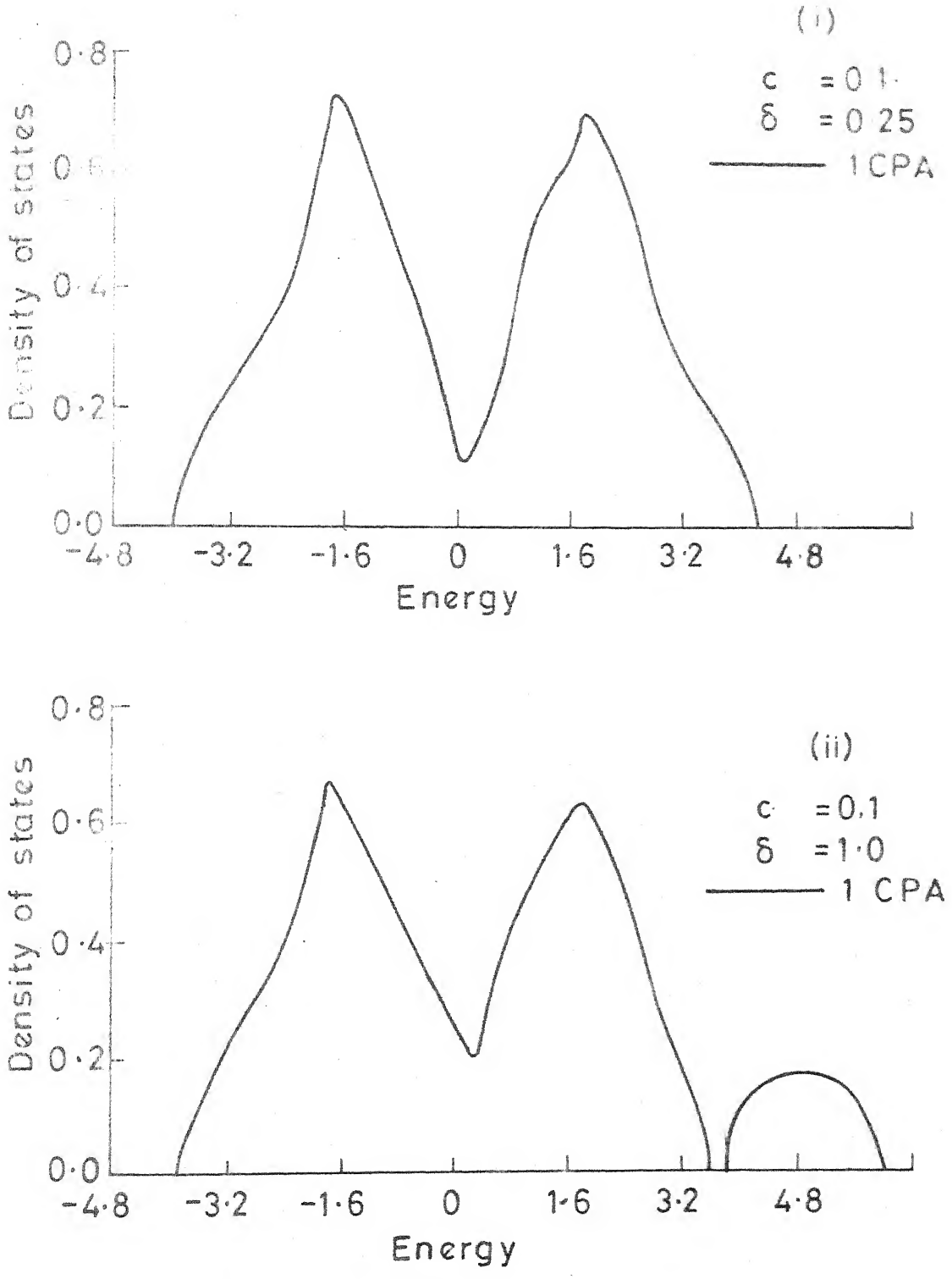
(i)
c = 0 1·
δ = 0 25
1 CPA
Density of states
0·8
0·4
0·2
0·0
-4·8
-3·2
-1·6
0
1·6
3·2
4·8
Energy
(ii)
c = 0.1
δ = 1·0
1 CPA
Density of states
0·8
0·6
0·4
0·2
0·0
-4·8
-3·2
-1·6
0
1·6
3·2
4·8
Energy

Fig. 3·3a

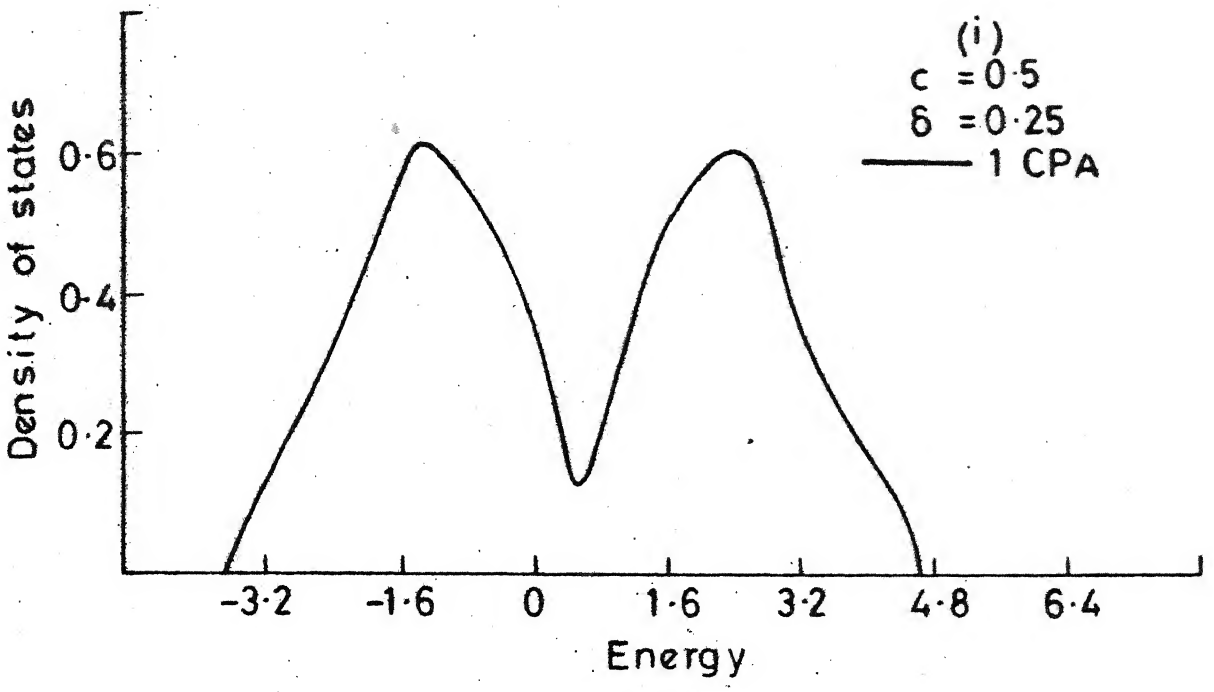
(i)
c = 0·5
δ = 0·25
1 CPA
Density of states
0·6
0·4
0·2
-3·2
-1·6
0
1·6
3·2
4·8
6·4
Energy

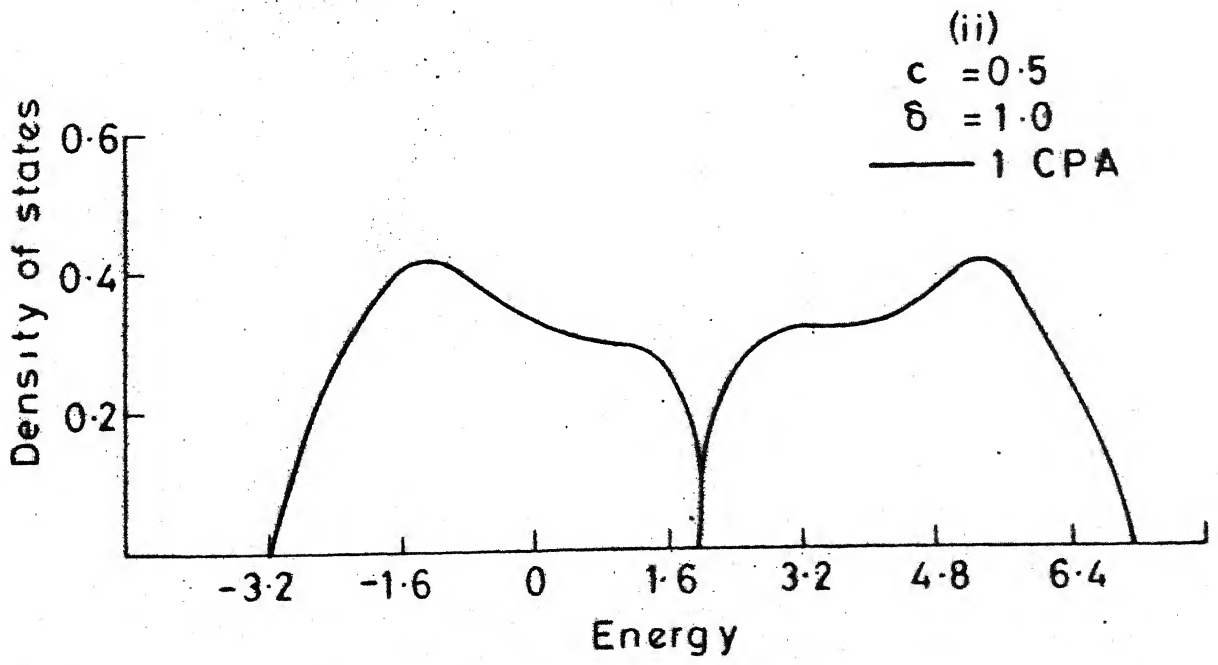
(ii)
c = 0·5
δ = 1·0
1 CPA
Density of states
0·6
0·4
0·2
-3·2
-1·6
0
1·6
3·2
4·8
6·4
Energy

Fig. 3·3b

with small and large separations of the well depths. Again the 1CPA exhibits a lack of structures other than those arising from the ordered diamond lattice. The Van Hove peaks of the ordered lattice are rounded due to disorder. These four 1CPA results will form a background against which we shall compare our cluster-CPA results, to ascertain the effects of clustering and off-diagonal disorder.

As mentioned in the previous section, the self-energy self-consistent equations are practically useful only if the iterative procedure converges. Fortunately, for all the subsequent cases not only did the precedure converge but, except for the edges of impurity bands, the convergence was rapid. In the exceptional cases the number of iterations required was large but tractable. For the sake of illustration, the self-consistent $\Sigma_o(E)$ and $\Sigma_1(E)$ for the alloy later illustrated in fig. 3.6a are presented in fig. 3.4. The effect of clustering is apparent in $\Sigma_o(E)$ which has considerable structure compared with the smooth $\Sigma_o(E)$ characteristic of the 1CPA. The effect of off-diagonal disorder and clustering is strikingly displayed in its effect on $\Sigma_1(E)$. In the 1CPA $\Sigma_1(E)$ is a real constant and is the average value of the overlap parameter $\bar{V} = c^2V_{AA}+(1-c)^2V_{BB}+ 2c(1-c)V_{AB}$, whereas in the cluster generalisation it is a complex function of the energy and has considerable structure.

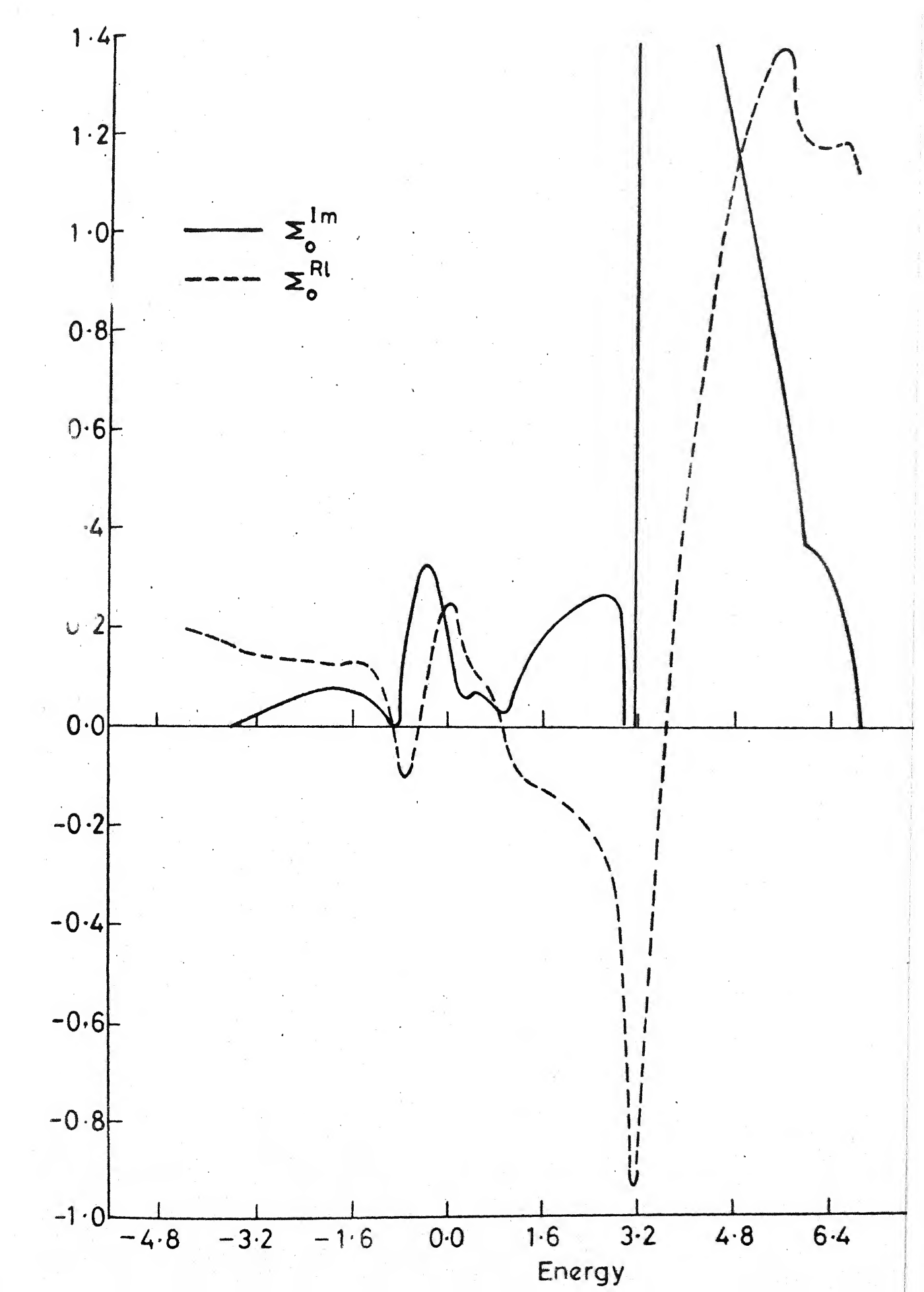
1·4
1·2
1·0
0·8
0·6
·4
0·0
-0·2
-0·4
-0·6
-0·8
-1·0
M_o^{Im}
M_o^{Rl}
−4·8
−3·2
−1·6
0·0
1·6
3·2
4·8
6·4
Energy

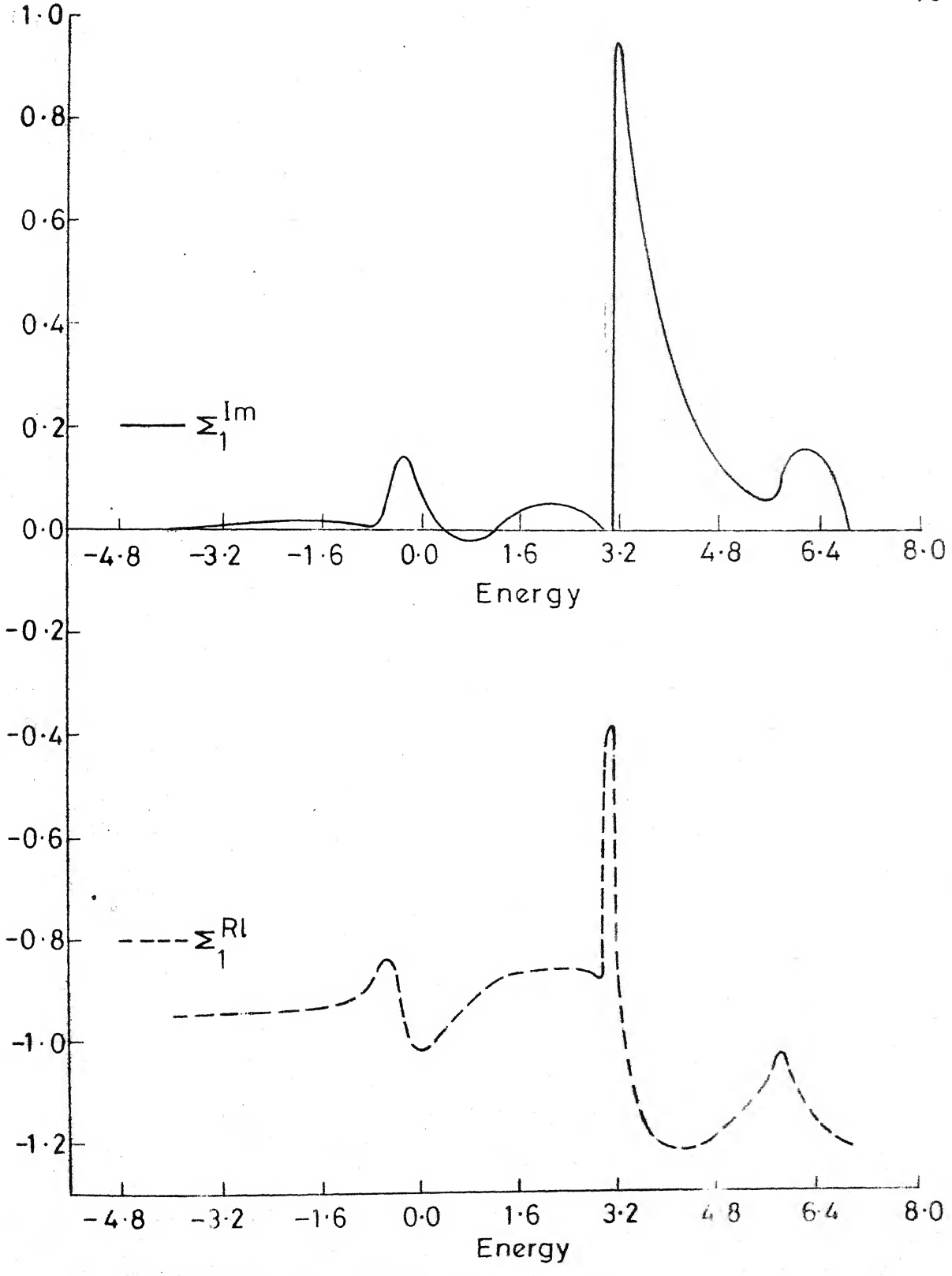
1·0
0·8
0·6
0·4
0·2
0·0
Σ_1^{Im}
-4·8
-3·2
-1·6
0·0
1·6
3·2
4·8
6·4
8·0
Energy
-0·2
-0·4
-0·6
-0·8
-1·0
-1·2
Σ_1^{Rl}
-4·8
-3·2
-1·6
0·0
1·6
3·2
4·8
6·4
8·0
Energy

Fig. 3·4b

The first set of results illustrated in fig. 3.5 considers only diagonal disorder in order that we may examine the effects of statistical clustering alone.

Figure 3.5a shows the density of states per site in units of π^{-1} for a concentrated 50-50 alloy with small separation ($\delta = 0.5$). Only half the density of states is shown as it is symmetric around the band centre. We first note that in this 'weak' scattering regime clusters do not introduce much structure. The bond and cluster CPAS are very similar. Some structure is seen in the cluster CPAS and is in good agreement with the results of Mookerjee (1975b) which were not self-consistent. Secondly, the density of states near the band centre actually increases as we go from 1CPA to CCPA, indicating that clusters inhibit band separation For 1CPA $\delta = 1$ is sufficient to separate the two bands, while for the CCPA $\delta > 1$. This is also indicated by the moment method of Desjonqueres and Cyrot-Lackmann (1978) and the self-consistent boundary site approximation of Kumar and Joshi (1978).

Figure 3.5b shows a 50-50 alloy with large separation ($\delta = 1$). There is now greater structure in the CCPA results. The characteristic peak due to states localised on isolated A atoms and two satellite humps due to states localised on bonding and antibonding states on AB pairs show up. These results are in good agreement with earlier work of Mookerjee (1975) and various boundary site approximations (Kumar et al 1975

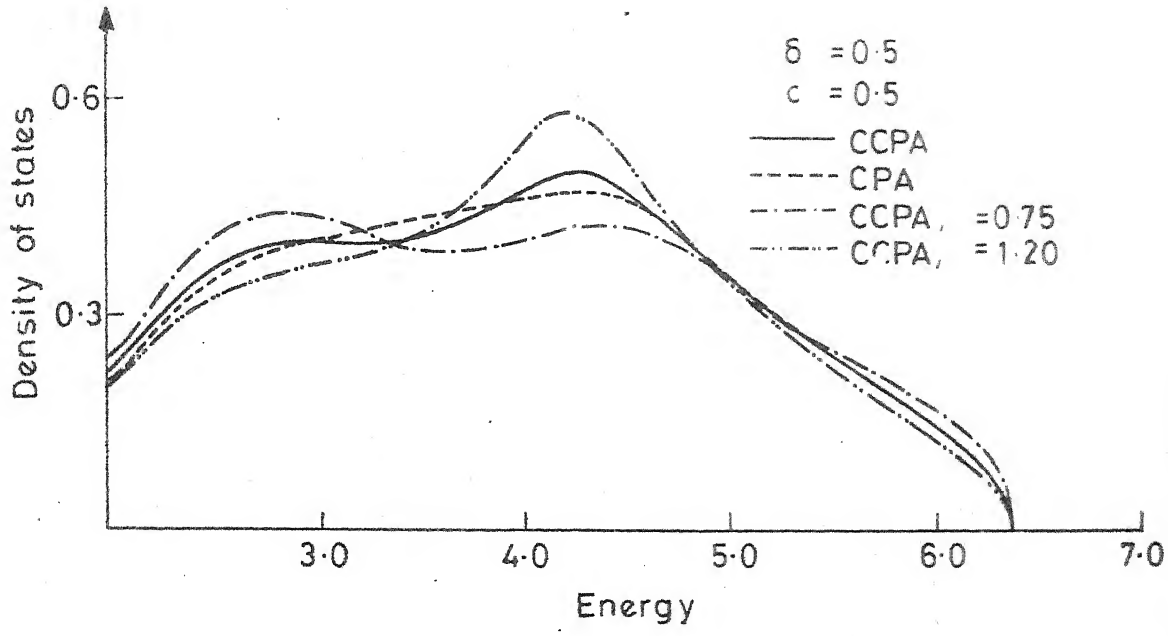

Fig. 3·5a

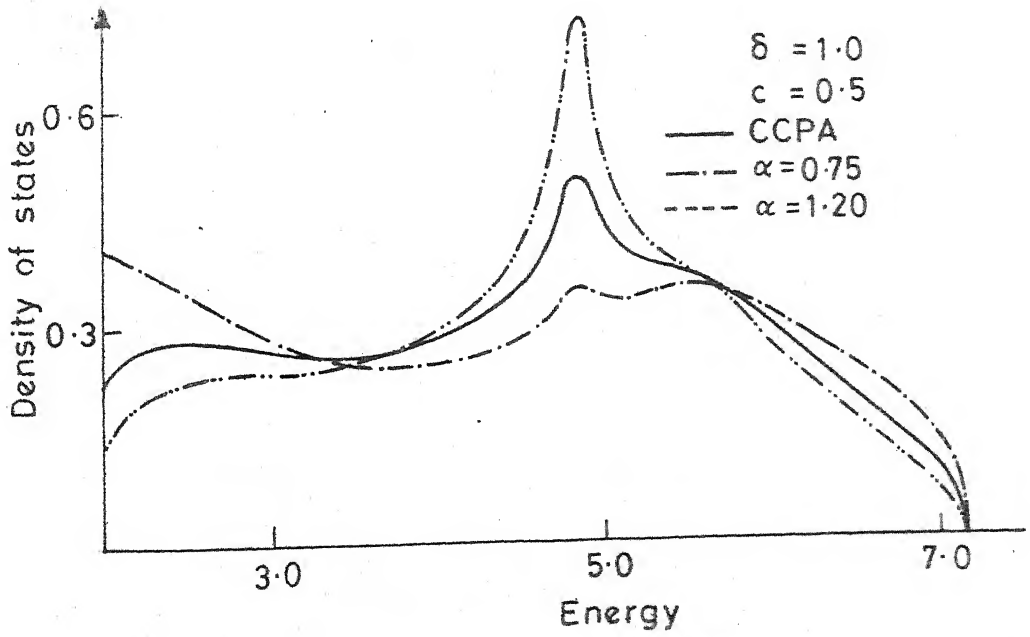

Fig. 3·5b

Kumar and Joshi 1978). The self-consistent central-site approximation of Brouers et al (1973) suffers from violation of herglotzicity at E = 2.25, leading to unphysical discontinuity of the density of states at that energy. There is no band separation in the CCPA.

Figure 3.5c shows results for the 50-50 alloy with a still larger separation ($\delta = 2$). The features described above show up even more clearly. Further, even in the CCPA there is now an unambiguous separation of the bands leading to a gap at the band centre.

Figure 3.5d shows a dilute alloy (90-10) with large separation ($\delta = 1$). This is the 'strong scattering' regime. The majority band is not much different from the pure host with the twin rounded peaks of the diamond lattice. The impurity band, however, shows considerable structure compared with the 1CPA. The three-peaked structure mentioned earlier is now even more prominent. For these parameter regimes the boundary site approximations start to show violation of herglotzicity. For $\delta = 2$, for example, around E = 3.2 and between 3.46 and 3.48 branch cuts appear off the real axis. This immediately restricts the use of these approximations precisely in those regimes of strong scattering where clustering has considerable effect. However, because of the graphical methodology and recursion techniques used in our work, herglotzicity is assured in our results for all energies and disorders.

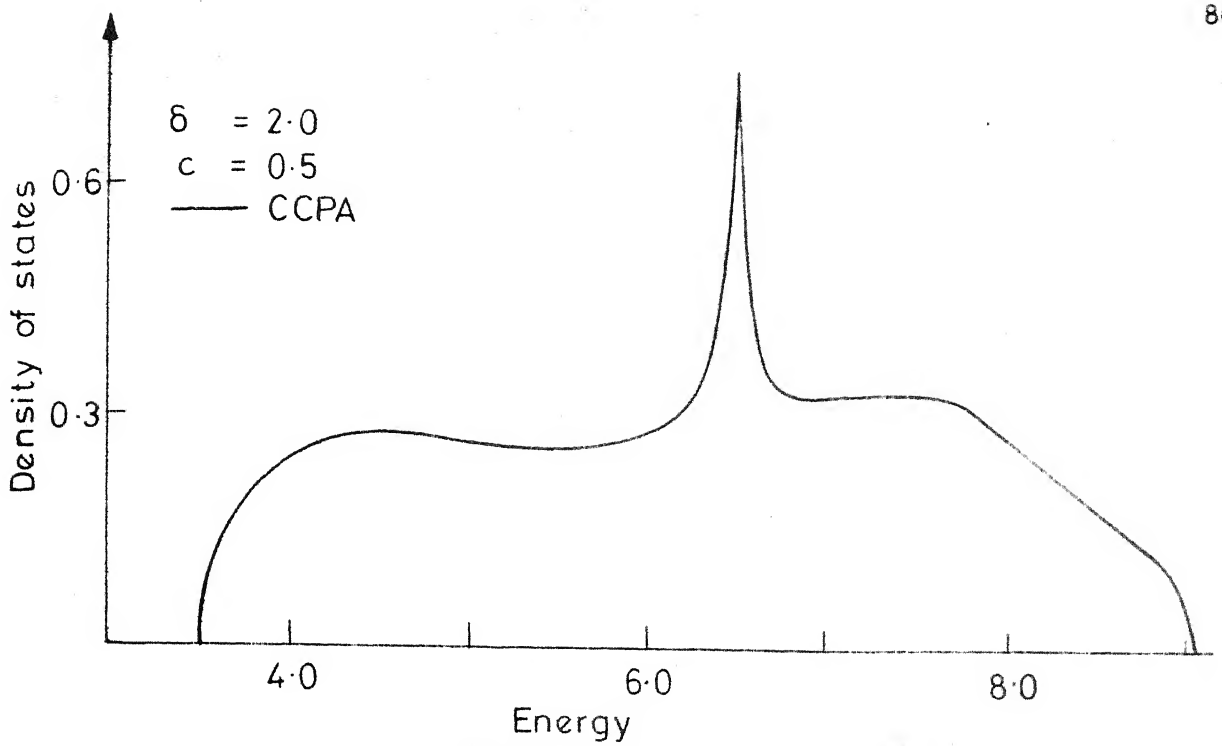

Fig. 3·5c

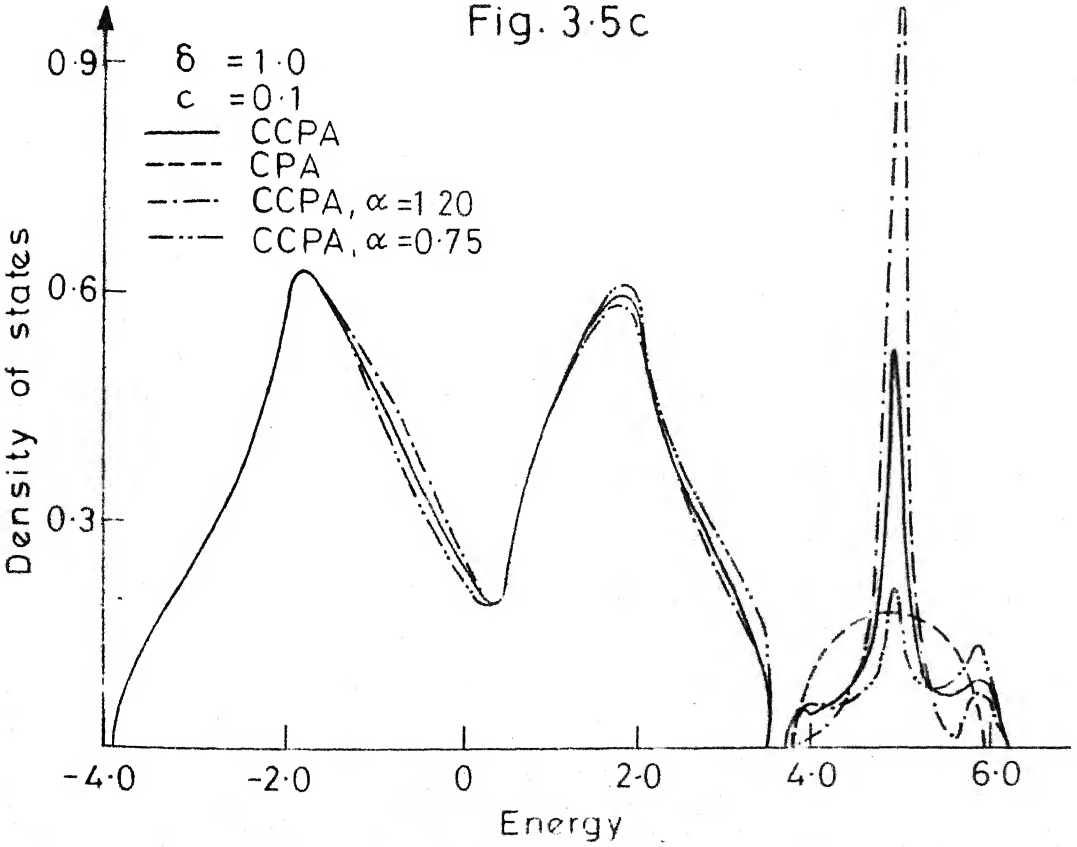

Fig. 3·5d

Fig. 3.5d also shows the effect of Markovian short-range order of the type described in the earlier section and characterised by a parameter α. $\alpha < 1$ enhances the probability of precipitation of A clusters in a B background. This is clearly exhibited by the enhancement of satellite hump due to isolated A clusters. $\alpha > 1$ enhances AB type pairs with a consequent rise in the central peak structure due to such pairs.

The next set of results introduces off-diagonal disorder in the overlap parameters. For any realistic model of an alloy it is ultimately essential to introduce off-diagonal disorder. It is interesting to note that most previous tractable CPAS involving off-diagonal disorder necessitated V_{AB} to be either the arithmetic or the geometric mean of V_{AA} and V_{BB}. This is an unnecessary restriction and ignores the effect of chemical affinites in bonding. Our formalism, on the other hand, has no such restriction. To start with we shall take V_{AB} to be the arithmetic mean of V_{AA} and V_{BB}, so that we may compare with existing results but subsequently we shall also present results when this is not so.

Fig.3.6a shows dilute (90-10) alloy with a large separation ($\delta = 1$) and off-diagonal disorder $V_{BB} = -1.0$, $V_{AA} = -2.0$ and $V_{AB} = -1.5$. These results are to be compared with fig.3.5d. Note first that because of the larger values of V_{AA} and V_{AB} the band is wider. The majority band resembles that of the host.

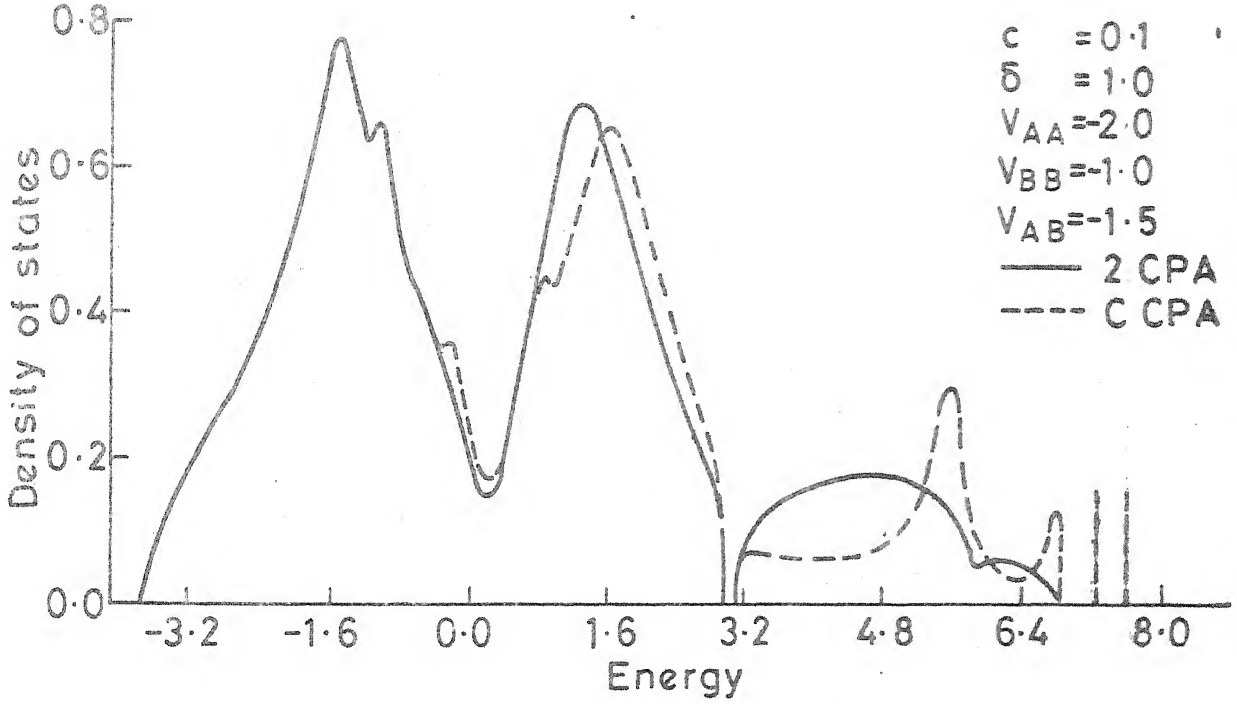
0·8
0·6
0·4
0·2
0·0
Density of states
-3·2
-1·6
0·0
1·6
3·2
4·8
6·4
8·0
Energy
c =0·1
δ =1·0
V_{AA}=-2·0
V_{BB}=-1·0
V_{AB}=-1·5
2 CPA
C CPA

Fig. 3·6a

The structure near the lower Van-Hove peak seems to be a feature of off-diagonal disorder and is also present in cases when δ is small (fig. 3.8). The striking new feature is the structure in the impurity band. Not only is the impurity band wider (as a consequence of larger overlaps between impurity and host and impurity and impurity), but there is a structure in the impurity band.

In order to analyse the origin of these structures, and to make sure that these structures do not arise due to spurious numerical errors, we shall examine the partial densities of states of specific cluster configurations embedded in the CCPA medium, as well as the corresponding eigenenergies of these isolated clusters. These details will unambiguously identify the origin of the structures in the impurity band. The exercise is of importance since we have no completely reliable self-consistent CCPA results in this regime to compare our results with, certainly none with off-diagonal disorder.

The configuration of the cluster corresponding to a given partial density of states in the impurity band is displayed alongside in fig. 3.6b. It is evident from figure 3.6b(i)-(vi) that the band between $E \simeq 3.20$ and $E \simeq 5.60$ is due to clusters of either host surrounded with impurities or vice-versa. Its width is associated with V_{AB}. On the other hand fig. 3.6b (vii)-(x) the band above $E \simeq 5.60$ and stretching up

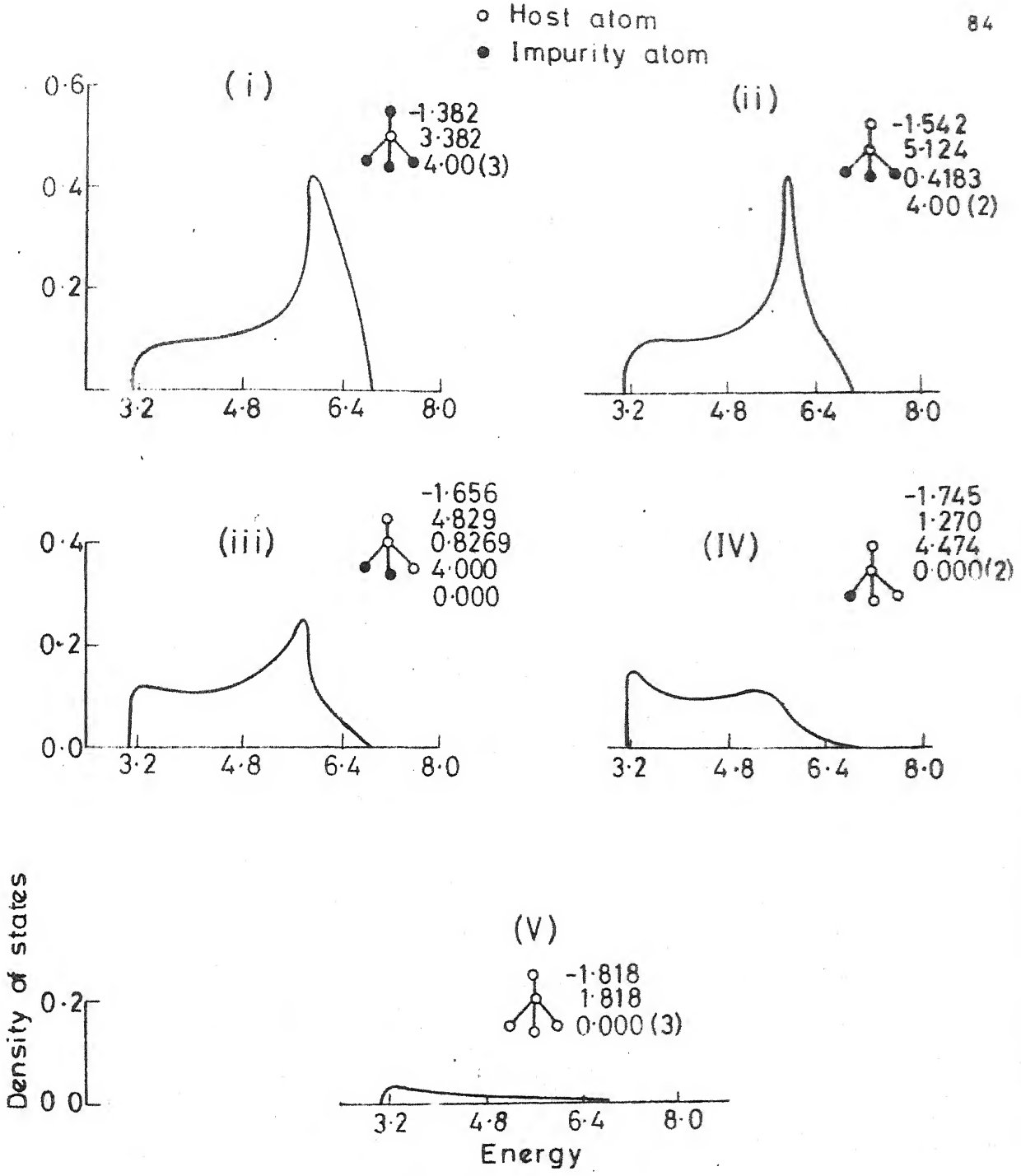
o Host atom
• Impurity atom
(i)
-1·382
3·382
4·00(3)
(ii)
-1·542
5·124
0·4183
4·00(2)
(iii)
-1·656
4·829
0·8269
4·000
0·000
(IV)
-1·745
1·270
4·474
0·000(2)
(V)
-1·818
1·818
0·000(3)
Density of states
Energy
3·2
4·8
6·4
8·0

Fig. 3·6b (i-v)

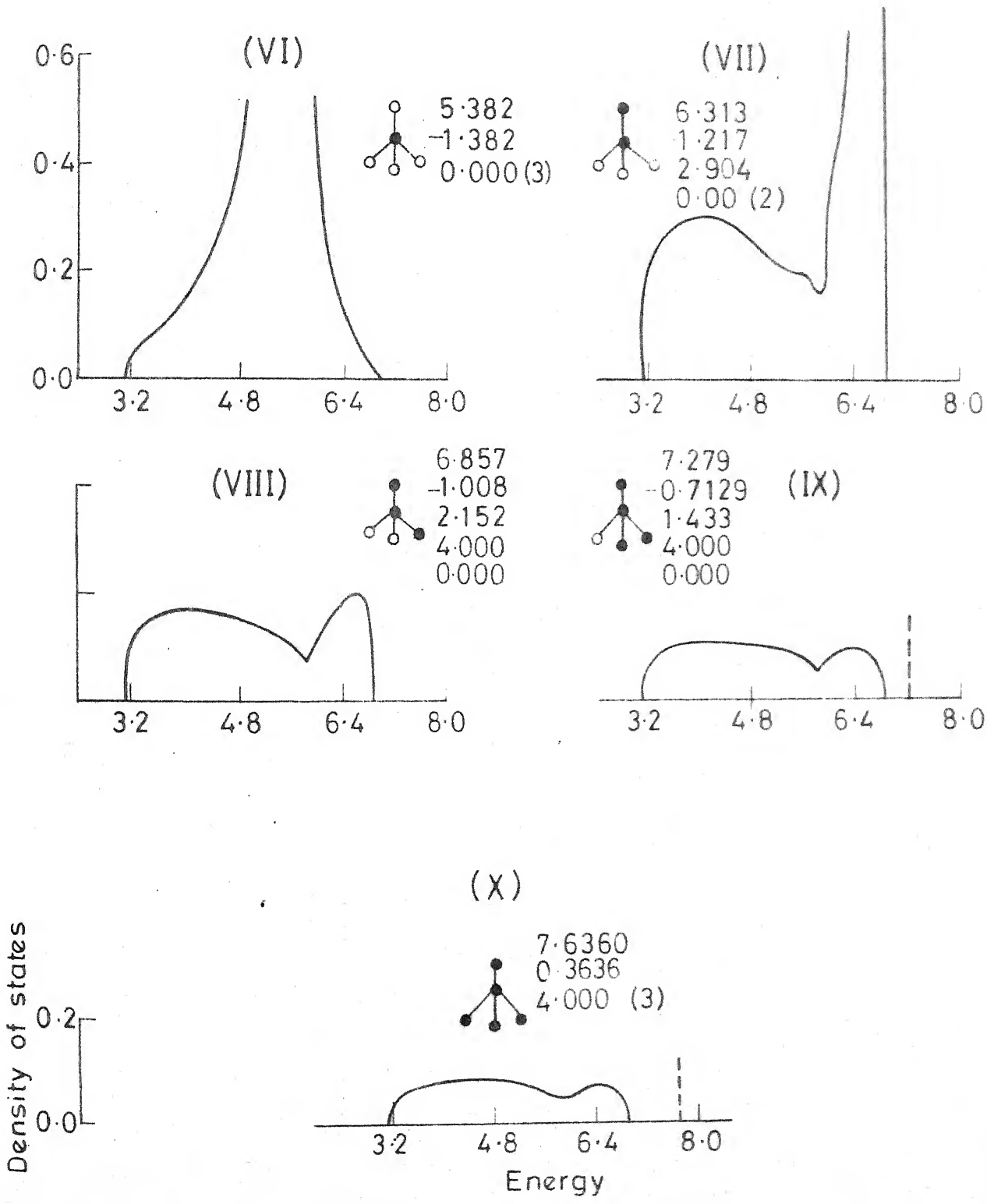
(VI)
5·382
−1·382
0·000 (3)
0·6
0·4
0·2
0·0
3·2
4·8
6·4
8·0
(VII)
6·313
1·217
2·904
0·00 (2)
3·2
4·8
6·4
8·0
(VIII)
6·857
−1·008
2·152
4·000
0·000
3·2
4·8
6·4
8·0
7·279
−0·7129
(IX)
1·433
4·000
0·000
3·2
4·8
6·4
8·0
(X)
7·6360
0·3636
4·000 (3)
Density of states
0·2
0·0
3·2
4·8
6·4
8·0
Energy

Fig 3·6b (VI – X)

to $E = 6.88$ is essentially due to clustering of impurities. Its width is related to V_{AA}. The isolated cluster eigenenergies also confirm this view point. This is a specific feature of off-diagonal disorder clustering and cannot be expected to be reproduced in any 1CPA in which the distinct effects of V_{AA}, V_{AB} and V_{BB} cannot show up. The small peak at $E = 6.80$ is seen as due to isolated impurities, while the bigger peak around $E = 5.60$ arises due to clusters in which the host atom is surrounded with impurities. These are to be compared with the central peak and satellite humps in the impurity band of fig. 3.5d (without off-diagonal disorder). The peak in the upper impurity band is due to large clusters of impurities (fig. 3.6b (vii)-(x)). This peak is small because the probability of such clusters is also small.

Two isolated cluster eigenvalues at $E = 7.279$ and $E = 7.636$ lie outside the CCPA impurity band (shown by broken vertical lines in fig (3.6a)). These arise from the cluster of the type shown in fig. 3.6b (ix)-(x). A self-consistent larger cluster theory would eventually include these in the tail. Such isolated structures were also seen by Kumar and Joshi (1978).

Figure 3.6c shows the effect of Markovian short-range order. As before $\alpha < 1$ diminishes the probability of unlike pairs. As a result, for $\alpha = 0.75$, the impurity peak due to

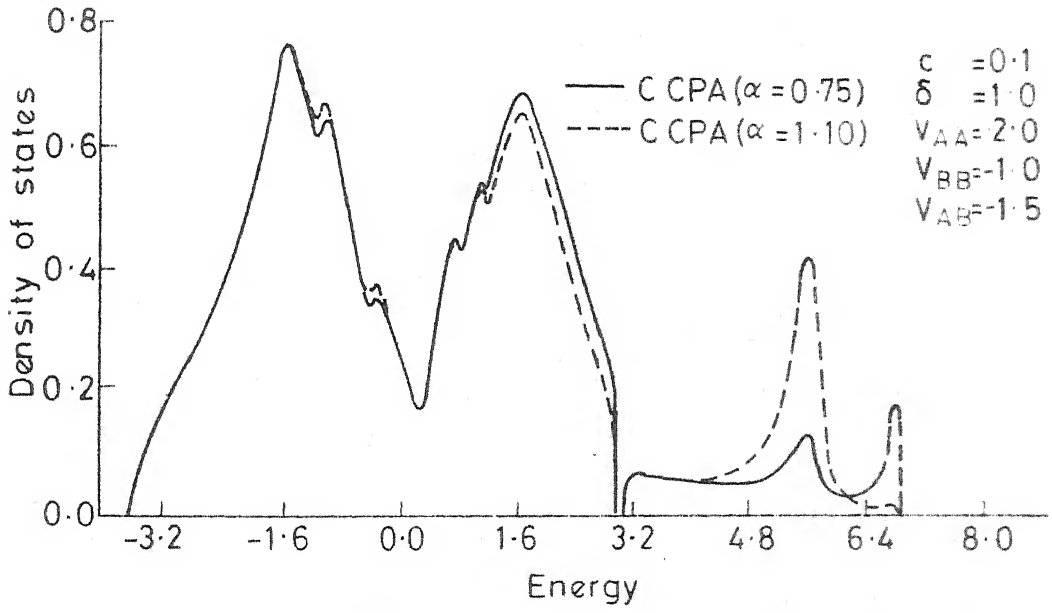
0·8
0·6
0·4
0·2
0·0
Density of states
C CPA (α = 0·75)
C CPA (α = 1·10)
c =0·1
δ =1·0
V_{AA}= 2·0
V_{BB}=-1·0
V_{AB}=-1·5
-3·2
-1·6
0·0
1·6
3·2
4·8
6·4
8·0
Energy

Fig. 3·6c

isolated A surrounded with B diminishes considerably. On the other hand $\alpha > 1$ increases the probability of precipitating clusters with unlike atoms, thus increasing the corresponding impurity peak. This effect shows up in all cases illustrated in these figures.

The partial densities of states and the short-range order effects serve to identify the origin of the structures seen in the impurity band.

Figure 3.7 shows the density of states of a dilute 90-10 alloy with off-diagonal disorder, but with a much weaker V_{AB} bonding. The qualitative features of the alloy in fig. 3.6a are retained. However, it is illustrative to note that since the overlap V_{AB} is weak, the peak due to impurity surrounded by host is not broadened, but remains a δ-function-like spike around $E = 4.3$.

In all the foregoing cases both 2CPA and the 5CPA curves are indicated. As expected, in all cases the 5CPA shows more structure than the 2CPA.

Fig. 3.8a shows a dilute 90-10 alloy with small separation. Apart from the structure near the lower Van Hove peak there are no striking features. Neither is there much difference between the 2CPA and 5CPA. This is to be expected in this 'weak scattering' regime.

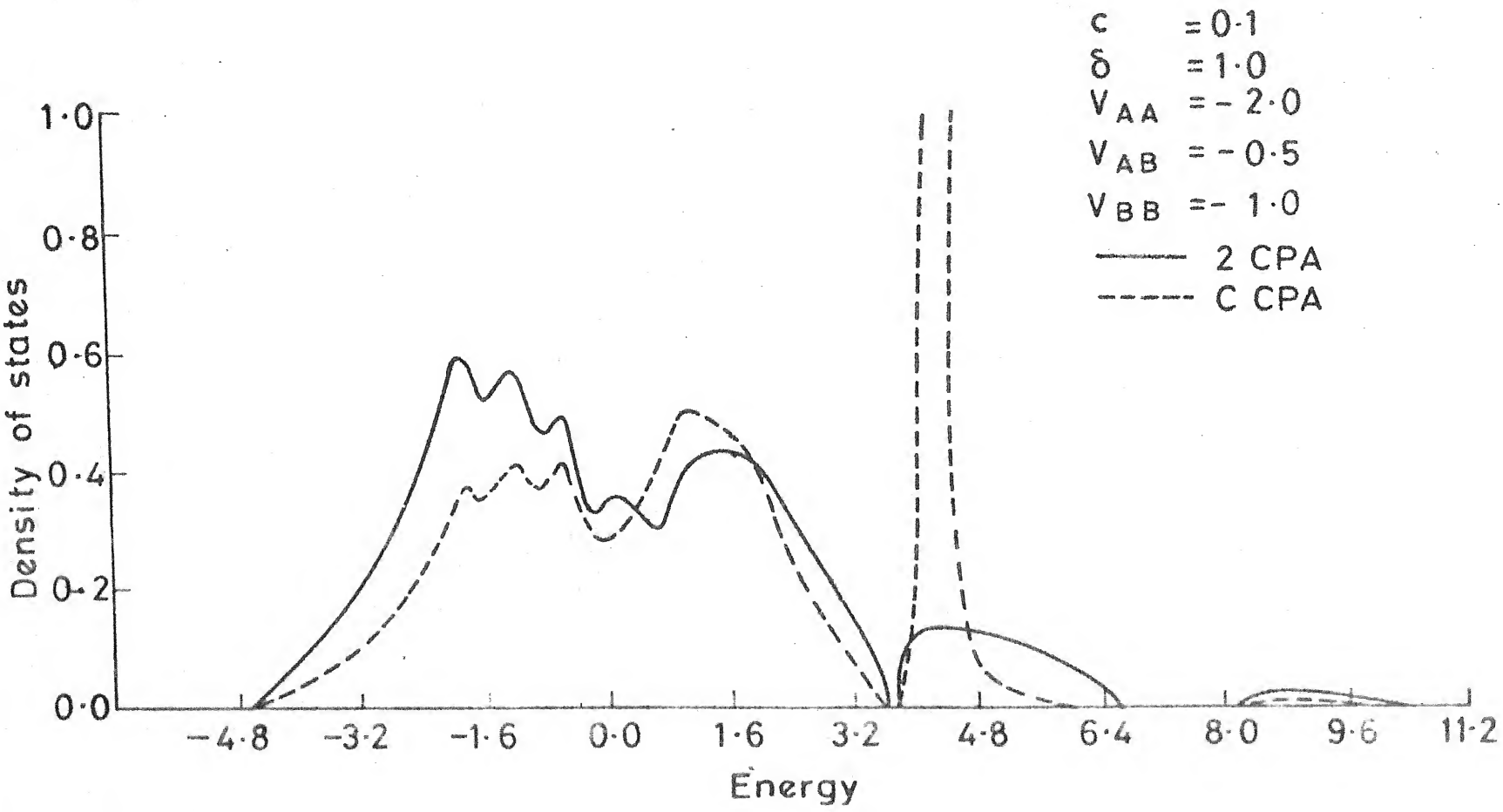
c = 0·1
δ = 1·0
V_{AA} = − 2·0
V_{AB} = − 0·5
V_{BB} = − 1·0
2 CPA
C CPA
Density of states
1·0
0·8
0·6
0·4
0·2
0·0
−4·8
−3·2
−1·6
0·0
1·6
3·2
4·8
6·4
8·0
9·6
11·2
Energy

Fig. 3·7

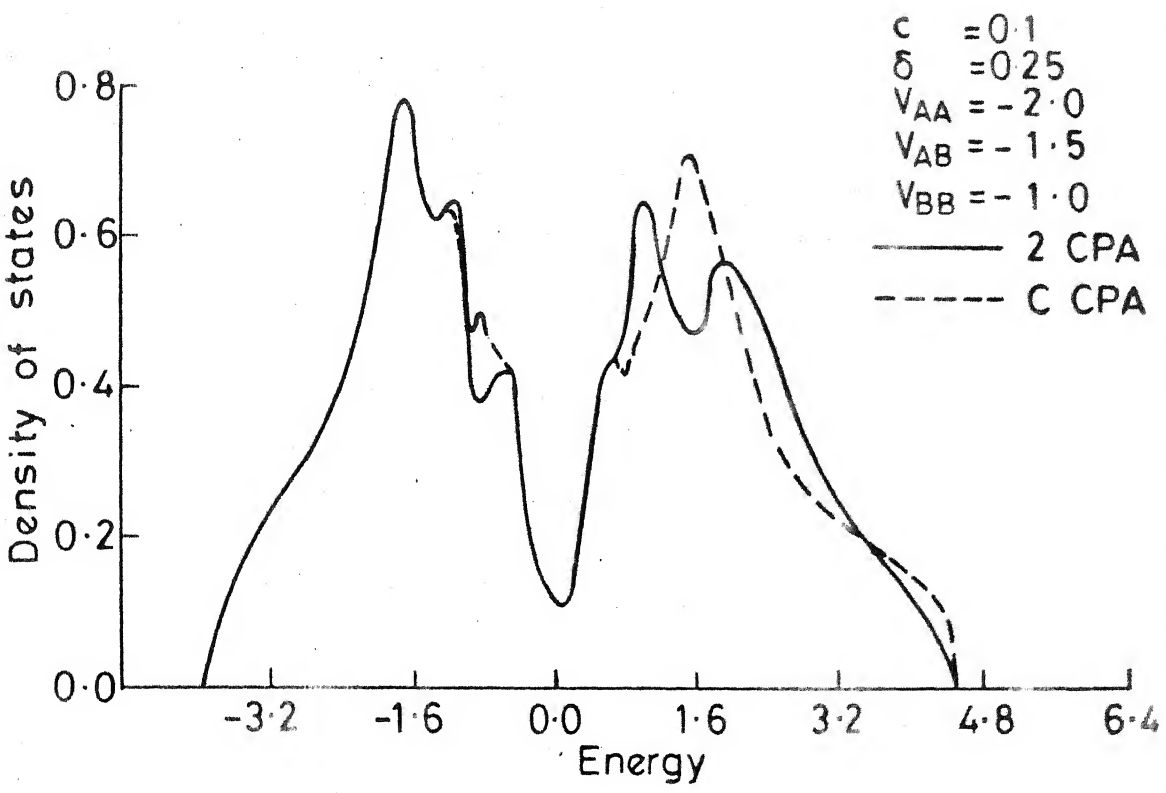

Fig. 3·8 a

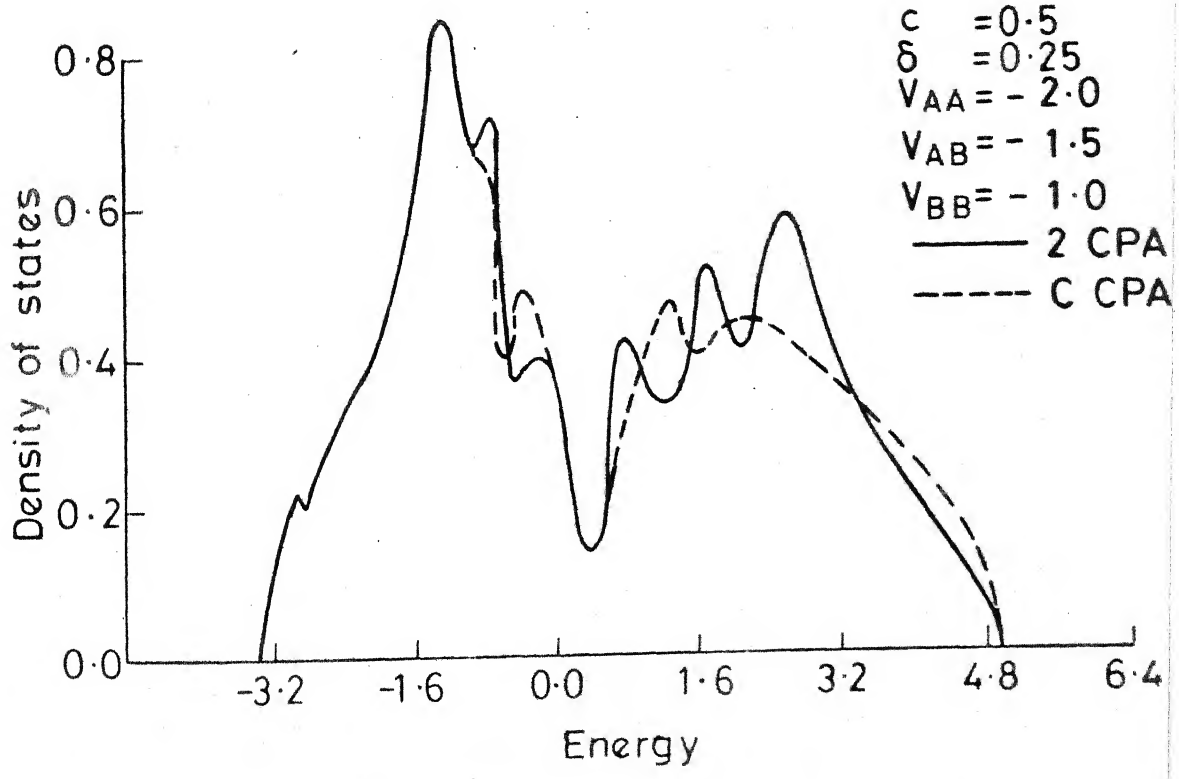

Fig. 3·8 b

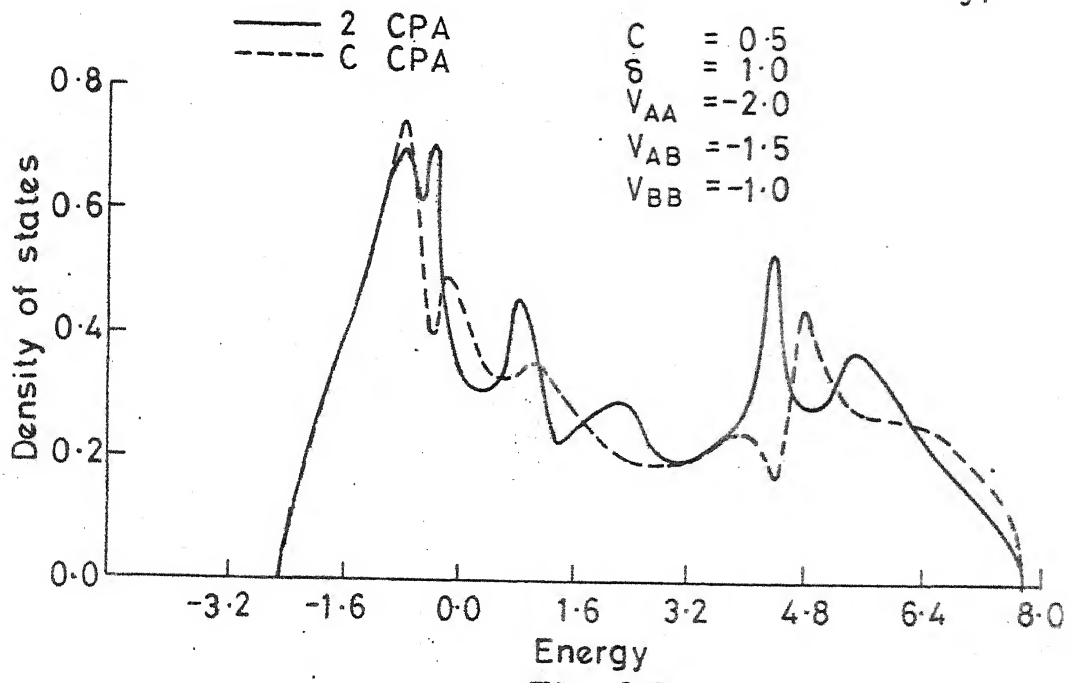

Fig. 3·9a

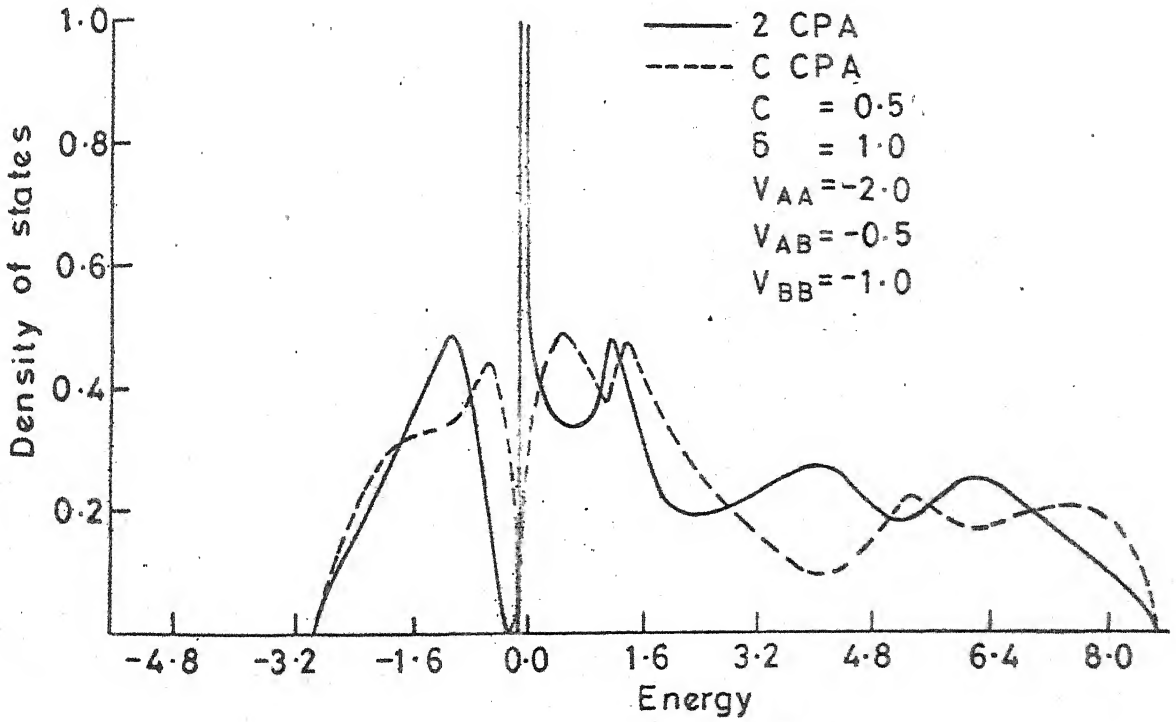

Fig. 3·9b

Figure 3.8b shows a concentrated 50-50 alloy with small separation. This is to be compared with fig. 3.5a. Unlike the case of purely diagonal disorder the density of states is not symmetric around the band centre. This is due to the different bandwidth of the host and impurity.

Finally, in figure 3.9 we have the last situation of a concentrated alloy (50-50) with large separations and different off-diagonal disorders. There is no symmetry around the band centres and there is a structure in the impurity band.

(b) B.C.C. Lattice

In this section we shall present the results for the density of states for a single s-orbital per site model on a b.c.c. lattice. The aim is a subsequent study of b.c.c. sd-metallic alloys like β-brass. These b.c.c. metallic alloys provide six sd^5 orbitals per site. Although, we have considered here only one orbital per site the generalisation to several orbitals per site is straight forward.

Figure 3.10 shows the 1CPA, 2CPA and CCPA density of states per site in the units of π^{-1} for a dilute 90-10 alloy with $\delta = 0.75$. In 1CPA there is no separate impurity band but in 2CPA and CCPA we observe a separate two peaked impurity band. Also there is an increase in the band-width from 1CPA to 2CPA and CCPA.

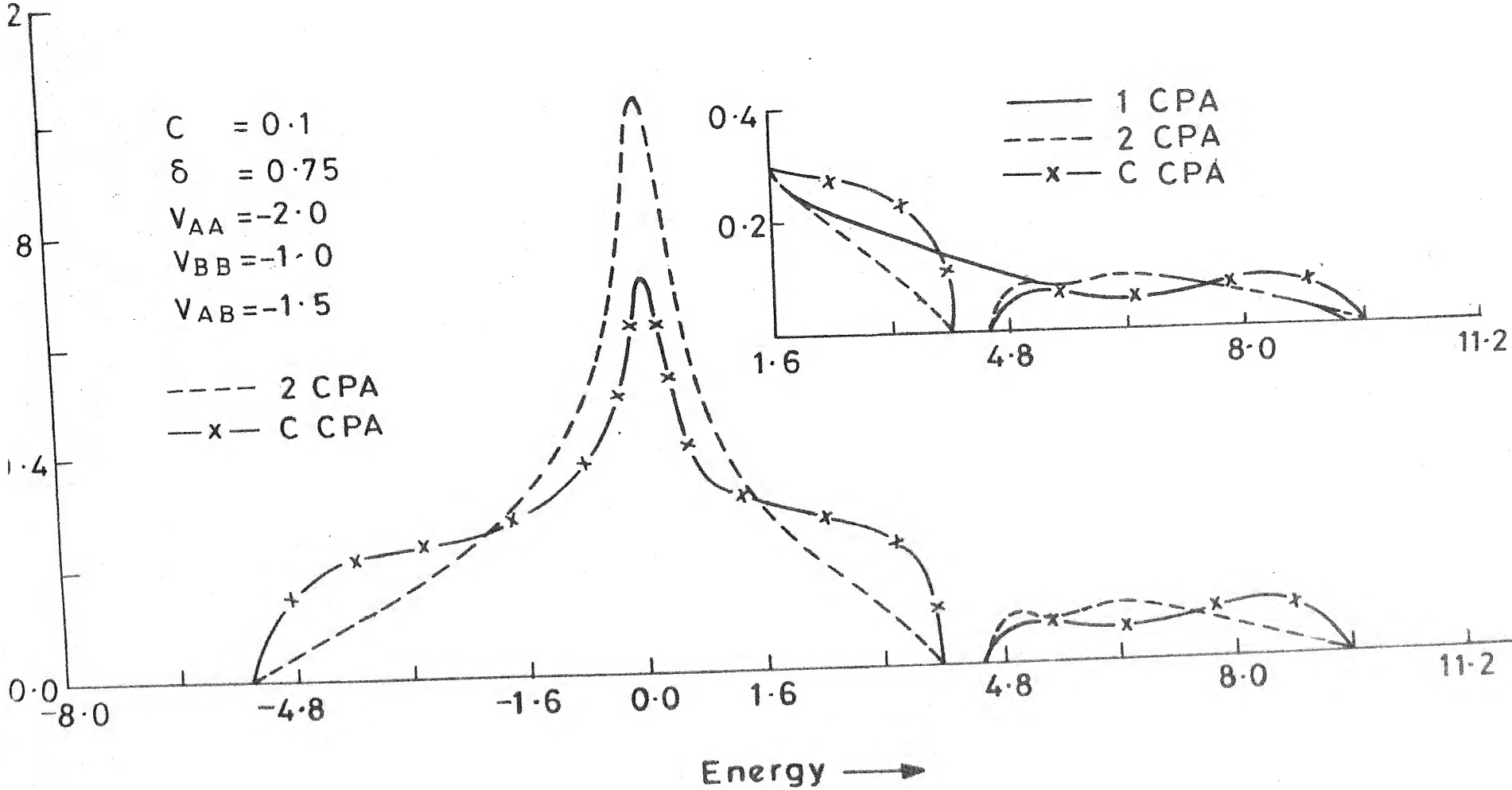
C = 0·1
δ = 0·75
V_{AA} = −2·0
V_{BB} = −1·0
V_{AB} = −1·5
2 CPA
C CPA
1 CPA
2 CPA
C CPA
2
8
1·4
0·0
0·4
0·2
−8·0
−4·8
−1·6
0·0
1·6
4·8
8·0
11·2
1·6
4·8
8·0
11·2
Energy

Figure 3.11a shows the 1CPA and 2CPA (without off-diagonal disorder) density of states for the dilute (c=0.1) alloy but with larger separation in well-depths (δ =1.0). This is the ''strong scattering'' regime. Here even in 1CPA we observe a separate impurity band. Figure 3.11b depicts the 2CPA (with off-diagonal disorder) and CCPA density of states for the same alloy. Here again there is an increase in the band-width as compared to 1CPA. The effect on majority band is very small and a single peak structure of the majority band is characteristic of the b.c.c. lattice and not a feature of disorder. Both 2CPA and CCPA show a two peaked structure in the minority (impurity) band. In order to identity the structure in the impurity band, the partial densities of states are shown in fig. 3.11c and 3.11d. The peak around $E \simeq 9.6$ is identified with an isolated impurity A in a B background (fig. 3.11c) while the peak around $E \simeq 8$ is identified with the cluster where AA interaction is dominant (fig. 3.11d).

Figure 3.12 shows the effect of Markovian short range order of the type described in the earlier section and characterized by a parameter α. $\alpha < 1$ enhances the probability of precipitation of A clusters in a B-background. This is clearly exhibited by the enhancement of the 1-st peak in fig. 3.11d. $\alpha > 1$ enhances AB type pairs which is exhibited by the enhancement of the second peak in fig. 3.11c.

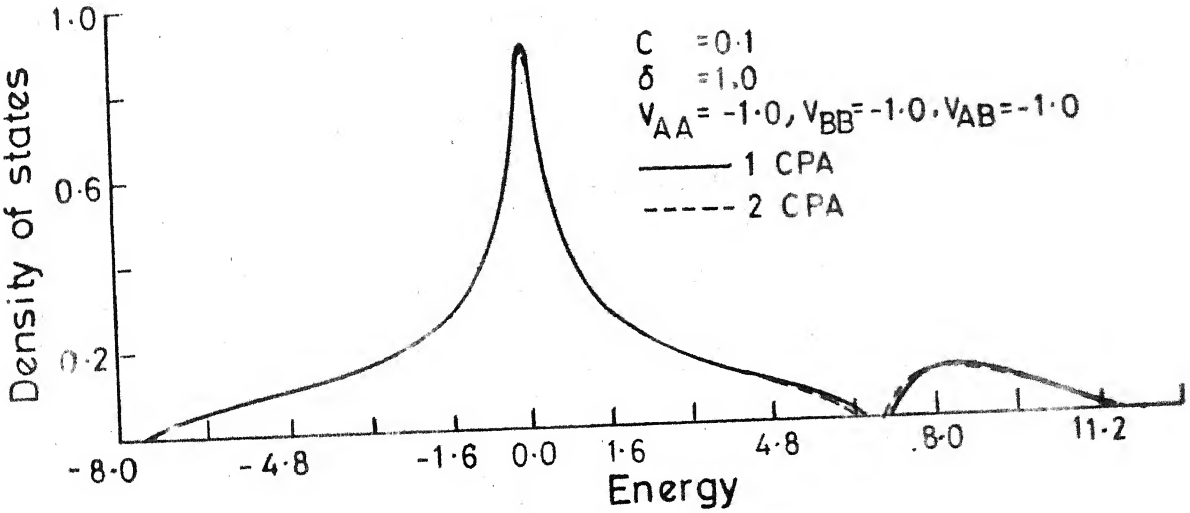

Fig. 3·11a

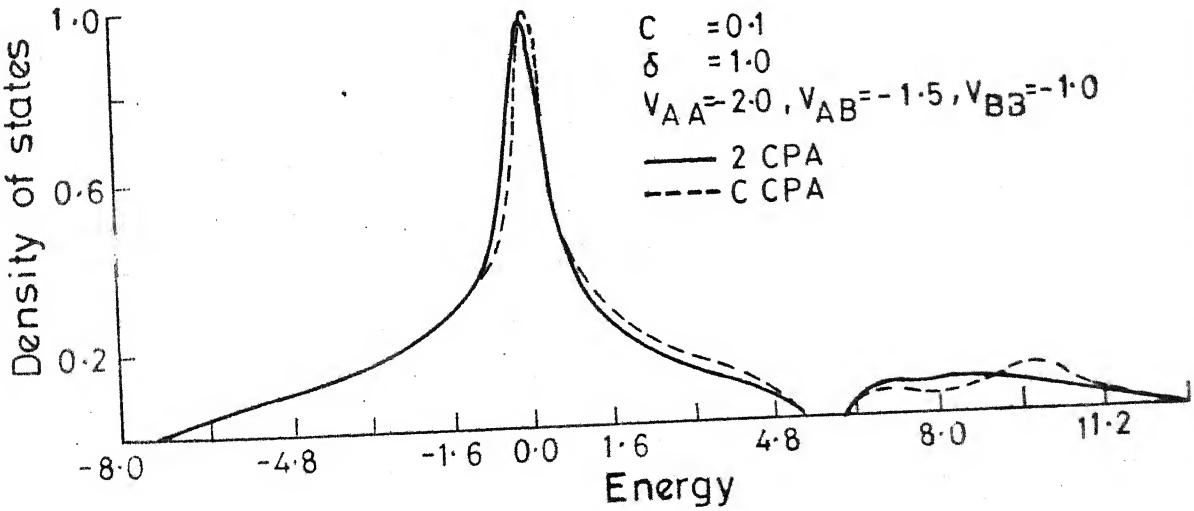

Fig. 3·11b

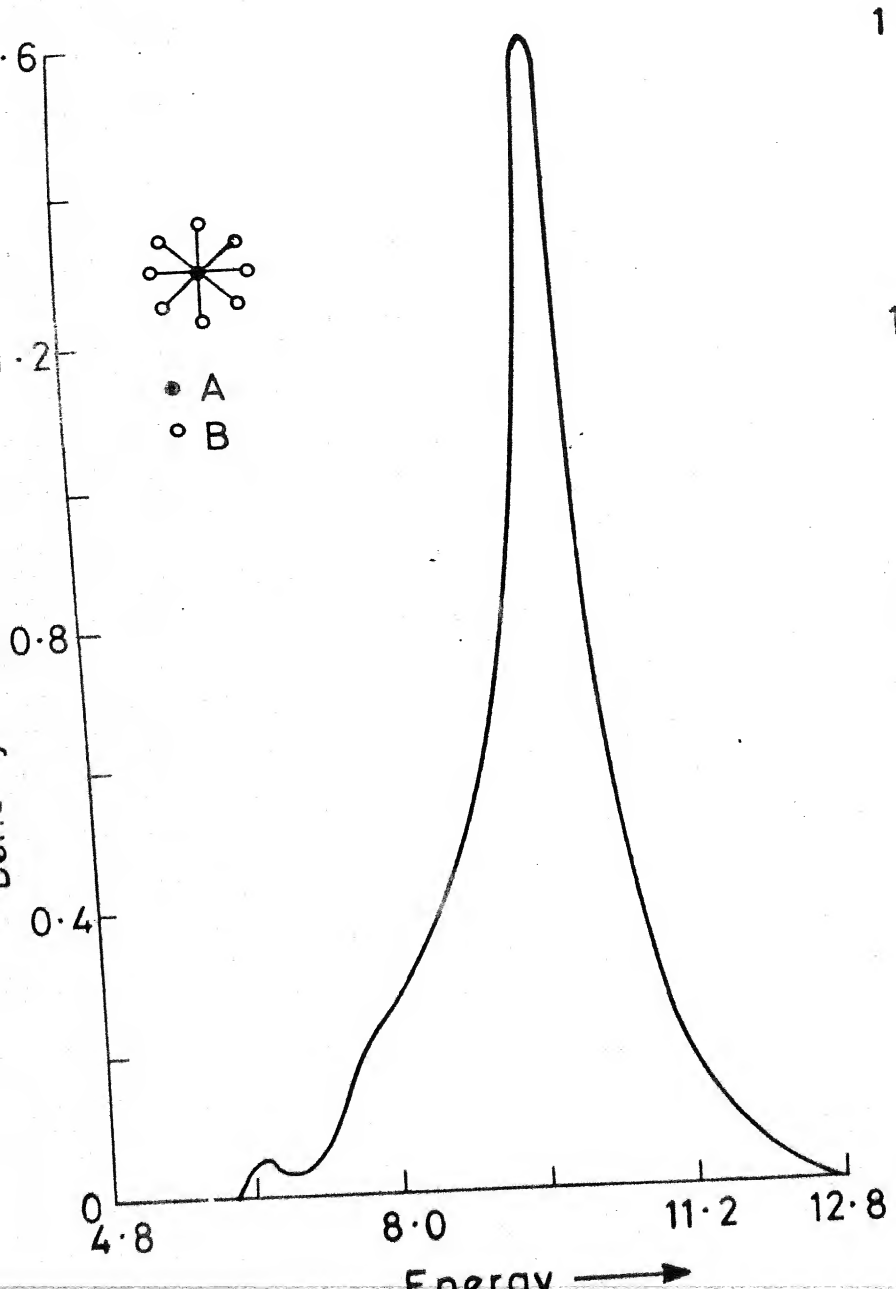
·6
·2
0·8
0·4
0
A
B
4·8
8·0
11·2
12·8
Energy

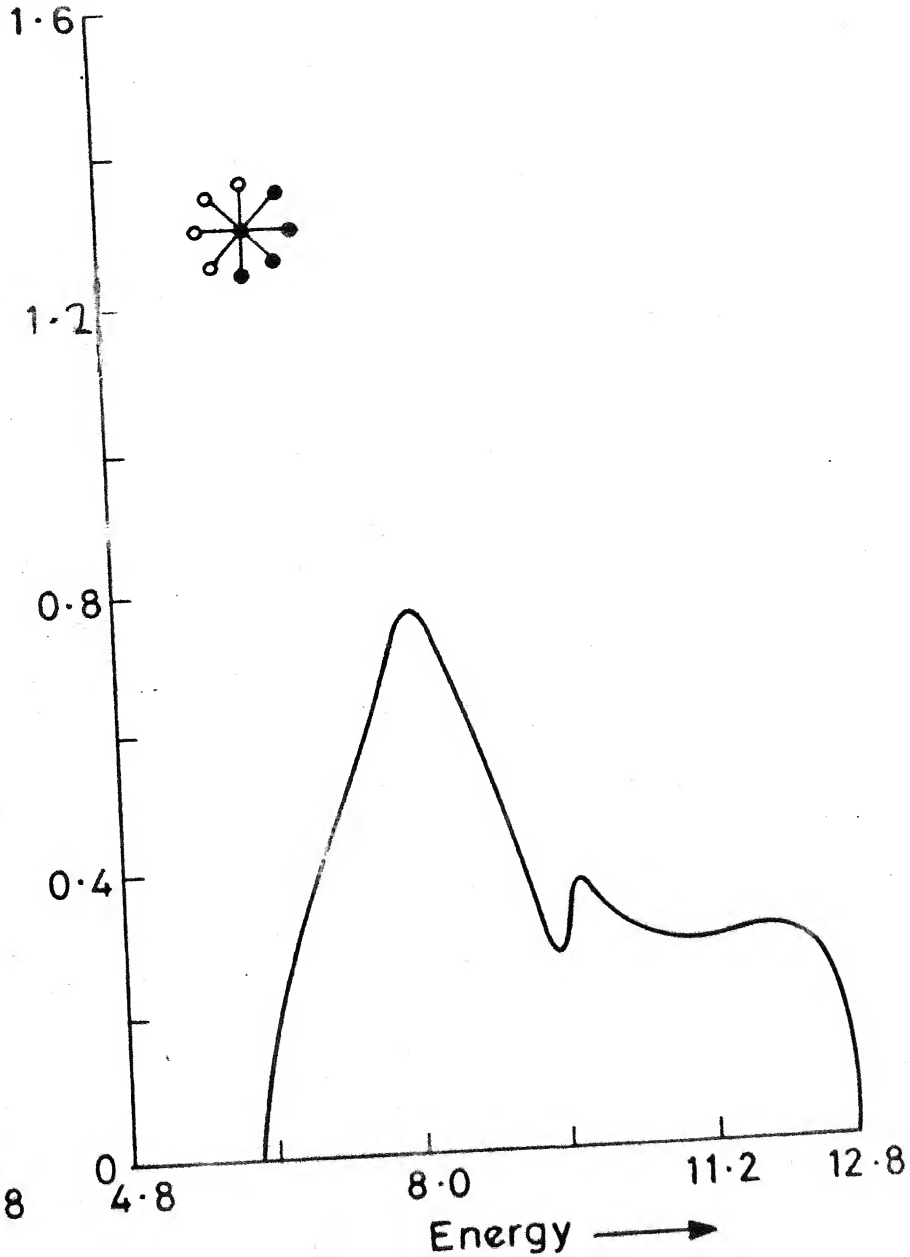
1·6
1·2
0·8
0·4
0
4·8
8·0
11·2
12·8
Energy

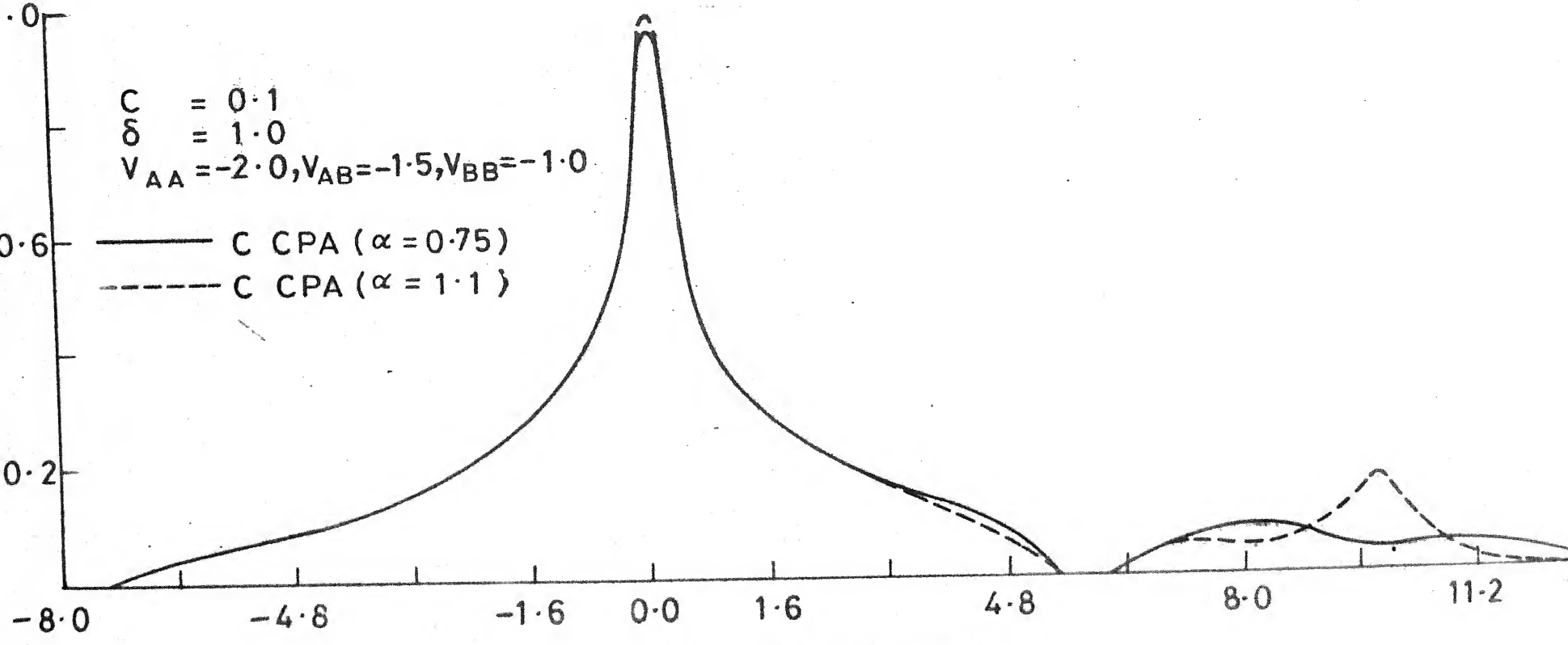
C = 0·1
δ = 1·0
V_{AA} = −2·0, V_{AB} = −1·5, V_{BB} = −1·0
C CPA (α = 0·75)
C CPA (α = 1·1)
·0
0·6
0·2
−8·0
−4·8
−1·6
0·0
1·6
4·8
8·0
11·2
Energy

Fig. 3.12

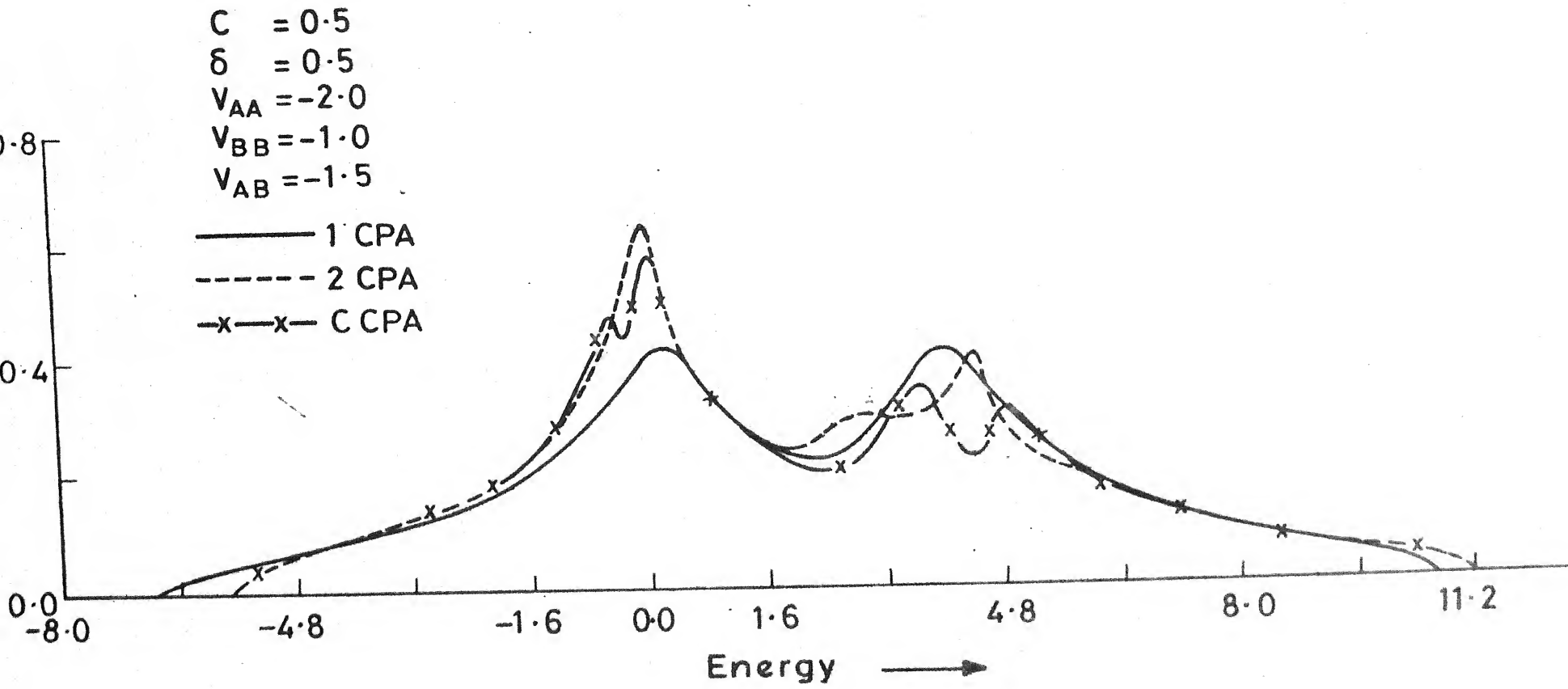
C = 0·5
δ = 0·5
V_{AA} = −2·0
V_{BB} = −1·0
V_{AB} = −1·5
1 CPA
2 CPA
C CPA
0·8
0·4
0·0
−8·0
−4·8
−1·6
0·0
1·6
4·8
8·0
11·2
Energy

Fig. 3·13

Figure 3.13 shows a concentrated 50-50 alloy with $\delta = 0.50$. Unlike the 1CPA case of purely diagonal disorder here in 2CPA and CCPA the density of states is not symmetric around the band centre. This is a feature of the off-diagonal disorder because of the different band-widths of the host and impurity.

These preliminary calculations on a simple but non-trivial three-dimensional model establish first, that the augmented-space formalism in conjunction to the real-space recursion techniques is a practical and useful method of generating physically valid (Herglotz) self-consistent cluster generalisations for resonably realistic models of alloys including off-diagonal disorder and short-range order. Secondly, the results themselves are illustrative of the effects of clustering, off-diagonal disorder and short-range order on the density of states. We have so far considered only one orbital per site. The generalisation to several orbitals per site is straightforward. This work provides us with a sufficient theoretical basis for application to the physically interesting situation of III-V ternary alloys like $Ga_cIn_{1-c}As$, $GaAs_cSb_{1-c}$ etc. These also form diamond lattices, but there are four sp^3 hybridised orbitals per site. This work has been reported in the next chapter.

CHAPTER IV

APPLICATION OF THE CLUSTER-COHERENT-POTENTIAL APPROXIMATION TO III-V SEMICONDUCTING ALLOYS

4.1 Introduction

The preliminary results of calculation on a simple model for random binary alloys discussed in the previous chapter were encouraging and provided us with sufficient theoretical basis to apply the method of self-consistent cluster-CPA to more realistic situations of III-V alloys.

The III-V semiconductors GaAs, InAs, GaSb, InSb, GaP and InP form zinc-blende structures (fig. 4.1). A zinc-blende structure consists of two interpenetrating f.c.c. sublattices, the anion (e.g. As) and the cation (e.g. Ga) sublattices, which are displaced from each other by a vector $\vec{\tau} = (\frac{1}{4},\frac{1}{4},\frac{1}{4})a$, where 'a' is the lattice constant. Consequently each anion in the crystal is surrounded by a tetrahedral arrangement of four cations and vice-versa. A schematic picture of the flattened network of the structure is shown in fig. 4.2.

Pairs of these semiconductors mix in all concentrations to form ternary substitutional disordered alloys. The sublattice of the common ion is 'ordered' while that of the other ion is occupied completely randomly.

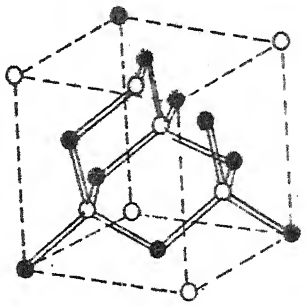

Zinc blende crystal structure
Fig. 4·1

O ANION
O CATION
a (0,0,0)
b (1/4,1/4,1/4)
c (1/2,1/2,0)
d (1/4,3/4,1/4)
e (0,1/2,-1/2)
f (-1/4,1/4,-1/4)
g (3/4,3/4,1/4)
h (1/2,1,1/2)
i (-1/4,3/4,-3/4)
$\vec{\tau}_1$ (1/8,1/8,1/8)
$\vec{\tau}_2$ (-1/8,-1/8,1/8)
$\vec{\tau}_3$ (-1/8,1/8,-1/8)
$\vec{\tau}_4$ (1/8,-1/8,-1/8)

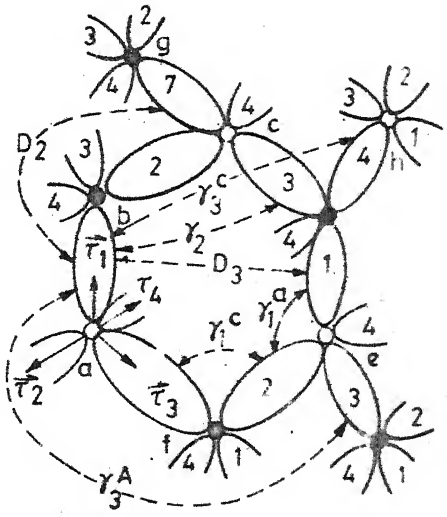

Cordinates are in the units of a, the lattice constan of the f.c.c. latti

Connectivities and coordinates in a flattened diagram for a zinc blende structure

Fig. 4·2

The aim of the work reported in this chapter is two fold. Firstly, the direct application of the formulation developed in the earlier chapters to a realistic system of interest. The basic Hamiltonian is set up in the bond-orbital basis with parameters fitted to experiment or in the pseudo-bond-orbital basis within the ab-initio chemical pseudo-potential formalism (Choudhry and Mookerjee 1980, Choudhry 1981). Secondly, as we adopt basically a tight binding view-point, we attempt with the help of the recursion-technique (see Appendix A) to develop a completely 'real' space method of generating the various constituent Green-functions.

In our former aim we have been successful, as reported below. In the latter, however, the attempt has been only partially successful. Of course, very accurate k-space methods exist for calculation of the Green functions - for example, the ray-integration technique (Chen 1977), which was further extended by Choudhry (Thesis 1981) to deal with off-diagonal Green function elements too. Green functions with vacancies (as required in our method) may also be derived from these by isolated impurity techniques. However, our aim was (to quote Heine) - ''throwing out $\vec{k}$space'' (Solid State Physics, Vol. 35). However a practical snag appeared, that to get results of accuracy comparable to that of $\vec{k}$-space technique, one has to carry out the recursion at least upto twenty to twenty-five steps. To make this feasible it requires

use of real space symmetries and an efficient way of extrapolating the asymptotic part of the continued fraction coefficients. Both these were beyond the know-how of our group here. If we compare a seven step continued fraction version of the density of states per bond (in the units of π^{-1}) for GaAs and InAs (fig. 4.5a,b) with a ray integrated version of density of states per atom (Chen and Sher 1978) as shown in fig. 4.6 then it is found that the overall features are reproduced with a s-like part, an internal gap, followed by a p-like part consisting of roughly two parts in a ratio of 1:2. However, the early truncation of the continued fraction produces spurious oscillatory dips. Since, the completion of this work, it has come to our notice (Kelly, private communication and Solid State Physics, Vol. 35) that efficient programmes have been developed that take into account real space symmetries (Kelly, Solid State Physics, vol. 35, p. 244) and truncation schemes which claim to achieve accuracies equal to the $\vec{k}$-space methods. The author proposes these as further extension of this work. However, he would like to emphasise the above, as a further justification, for starting to develop a fully real-space technique, wedded to the ideas of the augmented space method introduced in Chapter III.

4.2 Hamiltonian

The work by Harrison and his coworkers (1973-74) has demonstrated that the systematics of bonding of various

physical properties can be described by bond orbital model (BOM) in such covalently bonded systems. In this model the basis functions are centred on bonds connecting each anion and the nearest cations. These basis functions are constructed as linear combinations of sp^3 hybridised orbitals on adjacent atoms. This construction results in bonding and antibonding orbitals. Instead of atomic orbitals as basis, the bonding and antibonding orbitals form an equally valid basis. We may partition the Hamiltonian as $\underline{H} = \underline{H}_V + \underline{H}_C + \underline{H}_{VC}$ where $\underline{H}_V$ and $\underline{H}_C$ project on to the valence (or bonding) and conduction (or antibonding) subspaces respectively and $\underline{H}_{VC}$ is the hybridising term.

$$\underline{G}_V = \left[Z\underline{I} - \underline{H}_V - \underline{H}_{VC}^{\dagger} \underline{G}_C \underline{H}_{CV} \right]^{-P_V}$$

$$\underline{G}_C = \left[Z\underline{I} - \underline{H}_C \right]^{-P_C}$$

The valence band desnity of states is given by $-\frac{1}{\pi} \mathrm{Im} \sum_{\alpha} \underline{G}^{V}_{o\alpha, o\alpha}$. Within the bond orbital model, it is assumed that $\underline{H}_{CV}$ is small, and so we may completely neglect the antibonding part and work exclusively in the bonding subspace. In case there is a significant coupling between bonding and antibonding states, the bond orbital approximation is invalid, and bonding basis is incomplete to describe even the valence band only.

We use the chemical bonding orbitals as our basis set and using the notations of Chen and Sher (1978) we fix the

anion f.c.c. sublattice as the reference lattice on which each lattice point is represented by a lattice vector $\vec{j}$. The four bonding orbitals surrounding it may then be represented by $|\vec{j}\alpha\rangle$, $\alpha = 1,2,3,4$ centred at points specified by $\vec{j} + \vec{\tau}_\alpha$ where $\vec{\tau}_1 = (1,1,1)a/8$ $\vec{\tau}_2 = (-1,-1,1)a/8$, $\vec{\tau}_3 = (-1,1,-1)a/8$ and $\vec{\tau}_4 = (1,-1,-1)a/8$ where a is the lattice constant. The bond orbitals themselves are composed of symmetric linear combinations of the hybridised atomic orbitals $|a\rangle$ and $|c\rangle$ centred at the anion and cation atomic sites respectively i.e. $|\vec{j}\alpha\rangle = \frac{1}{N_n}[|a\rangle + |c\rangle] = |ac\rangle$ where N_n is the normalization constant $\sqrt{2(1+S)}$, S being $\langle a|c\rangle$ the orbital overlap of anion-cation pair, and

$$|a\rangle = \frac{1}{2}|s_a\rangle + \frac{\sqrt{3}}{2}|p_a\rangle$$
$$|c\rangle = \frac{1}{2}|s_c\rangle + \frac{\sqrt{3}}{2}|p_c\rangle \qquad (4.1)$$

where $|s_a\rangle$ and $|p_a\rangle$ are the s and p orbitals on the anions while $|s_c\rangle$ and $|p_c\rangle$ are those on the cations. The p-orbitals are taken to be directed along the bond in the above expressions. When expanded in terms of a bond basis set $\{|\vec{j},\alpha\rangle\}$ the BOM Hamiltonian takes the form

$$H_o = \sum_{\vec{j}\alpha,\vec{j}'\alpha'} |\vec{j},\alpha\rangle \langle\vec{j},\alpha|\underline{H}_o|\vec{j}'\alpha'\rangle \langle\vec{j}'\alpha'|$$

If we consider bond to bond interactions upto second nearest neighbour bonds, there are five distinct interactions

$\langle \vec{j},\alpha | \underline{H}_o | \vec{j}'\alpha' \rangle$ which are defined below (see fig. 4.2).

D : The bond energy $\langle \vec{j}\alpha | \underline{H}_o | \vec{j}\alpha \rangle$

γ_1^a : The matrix elements between adjacent bonds with an anion in common.

γ_1^c : The matrix elements between adjacent bonds with a cation in common.

D_2 : The matrix elements between parallel second nearest neighbour bonds.

γ_2 : The matrix elements between non-parallel second nearest neighbour bonds.

The corresponding Bloch basis functions can now be constructed from the bonding orbitals in the usual manner:

$$|\vec{k},\alpha\rangle = \frac{1}{\sqrt{N}} \sum_{\vec{j}} e^{i\vec{k}.(\vec{j}+\vec{\tau}_a)} |\vec{j},\alpha\rangle \qquad (4.2)$$

where N is the total number of anions or cations in the crystal and $\vec{k}$ the wave vector within the Brillouin zone.

The secular equation can, therefore, be written as

$$\det |E(\vec{k})\underline{I} - \underline{H}^{\alpha\alpha'}(\vec{k})| = 0 \qquad (4.3)$$

where

$$H^{\alpha\alpha'}(\vec{k}) = \sum_{\vec{j}} H^{\alpha\alpha'}_{\vec{o}\vec{j}} \exp\ i\vec{k}.(\vec{j}+\vec{\tau}_\alpha - \vec{\tau}_{\alpha'}) \qquad (4.4)$$

has been obtained by using the transformation of bases defined in equation (4.2). Here, one of the site suffixes

on the Hamiltonian in the real space has been fixed as the origin.

In the above description $H^{\alpha\alpha'}_{\substack{\rightarrow\\ij}}$, represents, for example a 4 x 4 matrix representing the energies and interactions between the four bonds emanating from the anion site at the origin. Similarly by assigning different values to the lattice vector $\vec{j}$, interactions between other bonds can be brought in.

Chen and Sher (1978) have shown that the inclusion of third-nearest neighbour interactions, does not change the band structure significantly. So, retaining the interactions upto second nearest neighbour parallel and nonparallel bonds only, the distinct matrix elements are D, γ_1^a, γ_1^c, D_2 and γ_2. In the work of Chen and Sher these form independent parameters. The $\vec{k}$ dependent 4 x 4 Hamiltonian matrix under this approximation is therefore,

$$H_{11} = D+2D_2\,[\cos(2x+2y) + \cos(2x+2z) + \cos(2z+2y)]\,.$$

$$H_{22} = D+2D_2\,[\cos(2x+2y) + \cos(2y-2z) + \cos(2x-2z)]\,.$$

$$H_{33} = D+2D_2\,[\cos(2x-2y) + \cos(2y-2z) + \cos(2x+2z)]\,.$$

$$H_{44} = D+2D_2\,[\cos(2x-2y) + \cos(2y+2z) + \cos(2x-2z)]\,.$$

$$H_{12} = 2\{\gamma 1S\cos(x+y) + 2\gamma_2\cos(x-y)\cos(2z)\} - 2i\gamma 1A\sin(x+y).$$

$$H_{13} = 2\{\gamma 1S\cos(x+z) + 2\gamma_2\cos(x-z)\cos(2y)\} - 2i\gamma 1A\sin(x+z).$$

$$H_{14} = 2\{\gamma 1S\cos(y+z) + 2\gamma_2\cos(y-z)\cos(2x)\} - 2i\gamma 1A\sin(y+z).$$

$$H_{23} = 2\{\gamma 1S \cos(y-z) + 2\gamma_2 \cos(2x) \cos(y+z)\} + 2i\gamma 1A \sin(y-z)$$

$$H_{24} = 2\{\gamma 1S \cos(x-z) + 2\gamma_2 \cos(2y) \cos(x+z)\} + 2i\gamma 1A \sin(x-z).$$

$$H_{34} = 2\{\gamma 1S \cos(x-y) + 2\gamma_2 \cos(2z) \cos(x+y)\} + 2i\gamma 1A \sin(x-y).$$

where $\gamma 1S = \frac{(\gamma_1^a + \gamma_1^c)}{2}$ and $\gamma 1A = (\gamma_1^a - \gamma_1^c)/2$ and x,y,z stand for $\frac{1}{4} k_x a, \frac{1}{4} k_y a, \frac{1}{4} k_z a$ respectively.

4.2.1 The Parameter Fitting Procedure

Chen and Sher have adopted the empirical parameterization approach. They have obtained the values of parameters by fitting energy separations at specific symmetry points on the Brillouin zone Γ, X, L etc. The results are given in the table 4.1. The parameter D has been determined emprically using the band energies and the experimental values of the photo-electric thresholds measured by Shevchik et al (1974).

Table 4.1

Material	Parameters (Mev)				
	D	$\gamma 1S$	$\gamma 1A$	D_2	γ_2
GaAs	-11.1687	-1.5187	-0.4250	0.3406	-0.1094
GaSb	- 9.6437	-1.2687	-0.3750	0.3906	-0.0594
GaP	-10.8125	-1.3625	-0.3250	0.3812	-0.1188
InAs	-10.0562	-1.3937	-0.5125	0.3844	-0.0656
InSb	- 9.5625	-1.3500	-0.3875	0.2937	-0.0563
InP	-10.2750	-1.3125	-0.4125	0.2625	-0.0375

In the table 4.1 we have shown only an optimised set of values. Often, variation in the values of a parameter obtained by fitting to experimental data, for a given material, is more than that over different materials. Chen and Sher finally impose an energy dependent Lorentzian broadening and vary the parameters in order that the broadened peaks thus obtained best resemble the experimental spectra obtained by Ley at el (1973).

The procedure adopted by Chen and Sher is arbitrary and its validity is also not clear. Further the bonding orbitals are not orthogonal. The arguments of Chen and Sher, willing away the overlap integrals, are of doubtful validity.

The alternative and much more satisfying procedure is the ab-initio chemical pseudo-potential approach of Anderson (1969) and Bullett (1975), as performed on GaAs, InAs etc. by Choudhry (Thesis 1981). Within this formalism the bases used need not be orthogonal. It is sufficient that they form a linearly-independent set. It must be mentioned that the chemical pseudo-potential calculations were not self-consistent, as such their accuracy is also in some doubt.

However, we were not interested in this aspect of the problem and for our CCPA calculations, we have used the parameters of Chen and Sher.

Table 4.2

Bond lengths, bond energies, and work functions for III-V semiconductors

Materials	Bond length (A^{o})	Bond energy (e.v.)	Work-function (e.v.)
GaAs	2.45	-5.6687	5.5
InAs	2.61	-4.7562	5.3
GaSb	2.65	-4.7437	4.9
InSb	2.81	-4.7625	4.8
GaP	2.36	-5.1125	5.7
InP	2.54	-4.5750	5.7

4.3 Recursion Calculation of Green Functions

The alloys under consideration are of the kind $Ga_cIn_{1-c}As$ as a common anion alloy and $GaAs_cSb_{1-c}$ as an example of 8(a) common cation alloy. These alloy in all proportions and therefore c may be anything between 0 and 1. Each of the six materials of table (4.1) have nearly the same bond length (table 4.2). Hence we shall assume that the interacation parameters corresponding to the pure materials are the same as those in the alloy. The vacuum state sets the zero of the energy scale.

In an alloy the question of interactions between two different kinds of bonds arises. For example in the case of

$Ga_cIn_{1-c}As$ alloys, a configuration of the kind

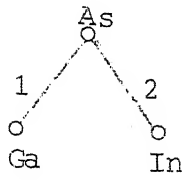

may be a part of the alloy. It is demonstrated below that the interaction H_{12}^{exact} between bonds 1 and 2 is the average of γ_1^a's corresponding to pure Ga-As and pure In-As crystals as a reasonable approximation.

Let the bonds 1 and 2 be described by the quantum states $|b_1\rangle$ and $|b_2\rangle$ respectively.

Then $$|b_1\rangle = \frac{1}{N} \left(|As_1\rangle + |Ga_1\rangle\right)$$

and $$|b_2\rangle = \frac{1}{N} \left(|As_2\rangle + |In_2\rangle\right)$$

in terms of sp^3 hybridised orbitals at various sites directed along the respective bonds and N is the normalisation constant $\simeq \sqrt{2}$, assumed to be the same for the GaAs and InAs bonds. We are concerned here with H_{12}^{exact} i.e.

$$\langle b_1|H^{exact}|b_2\rangle = \frac{1}{N^2}\left[\{\langle As_1| + \langle Ga_1|\}\, H \{|As_2\rangle + |In_2\rangle\}\right]$$

$$= \frac{1}{N^2}\left[\langle As_1|H|As_2\rangle + \langle Ga_1|H|As_2\rangle + \langle As_1|H|In_2\rangle + \langle Ga_1|H|In_2\rangle\right]$$

The first term is vanishing because of the orghogonality of two different hybridised orbitals at the same site.

The middle two terms would be identical in the unalloyed case due to the geometrical symmetry of the location of the orbitals involved. Hence this part of the expression is equivalent to the average of these corresponding to the pure cases. The last term is small compared with the middle two since it involves more distant orbitals. The approximation therefore involves the neglect of the variation in this term over the constituent materials.

In order to compare the results of cluster-CPA formalism with those of 1CPA and VCA we restrict ourselves to the one specific alloy i.e. $Ga_{0.5}In_{0.5}As$. However the procedure for other III-V alloys is quite similar.

In order to get the electronic density of states per bond scaled by π^{-1}, we have used the recursion method of Haydock (1972). The parameters used are those as used by Chen and Sher. The VCA parameters are given by the average of those of the constituents weighted by their respective concentrations. The VCA and the self-consistent 1CPA results are shown in fig. 4.7. The 1CPA results have been obtained by using the 1CPA equation:

$$\frac{c(e_A - \bar{e} - \underline{\Sigma})}{1-(e_A - \bar{e} - \underline{\Sigma})\, g(z - \underline{\Sigma})} + \frac{(e_B - \bar{e} - \underline{\Sigma})(1-c)}{1-(e_B - \bar{e} - \underline{\Sigma})\, g(z - \underline{\Sigma})} = 0,$$

where $\bar{e} = c\, e_A + (1-c)\, e_B$.

The VCA diagonal Green function is substituted as a zeroeth approximation and the quadratic equation in $\underline{\Sigma}$ thus obtained

is solved. The choice of the correct solution is ensured by checking that $\Sigma \to 0$ as $\delta \to 0$ and the imaginary part of σ remains negative throughout the band. At each step new $g(E-\sigma)$ is calculated and substituted back in the above equation. The process continues until self-consistent solution is obtained at a fixed energy. The energy is varied in regular steps across the whole of the valence band.

A comparison of VCA and 1CPA curves shows that the CPA rounds off the sharp peaks present in the VCA.

4.4 Cluster-CPA formalism

The single-site CPA completely ignores the effect of clusters and cannot adequately deal with off-diagonal disorder. Chen and Sher have treated diagonal disorder in 1CPA while off-diagonal disorder in VCA. This is not a consistent procedure and the randomness in the off-diagonal elements, particularly in the nearest neighbour overlaps, is significant. Here an attempt has been made to improve upon this drawback.

When GaAs and InAs are alloyed together they form a random alloy. One of the f.c.c. sublattices is completely occupied by the As atoms, while the other f.c.c. sublattice is randomly occupied by the Ga or In. The analysis therefore resembles that for the random binary rather than the ternary alloys. If we go to the bond-orbital basis and label our

bonds by the As positions, then the bonds are either As-Ga or As-In type randomly. The pseudo-Hamiltonian closely resembles that of an Anderson model.

$$\underline{H} = \sum_i D_i \underline{P}_i + \sum_{i,j \in \mathcal{N}_c} V_{ij}^{(c)} \underline{T}_{ij}^{(c)} + \sum_{i,j \in \mathcal{N}_a} V_{ij}^{(a)} \underline{I}_{ij}^{(a)}$$

$$+ \bar{D}_2 \sum_{i,j \in \mathcal{N}^{||}} \underline{T}_{ij} + \bar{\gamma}_2 \sum_{1,j \in \mathcal{N}^{\#}} T_{ij}$$

where $\underline{T}_{ij}^{(a)}$ (or $T_{ij}^{(c)}$) denotes nearest neighbour transfer between two bonds with an anion (or cation) in common. $\mathcal{N}_c$ (or $\mathcal{N}_a$) denotes nearest neighbour bonds with a cation (or anion) in common. $\mathcal{N}^{||}$ and $\mathcal{N}^{\#}$ denote next nearest parallel and non-parallel bonds (see fig. 4.2). Here i labels a bond $|r,n\rangle$. The set $\{D_i\}$ and the set $\{V_{ij}\}$ are both random, so that the model contains both diagonal and off-diagonal disorders. The second nearest neighbour parallel and non-parallel bond interactions D_2 and γ_2 respectively are treated in VCA, denoted by $\bar{D}_2$ and $\bar{\gamma}_2$. We may write $\underline{H}$ interms of the occupation number N_i for the (say) Ga-As bond. That is if $N_i = 1$, the bond is a Ga-As one and zero, if it is not. Then

$$D_i = D^{GaAs}(N_i) + D^{InAs}(1-N_i)$$

or

$$D_i = D^A N_i + D^B(1-N_i)$$

where D^A and D^B represent bond energies of Ga-As and In-As respectively.

Now $V_{ij}^{(c)}$ and $V_{ij}^{(a)}$ can be written as,

$$V_{ij}^{(c)} = \gamma_{1c}^{AA} N_i + \gamma_{1c}^{BB} (1-N_i),$$

$$V_{ij}^{(a)} = \gamma_{1a}^{AA} N_i N_j + \gamma_{1a}^{BB} (1-N_i)(1-N_j) + \gamma_{1a}^{AB}\{(1-N_i)N_j + N_i(1-N_j)\} \quad (4.7)$$

Here γ_{1a}^{AA} (or γ_{1a}^{BB}) represents first nearest neighbour bond interaction between two Ga-As (or InAs) bonds with As as common ion and γ_{1c}^{AA} (or γ_{1c}^{BB}) represents that between two nearest neighbour Ga-As (or In-As) bonds with Ga (or In) as common ion. γ_{1a}^{AB} represents nearest neighbour bond interaction between Ga-As and In-As bonds with As as common ion. So $\underline{H}$ can be written as

$$\underline{H} = \underline{H}_B + W \sum_i N_i \underline{P}_i + V_{1a} \sum_{ij} (N_i N_j)\, \underline{T}_{ij}^{(a)}$$

$$+ V_{2a} \sum_{ij} (N_i + N_j)\, T_{ij}^{(a)} + V_{2c} \sum_{ij} (N_i + N_j)\, \underline{T}_{ij}^{(c)}$$

$$+ (\bar{D}_2 - D_2^{BB}) \sum_{ij} \underline{T}_{ij} + (\bar{\gamma}_2 - \gamma_2^{BB}) \sum_{ij} T_{ij} \quad (4.8)$$

$$\underline{H}_B = D^B \sum_i P_i + \sum_{ij} \gamma_{1c}^{BB} T_{ij}^{(c)} + \sum_{ij} \gamma_{1a}^{BB} T_{ij}^{(a)}$$

$$+ D_2^{BB} \sum_{ij} T_{ij} + \gamma_2^{BB} \sum_{ij} T_{ij}$$

is the pseudo-Hamiltonian for the pure InAs case:

$W = D_A - D_B$ and

$$V_{1a} = \gamma_{1a}^{AA} + \gamma_{1a}^{BB} - 2\gamma_{1a}^{AB}$$

$$V_{2a} = \gamma_{1a}^{AB} - \gamma_{1a}^{BB} \quad (4.9)$$

$$V_{2c} = \frac{1}{2}(\gamma_{1c}^{AA} - \gamma_{1c}^{BB})$$

Here In-As has been used as solvent and Ga-As as solute. We might just as well reverse their roles.

In the absence of short range ordering due to chemical clustering

$$p(N_i) = c\delta(N_i-1) + (1-c)\,\delta(N_i) \tag{4.10}$$

where c is the concentration of Ga-As.

We now go over to the augmented space formalism. This has been described in great detail in Chapter III. Using the same notations introduced earlier, the augmented space Hamiltonian can be written as

$$\begin{aligned}\underline{\tilde{H}} = {} & \underline{H}^{B} \otimes \underline{I} + W \sum_i \underline{P}_i \otimes \underline{M}^{(i)} \otimes \underline{I}^{(i)} \\ & + V_{1a} \sum_{ij} \underline{T}_{ij} \otimes \underline{M}^{(i)} \otimes \underline{M}^{(j)} \otimes \underline{I}^{(ij)} \\ & + (V_{2a} + V_{2c}) \sum_{ij} \{\underline{M}^{(i)} \otimes \underline{I}^{(i)} + \underline{M}^{(j)} \otimes \underline{I}^{(j)}\} \\ & + (\bar{D}_2 - D_2^{BB}) \sum_{ij} \underline{T}_{ij} \otimes \underline{I} + (\bar{\gamma}_2 - \gamma_2^{BB}) \sum_{ij} \underline{T}_{ij} \otimes \underline{I}\end{aligned} \tag{4.11}$$

where $$\underline{M}^{(i)} = \begin{bmatrix} c & \sqrt{c(1-c)} \\ \sqrt{c(1-c)} & 1-c \end{bmatrix} \tag{4.12}$$

and $\underline{\tilde{H}} \in \mathcal{H} \otimes \prod^{\otimes} \phi^{(i)}$

The configurationally averaged Green's function is given by

$$\langle G_{ij}(Z) \rangle = \langle i, \tau^{o} | \, (Z\underline{I} - \underline{\tilde{H}})^{-1} \, | \, j, \tau^{o} \rangle \tag{4.13}$$

where $|\tau^{o}\rangle = \prod_i^{\otimes} |v_i^{o}\rangle$ is the augmented space configuration

''ground state'' (chapter III). The density of states is

$$\langle n(E)\rangle = -\frac{1}{\pi} \operatorname{Im}_{\eta \to 0^+} \langle G_{ii}(E+i\eta)\rangle \qquad (4.14)$$

The CCPA may be generated from (4.14) using the methodology described in Chapter III.

The calculation of self-consistent medium is of central interest. In order to illustrate the procedure we shall first consider a pair-CPA (2CPA). If we apply the delinking procedure described in Chapter III, the resulting graph has the following structure.

Each two bonds attached to a common ion in the original lattice have in augmented space an ''octagon'' decorating it. (fig. 4.3a). In the case of $Ga_cIn_{1-c}As$, there are two such octagons, one corresponding to two bonds with a cation in common and the other corresponding to two bonds with an anion in common. As a starting point, we treat the interaction between two bonds with a cation in common in VCA, and denote it by $\bar{\gamma}_{1c}$ i.e. there is no cation disorder and the interaction between two bonds with anion in common is taken into account exactly. We can do otherwise also, i.e. we can take into account exactly the cation disorder while treat the anion disorder in VCA. Our choice is governed by which disorder is more significant in our example. In order to take both types of disorder into account consistently, we must perform a 3CPA calculation. However in the present work we have

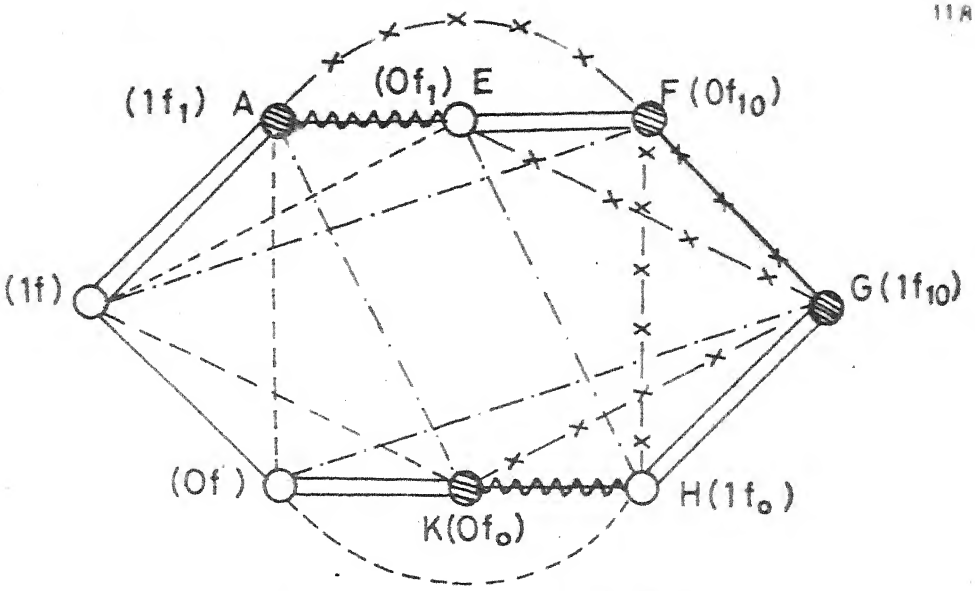

$V_1 = 2CV_{2a} + C^2 V_{1a} + \gamma_{1a}^{BB}$

$V_2 = V_{2a} + C(1-C) V_{1a} + \gamma_{1a}^{BB}$

$V_3 = 2(1-C) V_{2a} + (1-C)^2 V_{1a} + \gamma_{1a}^{BB}$

$\sqrt{C(1-C)}\,[V_{2a} + (1-C) V_{1a}]$

$\sqrt{C(1-C)}\,[V_{2a} + C V_{1a}]$

$C(1-C)\, V_{1a}$

$W\sqrt{C(1-C)}$

$\equiv D^B + CW$

$\equiv D^B + (1-C)\, W$

Fig. 4·3a

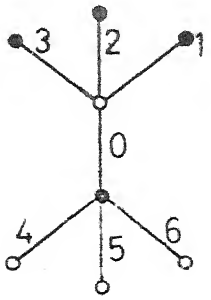

• Cation
o Anion

Fig. 4.3b

performed only a 2CPA calculation and a full 3CPA and other cluster CPA calculations have been left for later research work. The augmented space Hamiltonian with bond disorder, due to a common anion only, can be written as

$$\begin{aligned}\underline{\tilde{H}} = \underline{H}_0 \otimes \underline{I} + W \sum_i \underline{P}_i \otimes \underline{M}^{(i)} \otimes \underline{I}^{(i)} \\ + V_{1a} \sum_{ij} \underline{T}_{ij}^{(a)} \otimes \underline{M}^{(i)} \otimes \underline{M}^{(j)} \otimes I^{(j)} \\ + V_{2a} \sum_{ij} \underline{T}_{ij}^{(a)} \otimes [\, \underline{M}^{(i)} \otimes \underline{I}^{(i)} + \underline{M}^{(j)} \otimes \underline{I}^{(j)} \,] \\ + (\bar{\gamma}_{1c} - \gamma_{1c}^{BB}) \sum_{ij} \underline{T}_{ij}^{(c)} \otimes \underline{I} + (\bar{D}_2 - D_2^{BB}) \sum_{ij} \underline{T}_{ij} \otimes \underline{I} \\ + (\bar{\gamma}_2 - \gamma_2^{BB}) \sum_{ij} \underline{T}_{ij} \otimes \underline{I} \qquad (4.15)\end{aligned}$$

The eight vertices of the octagon (fig. 4.3a) correspond. to eight different configurations of the two bond cluster ($N \times 2^N$). We should notice here that each vertex of our graph now corresponds to a 'bond' and each link to the off-diagonal Hamiltonian matrix element in a bond rather than 'site' basis (In fact it is the 'covering' lattice formed by a bond-vertex interchange).

Now we apply the cluster delinking procedure described in Chapter III. The result is that no octagon belonging to a pair of two bonds with an anion in common has any connection to another corresponding to another pair of bonds with an anion in common. This again implements the idea that within 2CPA correlated scattering from three or more bonds is ignored.

The final effect is that each pair of bonds with an anion in common is renormalised. This gives rise to a matrix self-energy

$$\underline{\Sigma} = \begin{bmatrix} \Sigma_0 & \Sigma_1 \\ \Sigma_1 & \Sigma_0 \end{bmatrix}$$

Here Σ_0 is the self-energy of the bonds and Σ_1 is the overlap-self energy of a pair of bonds with an anion in common. The aim is to calculate $\underline{\Sigma}$ self consistently.

The renormalisation of pair of bonds with an anion in common follows in two steps:

(a) The decorating octagon is not an isolated octagon involving only the two spatial bonds (0 and 1). If we look at the vertex A (i.e. $1f_1$), the link AE($1f_1$ to $0f_1$) belonging to the octagon is only one of the six links emanating from A to the six nearest neighbour bonds of 0. The other remaining 5 bonds to $2f_1$, $3f_1$;.... also hang on to the bond A. Out of these 5 bonds, 2 hang on to the anion and 3 hang on to the cation constituting the bond 0 (see fig. 4.3b). These bonds themselves inturn have their own octagons decorating them (fig. 3.2c). Thus the link AE is itself immersed in a self-consistent medium. The same is true for the links FG and HK of the octagon. We may take this into account by saying that the medium renormalises the link AE, FG and HK. Once the renormalisation is accounted for the octagon is

effectively isolated. The renormalised vertices $\underline{\sigma}_0(Z)$ and links $\underline{\sigma}_1(Z)$ are found as follows Let us devide the lattice (of bonds,into two subspaces (1) An unrenormalised link AE, which we shall call system 1. It has a Hamiltonian

$$H^{(1)} = V_1 \ (\underline{T}_{AE} + \underline{T}_{EA})$$

(2) A lattice L, which is the original lattice minus the link AE and in which all bonds and those links which have an anion in common are renormalised by $\underline{\Sigma}$. This has a Hamiltonian

$$\underline{H}^{(2)} = \underline{\Sigma}_0(Z) \sum_{i\neq A,E} \underline{P}_i + \underline{\Sigma}_1(Z) \sum_{ij\neq A,E} \underline{T}_{ij} + \bar{\gamma}_{1c} \sum_{ij\neq A,E} \underline{T}_{ij}$$

$$+ \bar{D}_2 \sum_{ij} \underline{T}_{ij} + \bar{\gamma}_2 \sum_{ij} \underline{T}_{ij}$$

and a linking Hamiltonian

$$\underline{H}^{(int)} = \Sigma_1(Z) \sum_i (\underline{T}_{iA} + \underline{T}_{Ai} + \underline{T}_{iE} + \underline{T}_{Ei})$$

$$+ \bar{\gamma}_{1c} \sum_i (\underline{T}_{iA} + \underline{T}_{Ai} + \underline{T}_{iE} + \underline{T}_{Ei})$$

$$+ \bar{D}_2 \sum_i (\underline{T}_{iA} + \underline{T}_{Ai} + \underline{T}_{iE} + \underline{T}_{Ei}) + \bar{\gamma}_2 \sum_i (\underline{T}_{iA} + \underline{T}_{Ai} + \underline{T}_{iE} + \underline{T}_{Ei})$$

If we now use the notation $\underline{X}^{-P_Y}$ to denote the inverse of the operator $\underline{X}$ in the subspace y we get

$$\underline{G}^{(1)} = \underline{P}_1 \underline{G} \underline{P}_1 = \left[Z\underline{I} - \underline{H}^{(1)} - \underline{H}^{(int)} \underline{G}^{(2)} \underline{H}^{(int)} \right]^{-\underline{P}_1}$$

where $\underline{G}^{(2)} = \left[Z\underline{I} - \underline{H}^{(2)} \right]^{-\underline{P}_2}$

with $\underline{P}_1 + \underline{P}_2 = \underline{I}$ (4.16)

Examination of the form of above set of equations immediately indicates that the effect of the rest of the lattice hanging on to link AE, is to change the Hamiltonian $H^{(1)}$ to $H^{(1)} + \underline{\sigma}$ where the self energy $\underline{\sigma} = \begin{pmatrix} \sigma_o & \sigma_1 \\ \sigma_1 & \sigma_c \end{pmatrix}$ is given by

$$\sigma_{AA} = \sigma_{EE} = \sigma_o = (\Sigma_1 + \bar{\gamma}_{1c} + \bar{D}_2 + \bar{\gamma}_2)^2 \sum_{k,m \in \mathcal{N}_A} G^{(2)}_{k,m}$$

$$= \Sigma_1^2(2G0+2G1A) + \bar{\gamma}_{1c}^2(3G0+6G1c)$$

$$+ \Sigma_1 \bar{\gamma}_{1c}(4G2P+8G2A) + \bar{\gamma}_2^2(12G0+6G1A+6G1C+8G3AA$$

$$+ 18G3AC+6G3PA+6G3PC+24G4P+48G4A) + \bar{D}_2^2(6G0+6G3PA+6G3PC$$

$$+ 18G4P) + \bar{\gamma}_2\bar{D}_2(12G1A+12G1C+24G3AC+24G3AA+72G4A)$$

$$+ \Sigma_1 \bar{\gamma}_2(8G1C+3G2P+8G2A+8G3PA+16G3AA) + \bar{\gamma}_{1c}\bar{\gamma}_2(12G1A$$

$$+ 12G2P+12G2A+12G3PC+24G3AC) + \Sigma_1\bar{D}_2(4G1C+8G2A+12G3AA)$$

$$+ \bar{\gamma}_{1c}\bar{D}_2(6G1A+12G2A+18G3AC) \qquad (4.17a)$$

and

$$\sigma_{AE} = \sigma_{EA} = \sigma_1 = (\Sigma_1 + \bar{\gamma}_{1c} + \bar{D}_2 + \bar{\gamma}_2)^2 \sum_{k \in \mathcal{N}_A} \sum_{m \in \mathcal{N}_E} G^{(2)}_{k,m}$$

$$= \Sigma_1^2(2G0+2G1A) + (\bar{\gamma}_{1c})^2(2G3PC+7G3AC) + \Sigma_1 \bar{\gamma}_{1c}(4G2P+8G2A)$$

$$+ \bar{D}_2^2(G1A+2G1C+5G2A+2G3PC+5G3AC+12G4A+9G5AA)$$

$$+ \bar{\gamma}_2^2(2G0+8G1A+6G1C+4G2P+4G2A+8G4P+40G4A+22G3AC$$

$$= 4G3AA+8G3PC+8G5PA+30G5AA) + \bar{\gamma}_2\bar{D}_2(4G0+4G1C+8G1A$$

$$+ 4G2P+12G2A+20G4P+28G4A+20G3AC+24G5AA+12G5PA+8G3PC)$$

$$+ \bar{\gamma}_1 \bar{\gamma}_2(3G1C+3G2P+3G2A+3G3PA+16G3AA) + \bar{\gamma}_1 \bar{\gamma}_2(4G0$$

$$+ 8G1C+4G3PC+20G3AC+8G4P+28G4A) + \Sigma_1 \bar{D}_2(8G2A+4G1C$$

$$+ 12G3AA) + \bar{\gamma}_{1c} \bar{D}_2(2GC+4G1C+4G3PC+8G3AC+6G4P+12G4A)$$

(4.17b)

Here $\mathcal{N}_A$ denotes the neighbours (upto second nearest neighbour) of bond A. The different Green functions, used in the above expressions are specified below:

GC - diagonal matrix element of Green function

G1A - matrix element of the Green function between two bonds with an anion in common

G1C - matrix element of the Green function between two bonds with a cation in common

G2P - matrix element of Green function between two second nearest beighbour parallel bonds

G2A - matrix element of Green function between two second nearest neighbour non-parallel bonds.

G3PA - matrix element of Green function between two third nearest-neighbour parallel bonds with their closer ends adjacent to anions

G3PC - matrix element of Green function between two third nearest-neighbour parallel bonds with their closer ends adjacent to cations

G3AA - matrix element of Green function between two third nearest-neighbour non-parallel bonds with their ends adjacent to anions

G3AC - matrix elements of Green function between two third nearest-neighbour non-parallel bonds with their closer ends adjacent to cations

G4P - matrix element of Green function between two fourth nearest neighbour parallel bonds

G4A - matrix element of Green function between two fourth nearest-neighbour non-parallel bonds

G5PA - matrix element of Green function between two fifth nearest-neighbour parallel bonds with their closer ends adjacent to anions.

G5PC - matrix element of Green function between two fifth nearest-neighbour parallel bonds with their closer ends adjacent to cations

G5AA - matrix element of Green function between two fifth nearest-neighbour non-parallel bonds with their closer ends adjacent to anions

G5AC - matrix element of Green function between two fifth nearest-neighbour non-parallel bonds with their closer ends adjacent to cations

(b) Let us now work on the renormalised isolated octagon. As before let us divide the octagon into two subsystems a link B (0f, 1f) and the rest of the actaton M. Then

$$\underline{\tilde{H}}_B = \sum_{i,j \in Of,1f} \tilde{H}_{ij}, \quad \underline{\tilde{H}}^M = \sum_{i,j \neq Of,1f} \underline{\tilde{H}}_{ij}$$

$$\underline{\tilde{H}}^{BM} = \sum_{i \in B} \sum_{j \in M} (\underline{\tilde{H}}_{vj} + \underline{\tilde{H}}_{ji})$$

As before we have

$$\underline{G}^B = \underline{P}_B \underline{G} \underline{P}_B = [Z\underline{I} - \underline{H}^B - \underline{H}^{BM} \quad \underline{G}^M \underline{H}^{BM}]^{-\underline{P}_B}$$

$$\underline{G}^M = [Z\underline{I} - \underline{H}^M]^{-\underline{P}_M}$$

This immediately shows how the octagon renormalises the link B. We have

$$\Sigma_o = \underline{\tilde{H}}^B_{oo} + \sum_{j \neq 0} \sum_{k \neq 0} \tilde{H}^{BM}_{oj} G_{jk} \tilde{H}^{BM}_{ko}$$

$$\Sigma_1 = \underline{\tilde{H}}^B_{o1} + \sum_{j \neq 1} \sum_{k \neq 1} \tilde{H}^{BM}_{oj} G_{jk} \tilde{H}^{BM}_{k1} \qquad (4.18)$$

equations (4.17) and (4.18) together provide a self-consistant set of equations for the calculation of the self energy _ The various Green's functions involved can be easily calculated using the recursion technique. In case when we are using energy dependent Hamiltonians, the recursion has to be done separately for each value of energy.

4.5 Results and Discussion

Using the methodology described in the previous section, we have generated the valence-band density of states for $Ga_{0.5}\ In_{0.5}\ As$.

Fig. 4.4. displays the the electronic density of states (EDOS) curve for Ga-As with nearest-neighbour bond interaction only, with eight and nine step recursions. The termination of the continued fraction of coefficients is based on Gershgorin theorem (see appendix-A). Here there are too many oscillations in the EDOS-curve and we cannot distinguish between two parts of the p-like part of the band.

Figure 4.5a shows the EDOS-curves for Ga-As with six and seven step recursions, with second nearest-neighbour bond interactions also. Here we could not go beyond seven steps because of time and storage-space problems. Figure 4.5b shows the seven step recursion curve for InAs.

If we compare the seven step recurion EDOS-curves for GaAs and InAs with the EDOS-curves obtained by $\vec{k}$-space methods (fig. 4. 6a, 4.6b) for these materials then we note that the recursion curves have almost all the qualitative features of the curves obtained by $\vec{k}$-space methods:

(i) There is one s-like part with a peak and a secondary peak simulating the $\vec{k}$-space hump. This has 25 per cent of the total area (under the full curve) under it.

(ii) A central gap insensitive to how the continued fraction-expansion is terminated.

(iii) A p-like part with one peak with 25 per cent of the total area under it, separated by a dip from a section

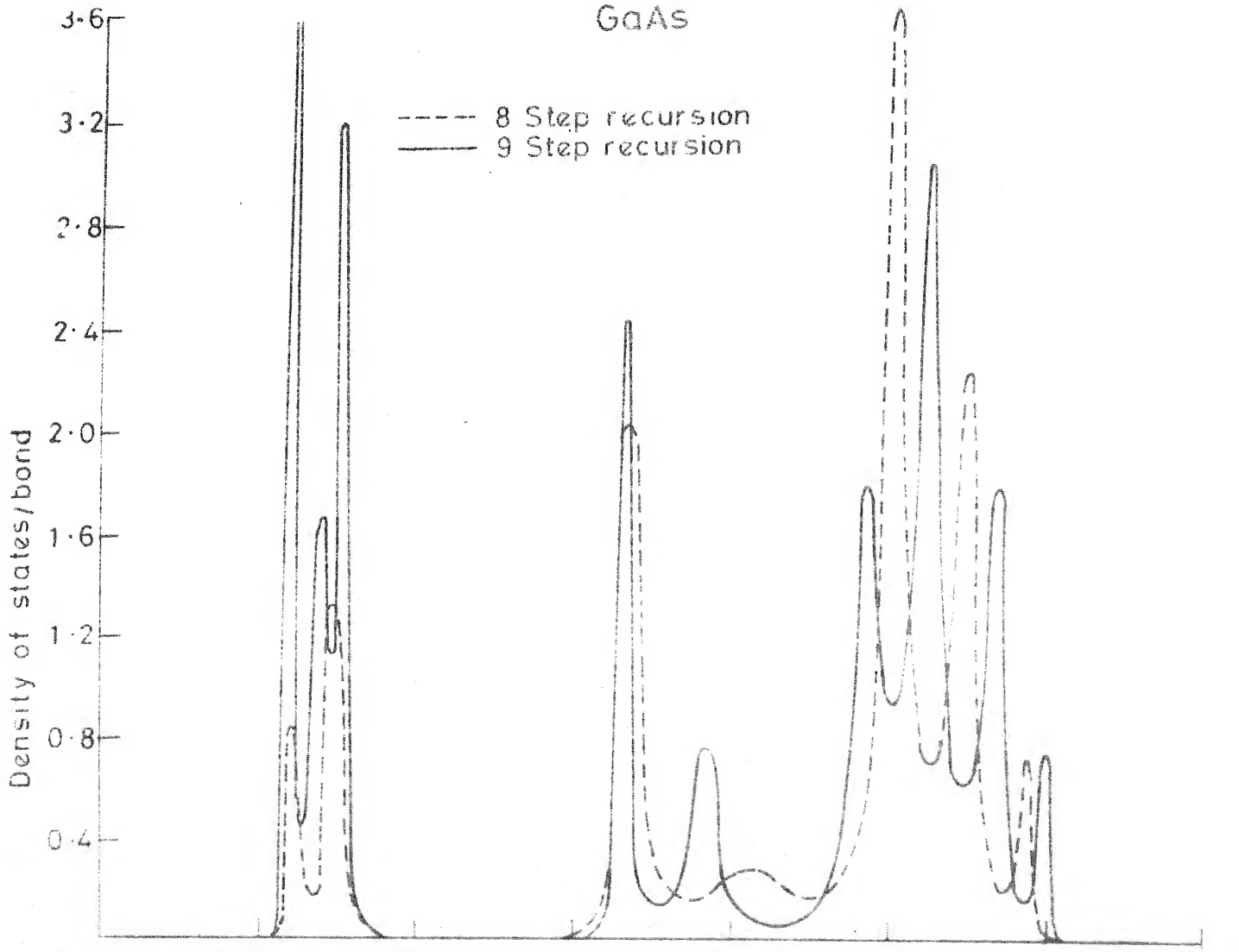
GaAs
8 Step recursion
9 Step recursion
Density of states/bond
3·6
3·2
2·8
2·4
2·0
1·6
1·2
0·8
0·4
-20·00
-17·60
-15·20
-12·80
-10·40
-8·00
-5·60
-3·20
Energy

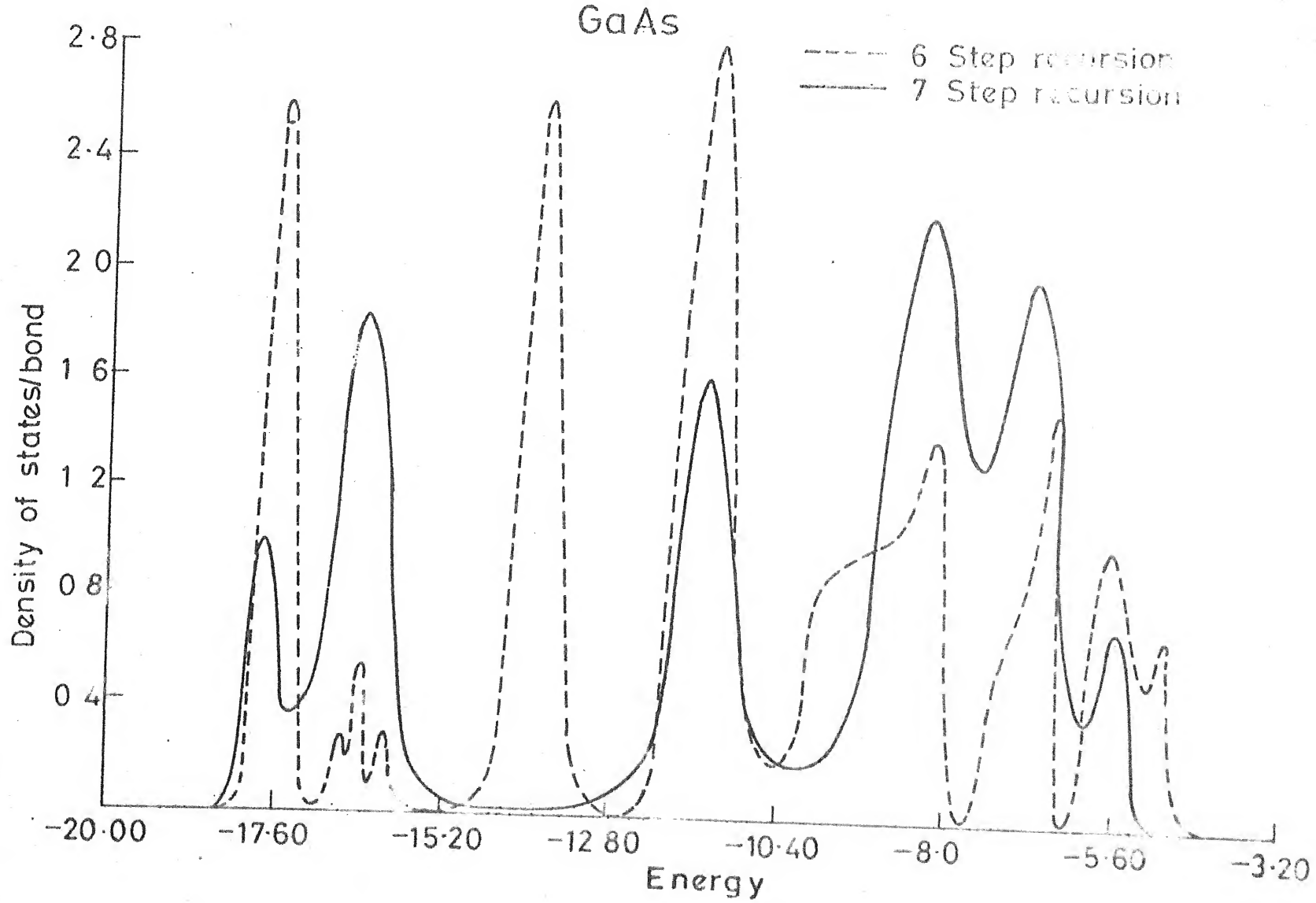
GaAs
6 Step recursion
7 Step recursion
Density of states/bond
2·8
2·4
2 0
1 6
1 2
0 8
0 4
−20·00
−17·60
−15·20
−12 80
−10·40
−8·0
−5·60
−3·20
Energy

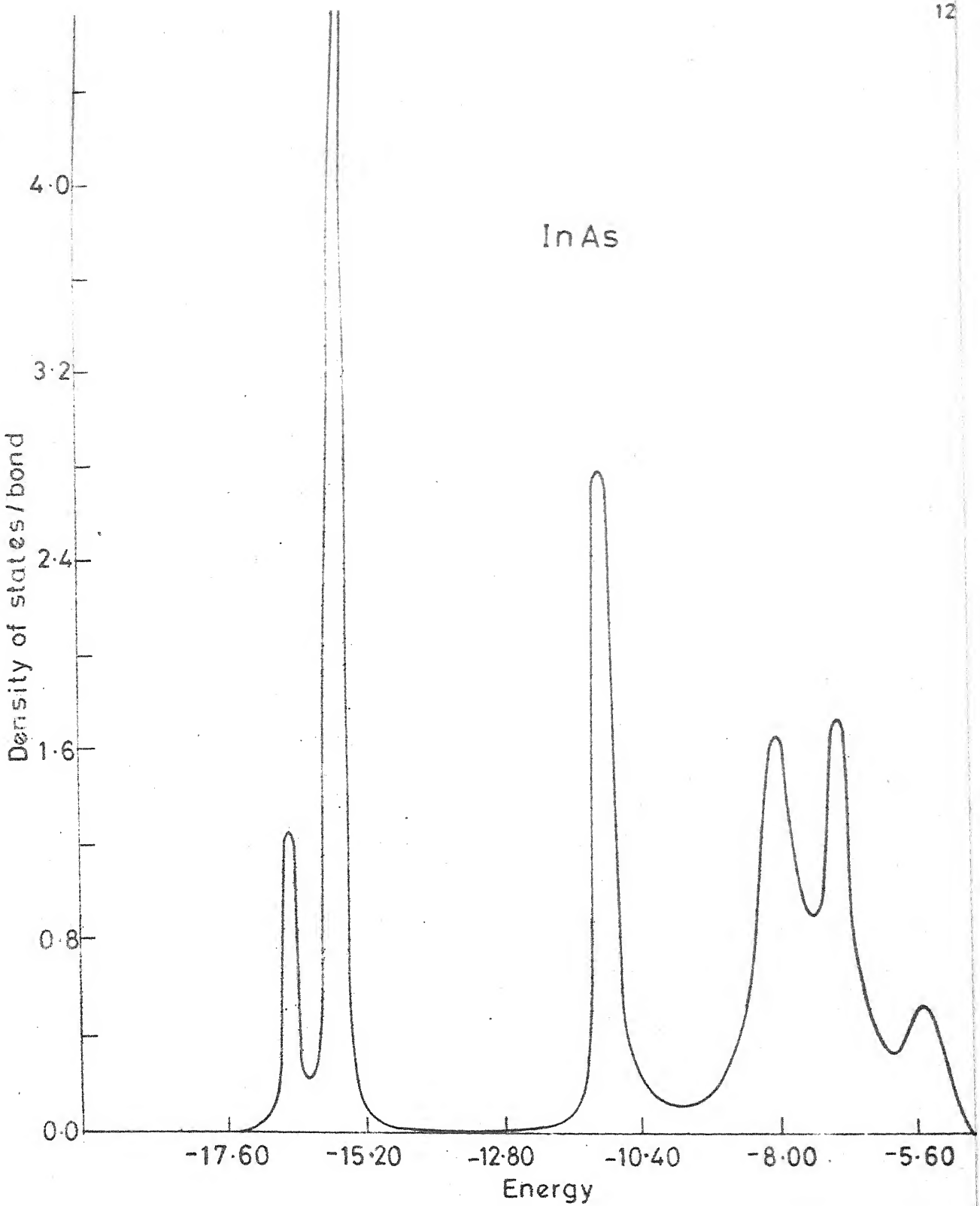
InAs
Density of states / bond
4·0
3·2
2·4
1·6
0·8
0·0
-17·60
-15·20
-12·80
-10·40
-8·00
-5·60
Energy

Fig. 4·5b

InAs

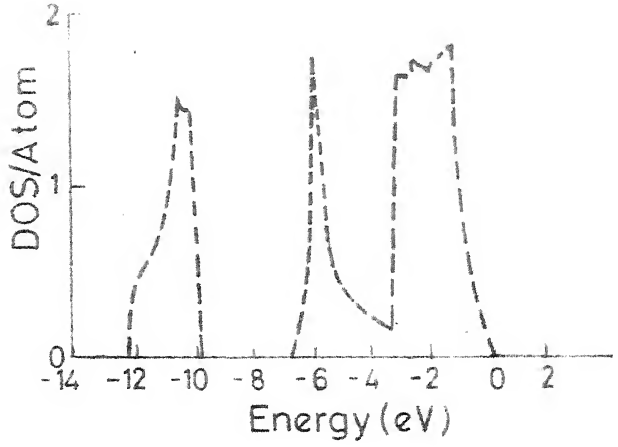

Fig. 4·6a

GaAs

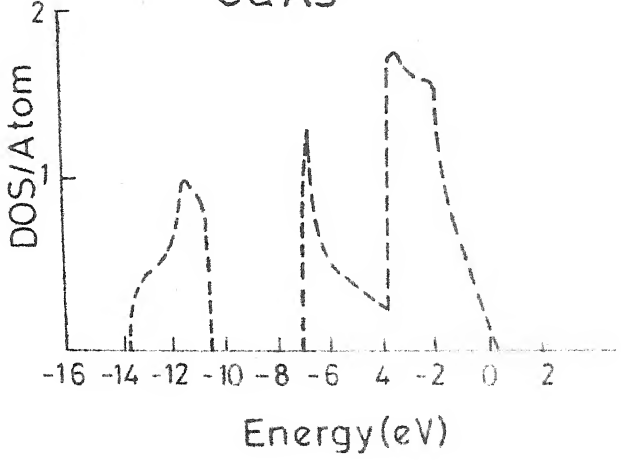

Fig. 4·6b

with 50 per cent of the total area under it. However here the k-space results show a table like shape which in seven step recursion is simulated by several peaks. This separation of the p-like parts is a feature of the two different types of second nearest-neighbour overlaps and shows up only when second neighbour overlaps, are introduced.

These oscillations are spurious and can be eliminated by going down a few more steps in the recursion. This can be done by the inclusion of symmetries of the covering lattice or alternatively, by the use of finite clusters and subsequently using the 'super-smooth' type of programme of Cambridge-group (Solid State Physics, Vol. 35). Unfortunately both of these were beyond the know-how of the group here, when the work on this problem was in progress.

In fig. 4.7 we have shown the 1CPA and VCA results for $Ga_{0.5}In_{0.5}Ah$. It is to be noted that the single site CPA does not have much effect other than smoothening the VCA results to a non-significant degree.

Figure 4.8 depicts the 2CPA result. If we compare this with the 1CPA result, then we observe that there is no change in the internal band gap. There is a slight increase in the band width and a slight enhancement of the s-type peak, which reflects the effect of InAs. The lower p-type peak gets lowered and broadened.

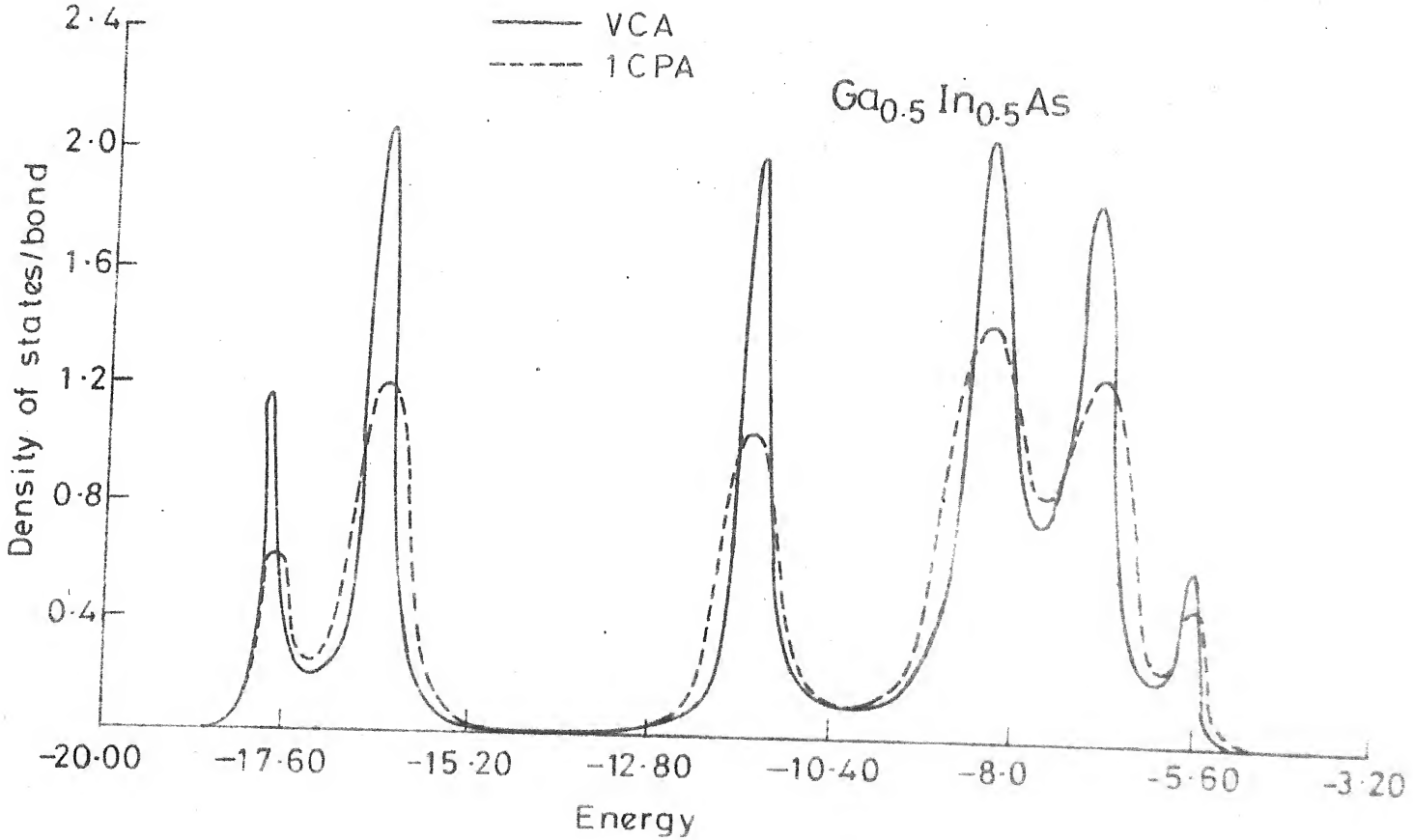
VCA
ICPA
$Ga_{0.5}In_{0.5}As$
Density of states/bond
2·4
2·0
1·6
1·2
0·8
0·4
-20·00
-17·60
-15·20
-12·80
-10·40
-8·0
-5·60
-3·20
Energy

Fig. 4·7

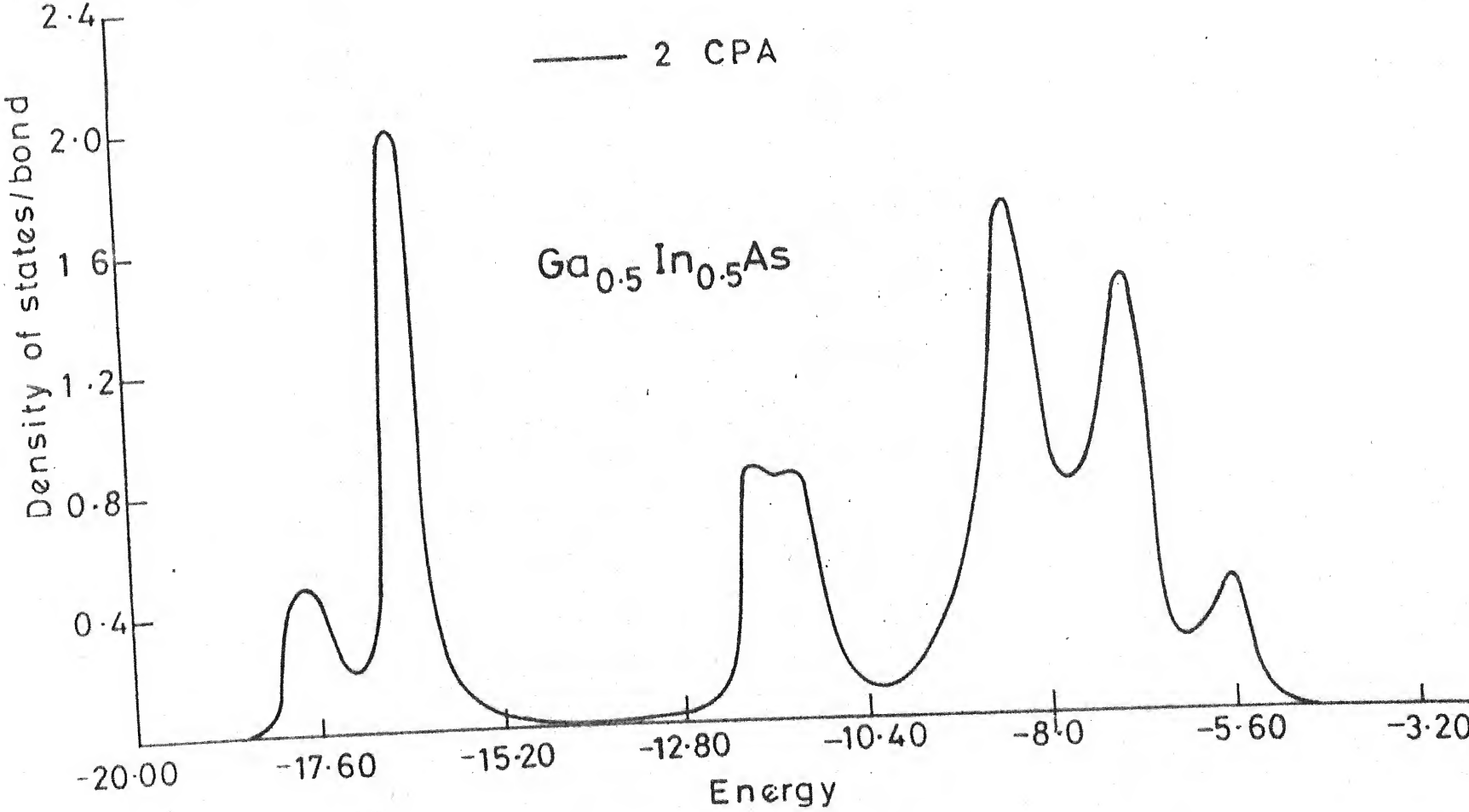
2 CPA
$Ga_{0.5}In_{0.5}As$
Density of states/bond
2·4
2·0
1 6
1·2
0·8
0·4
-20·00
-17·60
-15·20
-12·80
-10·40
-8·0
-5·60
-3·20
Energy

Fig. 4·8

The important thing to note is that no new structure appears in 2CPA. This is because of the fact that there is very small difference between GaAs and InAs parameters. This is in accordance with our predictions based on model calculations on diamond lattice (Chapter III). There also, when the difference in parameters was small, no new structure appeared.

In conclusion, we have presented a method of obtaining a self-consistent cluster CPA. In particular, we have applied it to ternary $Ga_cIn_{1-c}As$ and calculated the valence band density of states incorporating off-diagonal disorder. This is the main contribution of this work.

CHAPTER V

CONCLUSION

Our attempt to extend the theory of disordered alloys beyond 1CPA has resulted into the development of a self-consistent cluster coherent-potential approximation (CCPA), which can be applied to alloys of materials very different in mass, potentials and bond lengths. This is a significant development.

Though, the problem has been formulated only for electrons, the same model and mathematical treatment carry over to different kinds of elementary excitations like phonons and magnons.

To sum up, the following are the achievements of this work:

(1) A self-consistent CCPA based on augmented space formalism of Mookerjee, has been developed to take into account the effect of large clusters.

(2) The analytical properties (Herglotzicity)of the Green function are maintained in the CCPA-theory at all energies, concentrations and degrees of disorder.

(3) The CCPA theory takes into account exactly the effects of off-diagonal disorder and Markovian type short-range order. This is a significant advance over earlier work.

(4) The CCPA theory has been successfully applied to III-V ternary alloys which is the begining of application of the theory to realistic alloys.

However, there are a few refinements still essential, over the calculations presented here. They are

(1) The real-space methods for the calculation of different Green functions ($\underline{G}_{ij}$) need further refinement. In the calculation of density of states of pure GaAs and InAs we could go down only upto seventh step in the recursion because of which there are some spurious oscillations, near the Von-Hove singularities in the density of state curves. These oscillations can be avoided by going down more steps in the recursion. This can be facilitated by the use of real space symmetries which will reduce the working tune enormously. Haydock (Solid State Physics, Vol. 35) has shown that the entire basis $|\phi_i\rangle$ of tight-binding functions is unnecessary, for the recursion method, only those combinations which have the symmetry of the lattice and the starting state $|C\rangle$, (see appendix A) contribute. This drastically reduces the 'effective' basis and thus the time and storage-space required.

Another approach is to take a finite cluster and use the 'super smooth' programme of the Cambridge group to smoothen out the resulting histograms.

(2) Performing a CCPA calculation which takes into account the full off-diagonal disorder i.e. both anion and cation disorder in the case of III-V semi-conductors. This is possible again, by the use of 'super-smooth' programmes or by the exploitation of the symmetries of the underlying lattice in the recursion programme.

(3) Instead of using parametrization procedure (which is very ambiguous) of Chen and Sher the chemical-pseudopotential method may be used for the calculation of different near neighbour interaction parameters in III-V semiconductors.

(4) The variation of bond length has also been neglected. In the pseudopotential scheme, the interactions can be recalculated at the interatomic distances corresponding to specific alloys. In this way, the approximation made for Ga-As-In kind of near neighbour bond interactions can also be refined. This involves the calculation of somewhat more number of interaction parameters.

(5) The effect of conduction band on valence band has been ignored completely. Just as bonding orbitals yield Green functions for valence bands, anti-bonding orbitals determine the conduction band. The full band i.e. both conduction and valence bands can be obtained by using atomic-orbitals as basis. The

effect of conduction band seems to alter the top of valence band which is important for all transport properties.

Though, we have concentrated mainly on the problem of determination of electronic density of states or $\langle G(E) \rangle$, it is possible to extend this formalism for the calculation of different electronic properties of the disordered systems.

The formalism can be used to explain optical properties or the phenomenon of photo-emission in solids. Here the number of random variables will be more, but still the problem can be tackled and optical-transition probability can be calculated (Joshi and Mookerjee 1982). Also by the use of Ward's identity and accompanying Bethe-Salpeter equation, we can make predictions about conductivity and dielectric response of a disordered system.

The effect of bigger clusters can be included by performing a recursion calculation in the full augmented space.

So far we have confined ourselves only to crystalline systems with compositional disorder. Amorphous alloys, where there is a departure from perfect crystallinity, but there is an underlying distorted network on which the atoms sit (Polk 1971, Connell and Temkin 1974), may also be talked by the use of 'distorted' orbitals as basis. In such cases, Hamiltonian matrix elements will have continuous rather than bimodal distributions, but the augmented space techniques are general enough to consider these too.

REFERENCES

Aiyer, R.N., Elliott, R.J., Krumhansl, J.A. and Leath, P.L. (1969) Phys. Rev. 181, 1006.

Alben, R., Blume, M., Krakauer, M. and Schwartz, L. (1975) Phys. Rev. B12 4090.

Anderson, P.W. (1958) Phys. Rev. 109 1492

(1969) Phys. Rev. 181 25.

Anderson, P.W. and Mcmillan, W.L. (1967) Proceedings of the International School of Physics 'Enrico Fermi', edited by H. Suhl (Academic, New York).

Bishop, A.R., Mookerjee, A. (1974) J. Phys. C7 2165.

Blackmann, J.A., Esterling, D.M. and Berk, N.E. (1971) Phys. Rev. B4 2412.

Brouers, F., Cyrot, M. and Cyrot-Lackmann, F. (1973a) Phys. Rev. B7 4370.

Brouers, F., Ducastelle, F., Gutier, F. and Van Der Rest, J. (1973b) J. Phys. F3 2120.

Bullett, D.W. (1975) J. Phys. C8 2695.

Bullett, D.W. (1980) Solid State Physics, Vol. 35 (Academic Press Inc. New York).

Butler, W.H. (1972) Phys. Lett. 39 A203.

Butler, W.H. (1973) Phys. Rev. B8 4499.

Capek, V. (1971) Phys. Stat. Solidi (b) 43 61.

Chen, A.B. (1977) Phys. Rev. B16 3291.

Chen, A.B. and Sher, A. (1978) Phys. Rev. B17 4726.

Choudhry, V. (1981) Ph.D. Thesis I.I.T. Kanpur (unpublished)

Connell, G.A.N. and Temkin, R.J. (1974) Phys. Rev. B9 5323.

Cyrot-Lackmann, F. and Ducastelle, F. (1971) Phys. Rev. Lett 27 429.

Dean, P. (1972) Rev. Mod. Phys. 44 127.

Desjonquerer, M.C. and Cyrot-Lackmann F. (1978) J. Phys. F: Met. Phys. 7 61.

Diehl, H.W., Leath, D.L. (1979a) Phys. Rev. B19 596.

(1979b) Phys. Rev. B19 879.

Ducastelle, F. (1971) J. Phys. C4 L75.

(1974) J. Phys. C7 1795.

Elliott, R.J. Krumhansl, J.A. and Leath, P.L. (1974) Rev. Mod. Phys. 46 465.

Franklin (1968) Matrix Theory (Prentice-Hall, Englewood Cliffs, N.J.).

Freed, K.F. and Cohen, M.H. (1971) Phys. Rev. B3 3400.

Foo, E-Ni, Bose, S.M. and Ausloos, M. (1973) Phys. Rev. B7 3454.

Harrison, W.A. (1973) Phys. Rev. B8 4487.

Harrison, W.A. and Ciraci, S. (1974) Phys. Rev. B10 1516.

Haydock, R. (1972) Ph.D. Thesis, Univ. of Cambridge.

Haydock, R. Heine, V. and Kelly, M.J. (1972) J. Phys. C5 2845

(1975) J. Phys. C8 2591

Haydock, R. and Mookerjee, A. (1974) J. Phys. C7 3001.

Heine, V. (1980) Solid State Physics, Vol. 35 (Academic Press, Inc. New York).

Hermann, F., Skillmann, S. (1963) Atomic Structure Calculations, Prentice Hall Inc. New Jersey.

Kaplan, T., Gray, L.J. (1976) Phys. Rev. B14 3462

Kaplan, T., Gray, L.J. (1977) Phys. Rev. B15 3260.

(1978) Phys. Rev. B12 4607.

Kaplan, T., Leath, P.L., Gray, L.J., Diehl, H.W. (1980) Phys. Rev. B21 4230.

Kelly, M.J. (1980) Solid State Physics, Vol. 35 (Academic Press) Inc. New York.

Kumar, D., Kumar, V. and Joshi, S.K. (1975) Phys. Rev. B11

Kumar, V. and Joshi, S.K. (1975) J. Phys. C8 L148.

Kumar, V. and Joshi, S.K. (1978) Phys. Rev. B6 2515

(1978) Ind. J. of Phys. Comm. Vol. Part II.

Kumar, V., Mookerjee, A. and Srivastava, V.K. (1980) ICTP Preprint Ic/80/142.

Kumar, V., Mookerjee, A. and Srivastava, V.K. (1982) To be published in J. Phys. C.

Leath, P.L. (1968) Phys. Rev. 171 725.

(1970) Phys. Rev. B2 3078.

(1972) Phys. Rev. B5 1643.

Ley, L., Pollak, R.A., McFreely, F.R., Kowalczyk, S.P. and Shirley, A. (1973) Phys. Rev. B9 600.

Matsubara, T. and Kaneyoshi, T. (1966) Prog. Theor. Phys. 36 695.

Matsubara T. and Toyozawa, Y. (1961) Prog. Theor. Phys. 26 739.

Mookerjee, A. (1973a) J. Phys. C6 L205.

(1973b) J. Phys. C6. 1340.

(1975a) J. Phys. C8 29.

(1975b) J. Phys. C8 1524.

Mookerjee, A. (1979) Disordered Systems (Monograph-Hindustan Publishing Corporation India).

Mookerjee, A. and Chowdhry, V. (1980) ICTP, Trieste, preprint Ic/80/143.

Mookerjee, A. and Joshi, P. (1982) (unpublished).

Nickel, B. and Butler, W.H. (1973) Phys. Rev. Lett. 30 373.

Nickel, B. and Krumhansl, J.A. (1971) Phys. Rev. B4 4354.

Niizeki, K. (1975) Prog. Theor. Phys. 53 74.

Payton, D.N. and Visscher, W.M. (1967) Phys. Rev. 154 802.

Polk, D.E. (1971) Jrnl. Non-cryst. Solids 5 365.

Schwartz, L.M. and Siggia, E. (1972) Phys. Rev. B5 383.

Shevchik, N.J., Tejeda, J. and Cardona, M. (1974) Phys. Rev. B9 2627.

Shiba, H. (1971) Prog. Theor. Phys. 46 77.

Solid State Physics (1980) Vol. 35 (Academic Press Inc. New Y

Soven, P. (1967) Phys. Rev. 156 809.

Srivastava, V. and Joshi, S.K. (1973) J. Phys. F. Metal Phys. 3 L179.

Tsukda, M. (1972) J. Phys. Soc. Japan 36 1477.

Vander Rest, J. Gautier, F. and Brouers, F.

(1975a) J. Phys. F5 2283.

(1975b) J. Phys. F5 995.

Yonezawa, F. and Matsubara, T. (1966a) Prog. Theor. Phys. 35 357

(1966b) Prog. Theor. Phys. 35 759

Yonezava, F. (1968a) Prog. Theor. Phys. 39 1076.

(1968b) Prog. Theor. Phys. 40 734.

Ziman, J.M. (1969) J. Phys. C2 1230.

APPENDIX A

RECURSION METHOD

The 'recursion' method developed by Haydock et al (1972, 1975) facilitates the determination of the Green function. Given the Hamiltonian of a system, in suitable Hilbert space the recursion method sets up a basis in which the Hamiltonian has a tridiagonal representation, from which the matrix elements of the Green function may be derived. Equivalently, given the Hamiltonian matrix $\underline{H}$, the recursion method generates a unitary transformation $\underline{U}$ such that

$$\underline{U}\,\underline{H}\,U^{-1} = \underline{H}_{TD}$$

where $\underline{H}_{TD}$ is tridiagonal.

Let us start with a suitable Hamiltonian $\underline{H}$ in a Hilbert space $\mathcal{H}$. The quantity of interest is the resolvent of $\underline{H}$, also called the Green operator

$$G(Z) = \lim_{Z \to E+i0^+} (Z\underline{I} - \underline{H})^{-1}$$

$\underline{H}$ is self-adjoint and maps the Hilbert space on to itself i.e. if $|u_n\rangle$ is in $\mathcal{H}$ so is $H|u_n\rangle$. Now beginning with a given starting element $|u_o\rangle$ and an arbitrary sequence of numbers $\{a_n, b_n\}$ let us define a sequence of elements $\{|u_n\rangle\}$ by

$$|u_n\rangle = \underline{H}|u_{n-1}\rangle - a_{n-1}|u_{n-1}\rangle - b_{n-1}^2|u_{n-2}\rangle, \quad b_o = 0 \qquad (A\text{-}1)$$

This sequence terminates at n if $|u_{n+1}\rangle$ is the null vector ($b_n=0$), otherwise we generate an infinite sequence of elements. The numbers $\{a_n, b_n\}$ are real if $\underline{H}$ is Hermitian. If the sequence of elements $\{|u_n\rangle\}$ is such that $\langle u_n|u_m\rangle = 0$ for $n \neq m$ then equation (A-1) immediately implies

$$a_n = \frac{\langle u_n|H|u_n\rangle}{\langle u_n|u_n\rangle} \quad \text{and} \quad b_n^2 = \frac{\langle u_{n-1}|Hu_n\rangle}{\langle u_{n-1}|u_{n-1}\rangle} = \frac{\langle u_n|u_n\rangle}{\langle u_{n-1}|u_{n-1}\rangle} \qquad \text{(A-2)}$$

If we take $\{|u_n\rangle\}$ as our basis of representation, the Hamiltonian $\underline{H}$ becomes tridiagonal with the a_n's down the diagonal and b_n's down the off-diagonal positions.

If $\underline{H}$ is a non-Hermitian matrix (as is often the case with effective Hamiltonians arising out of the chemical pseudo-potential approach or any coherent potential approximation) then, alternatively we choose an arbitrary set of complex numbers $\{a_n, b_n, c_n\}$ as follows

$$b_o|u_1\rangle = (\underline{H}-a_o)|u_c\rangle \ , \ c_o = 0 \qquad \text{(A-3)}$$

for $n > 0$

$$b_n|u_{n+1}\rangle = (\underline{H}-a_n)|u_n\rangle - c_n|u_{n-1}\rangle$$

Using equation (A-3) it is easy to see that

$$a_n = \langle u_n|\underline{H}|u_n\rangle \ , \quad c_n = \langle u_{n-1}|\underline{H}|u_n\rangle \qquad \text{(A-4)}$$

$$b_n = \langle u_n|(H-a_n)^\dagger \ (H-a_n)|u_n\rangle - |c_n|^2 \ .$$

if we assume $\langle u_n|u_m\rangle = \delta_{nm}$.

The reason why this method is called recursion method now becomes clear. Starting from a Hamiltonian and starting element $|u_o\rangle$ with $b_o=0$ we may generate, with the help of equation (A-1), a_o, b_o and thus $|u_1\rangle$. Now we may determine in turn a_1, b_1 and thus $|u_2\rangle$ and so on recursively. As a calculation technique this method is very economical. At each stage we need to store $|u_n\rangle$ and $|u_{n-1}\rangle$ and the coefficients calculated upto that stage. All extraneous information is left out.

Given H_{TD} it is simple to construct various matrix elements of the Green function. We can evaluate the local matrix element

$$G_{oo}(E) = \langle O|(E\underline{I}-\underline{H})^{-1}|O\rangle$$

$$= \langle O|(E\underline{I}-\underline{H}_{TD})^{-1}|O\rangle,$$ if, as we can,

we insist that $|O\rangle$ remains as the first member of the new basis $\{|u_n\rangle\}$ i.e. $|u_o\rangle = |O\rangle$. The off-diagonal element of the Green operator $G_{01}(E)$ may also be calculated in same way. If we start with

$$|u_o\rangle = \frac{1}{2}\left[|01 + |1\rangle\right]$$

Here $G_{01}(E) = \langle O|(E\underline{I}-\underline{H})^{-1}|1\rangle$ and

$$\langle u_o|(E\underline{I}-\underline{H})^{-1}|u_o\rangle = \frac{1}{2}\left[G_{oo} + G_{11}+G_{01}+G_{10}\right]$$

but $G_{oo} = G_{11}$ and $G_{o1} = G_{10}$ so

$$G_{10}(E) = \langle u_o|(E\underline{I}-H)^{-1}|u_o\rangle - G_{oo}(E)$$

Here the first term of the right hand side of above equation can be calculated by continued fraction expansion with $|u_o\rangle = \frac{1}{2}[|0\rangle + |1\rangle]$ and G_{oo} is the term which has already been obtained by the same procedure with $|u_o\rangle = |0\rangle$. Hence we can calculate $G_{10}(E) = G_{01}(E)$.

Let D be the determinant of the matrix $(E\underline{I}-\underline{H}_{TD})$ and $D_n(n=0,1,3,\ldots)$ be the determinant of the matrices derived from $(E\underline{I}-\underline{H}_{TD})$ after rows and column from 0 to n have been eliminated. Then if we wish to obtain $G_{oo}(E) = D_o/D$ we may use the Cauchy expansion for the determinant D_n and write down a recursion relation for D_n as

$$D_n = (E-a_n)D_{n+1} - b_n^2 D_{n+2} \tag{A-5}$$

$G_{oo}(E)$ becomes a continued fraction expansion from the repeated application of equation (A-5).

$$G_{oo}(E) = \frac{D_o}{(E-a_o)D_o - b_1^2 D_1} = \frac{1}{(E-a_o) - b_1^2 D_1/D_o} \tag{A-6}$$

$$= \cfrac{1}{E-a_o - \cfrac{b_1^2}{E-a_1 - \cfrac{b_2^2}{E-a_2 - \cfrac{b_3^2}{\ddots \cfrac{b_{n-1}^2}{E-a_{n-1}^2 - b_n^2\left(\frac{D_n}{D_{n-1}}\right)}}}}}$$

By the recursion method we can calculate iteratively (a_b, b_n) from $n=o$ to some N. The resolvent is then

calculated by fixing $\frac{D_{N+1}}{D_{N+2}}$ in one of the ways described in the next subsection (A-1) and inserting this value at the N-th level of the continued fraction

The density of states can be expressed as:

$$n(E) = \underset{Z \to E+i0^+}{\mathrm{Im}} \cfrac{-1/\pi}{Z-a_o-\cfrac{b_1^2}{Z-a_1-\cfrac{b_2^2}{Z-a_2-\cfrac{b_3^2}{\ddots}}}} \qquad (A\text{-}7)$$

The tridiagonalisation of $\underline{H}$ reduces the original system to a fictitions linear chain of atoms with local orbitals with diagonal energies a_n and overlap elements b_n.

(A-1) Termination of Continued Fraction

In most of the cases (a_n, b_n^2) settle down quickly and tend towards a symptotic values (a_∞, b_∞^2). By setting $(a_n, b_n^2) = (a_\infty, b_\infty^2)$ for $n > N$ we can evaluate the remainder of the continued fraction expansion analytically. We write:

$$G_\infty(E) = \cfrac{1}{E-a_{N+1}-\cfrac{b_{N+2}^2}{E-a_{N+2}-\cfrac{b_{N+3}^2}{\ddots}}} = \frac{1}{E-a_\infty-b_\infty^2\, G_\infty}$$

and solve for $G_\infty(E)$ yielding

$$G_{\infty}(E) = \frac{1}{2b_{\infty}^2}\left[(E-a_{\infty}) - \sqrt{(E-a_{\infty})^2-4b_{\infty}^2}\ \right] \qquad (A\text{-}8)$$

we reject the second solution of the quadratic as $G_{\infty}(E)$ must vanish as $E \to \infty$ in order that the resolvent preserve its analytic character (of the form E^{-1}) there. It is clear that $G_{\infty}(E)$ is real for real E outside the range $(a_{\infty}-2|b_{\infty}|)$ and $(a_{\infty}+2|b_{\infty}|)$, so that the continued fraction will be real. Inside the same interval $G_{\infty}(E)$ has a branch cut and we obtain a band of allowed energies. If we underestimate the value of b_{∞}^2, we will get spurious structure in the interval $(a_{\infty}-2|b_{\infty}|)$, $a_{\infty}+2|b_{\infty}|)$ but if we overestimate b_{∞}^2 the band width is artificially large but the spectral weight in the spurious tails is extremely small (Haydock et al 1975).

In the tables (A-1) and (A-2) the values of (b_N^2) for diamond and b.c.c. lattices (with one orbital per site) respectively, are given. Here the well depths and overlaps are zero and -1 respectively. The well depth being zero all the a_N's are zero both in diamond and b.c.c. lattices. It is easy to see that in case of diamond lattice $a_{\infty} = 0$ and $b_{\infty}^2 = 4$ while in case of b.c.c. lattice $a_{\infty} = 0$ and $b_{\infty}^2 = 16$. The corresponding density of state curves are shown in figs. A1 and A2 respectively. With the number of coefficients N = 18, the density of state curves are fairly good.

Table A-1

Recursion-coefficients for Diamond Lattice

N	b_N^2	N	b_N^2
1	4.000	10	3.723
2	3.000	11	4.210
3	5.000	12	3.830
4	3.400	13	4.185
5	4.365	14	3.793
6	3.747	15	4.216
7	4.292	16	3.817
8	3.663	17	4.148
9	4.352	18	3.873

Table A-2

Recursion-Coefficients for B.C.C. Lattice

N	b_N^2	N	b_N^2
1	8,000	10	16.47
2	19.00	11	15.58
3	14.26	12	16.39
4	17.32	13	15.65
5	15.01	14	16.33
6	16.83	15	15.70
7	15.31	16	16.28
8	16.61	17	15.74
9	15.48	18	16.25

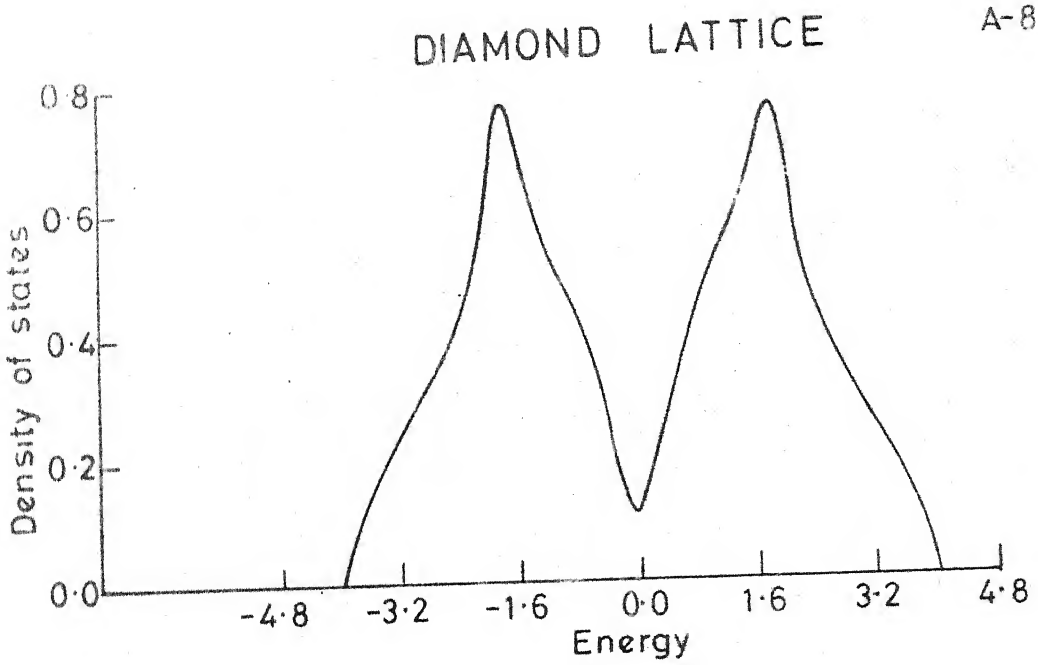
DIAMOND LATTICE
Density of states
0·8
0·6
0·4
0·2
0·0
-4·8
-3·2
-1·6
0·0
1·6
3·2
4·8
Energy

Fig. A1

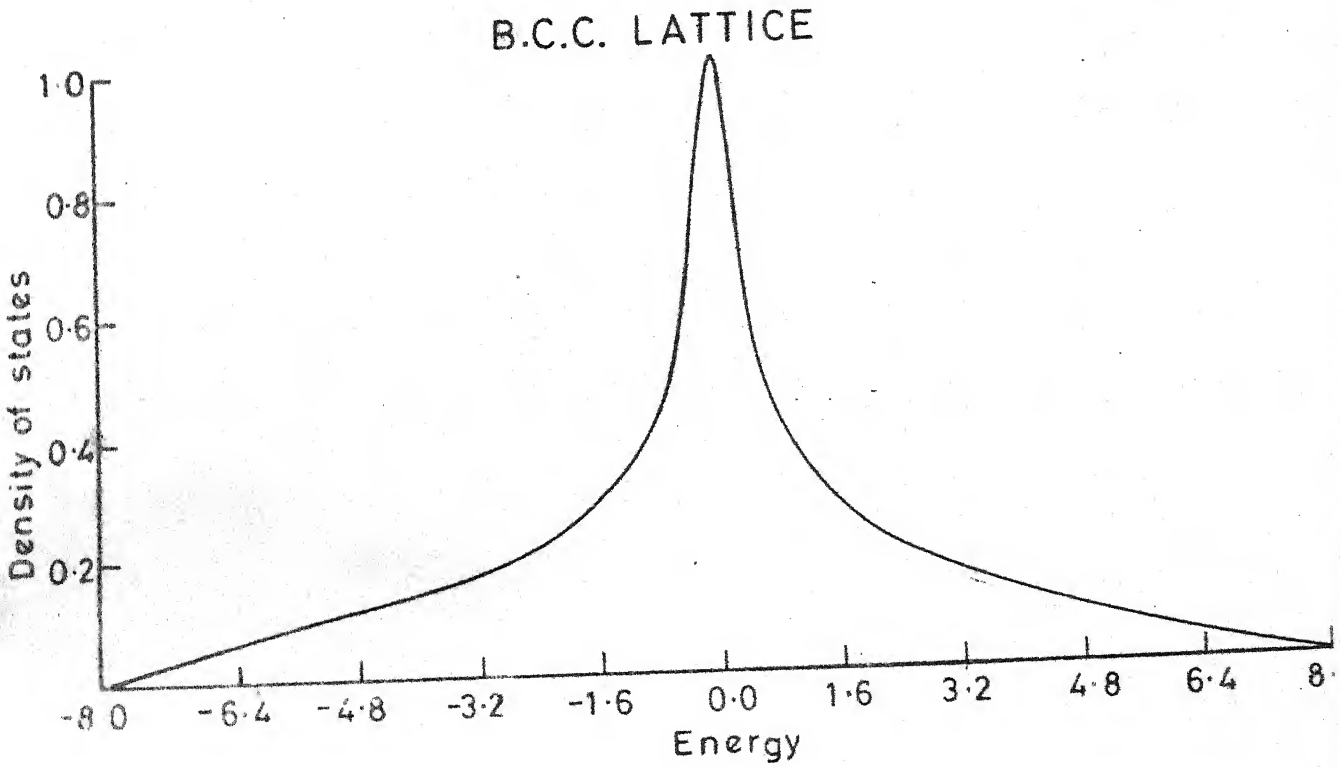
B.C.C. LATTICE
Density of states
1·0
0·8
0·6
0·4
0·2
-8·0
-6·4
-4·8
-3·2
-1·6
0·0
1·6
3·2
4·8
6·4
Energy

Fig. A2

When we have several orbitals per site (e.g. four sp^3 orbitals per site in case of III-V semi-conductors) a_n and $|b_n|^2$ do not settle down so quickly, as they incorporate the detailed information of internal band - edges and singularities. Hence it becomes difficult to choose an appropriate $\{a_\infty, |b_\infty|^2\}$. This can be done in a reasonable manner by several methods (Solid State Physics Vol. 35). We shall not go into details of these methods but shall describe a method based on Gershgorin theorem (Franklin 1968) which is, in general, suited for the estimates of $(a_\infty, |b_\infty|^2)$ in case of isolated bands e.g. the valence bands of III-V semiconductors.

The Gershgorin theorem states that for any Hermitian matrix $\underline{M}$, its eigenvalues E must lie within the union of regions defined by the relations:

$$M_{ii} - \sum_j |M_{ij}|^2 \leq E \leq M_{ii} + \sum_j |M_{ij}|^2 \qquad \text{(A-9)}$$

for all i. Therefore by direct examination of any Hamiltonian matrix, we can determine upper bounds for the limits of the band, where the density of states is non-zero. This theorem gives very good estimates of $(a_\infty, |b_\infty|^2)$ when applied to the tridiagonal matrix (Kaplan 1978). We can thus determine the maximum energy (E_{max}) and the minimum energy (E_{min}) limits for the band. Now knowing the fact that

$$(a_\infty - 2|b_\infty|) \leq Z \leq (a_\infty + 2|b_\infty|)$$

we have

$$a_\infty = \frac{1}{2}(E_{max} + E_{min})$$
$$|b_\infty|^2 = \frac{1}{16}(E_{max} - E_{min}) \qquad \text{(A.10)}$$

In case of valence bands of III-V semiconductors, the band width and the internal gap produced by a seven step continued fraction version, are in very good agreement with those obtained by experimental and $\bar{k}$-space methods (see Chapter IV). However, the early truncation of the continued fraction produces spurious oscillatory dips in order to preserve normalisation. This has been reported earlier by Haydock et al (1975) also. These spurious oscillations can be eliminated by going down more steps in the recursion, which is possible by the inclusion of symmetries of the covering lattice or by the use of finite clusters and subsequently using the 'super-smooth' type of programme of the Cambridge-group (Solid State Phys. Vol. 35). These techniques have not yet been mastered by us and should be incorporated.

The only thing that remains is the consideration of singularity structure of the density of states. In the complex Z-plane, the Green function exhibits all three types of singularities: simple poles, branch points and essential

singularities. The first few coefficients $(a_n, |b_n|^2)$, in the continued fraction expansion of Green function, are sufficient for the location of simple poles and the value of Green's function near singularities, but the position of band edges (branch points) and Von-Hove singularities (essential singularities) is determined by the asymptotic behaviour of $(a_n, |b_n|^2)$ for large n. It is not possible to tell the nature of singularity from first few $(a_n, |b_n|^2)$. Our termination of the continued fraction expansion after certain finite number of terms makes it impossible to determine the precise analytic structure of the singularities but the first few coefficients quite accurately distribute the spectral weight about the singularity (Haydock et al 1975).

APPENDIX B

RESOLVENT OR THE GREEN OPERATOR

The resolvent or the Green operator $\underline{G}$ corresponding to the Hamiltonian $\underline{H}$ is defined to be

$$\underline{G}(Z) = (Z\underline{I}-\underline{H})^{-1} \qquad (B-1)$$

where $\underline{I}$ is the identity operator. It is defined for all values of Z, the generalised complex energy variable, except on a domain viz. the spectrum of the Hamiltonian $\underline{H}$. For a self-adjoint $\underline{H}$, the spectrum of $\underline{H}$ lies entirely on the real axix in the complex Z-plane. For a finite system the resolvent has a finite number of poles (degenerate or otherwise) on the real axis. For an infinite system we can have (1) a set of poles (2) a branch cut i.e. an infinite, absolutely continuous (dense, compact) set of poles (3) essential singularities-like winding points (4) an infinite singularly continuous set of poles (dense, non-compact) as in the case of Anderson localised states in random Hamiltonians. The Green operator has poles at each spectral point , i.e. eigenvalue. Projection on to the corresponding eigen-state is the residue at that point. The diagonal member $\underline{G}_{ss}(Z)$ of any representation of $\underline{G}(Z)$ with respect to any linearly independent basis $\{|s\rangle\}$ is analytic everywhere in $\text{Im } Z \neq 0$. Also $\text{Im } G_{ss}(Z) < 0$ if $\text{Im } Z > 0$ and $\text{Im } G_{ss}(Z) > 0$ if $\text{Im } Z < 0$. If the spectrum

of $\underline{H}$ is bound from above, clearly $G_{ss}(Z) \sim \frac{1}{Z}$ as $Z \to \infty$ along the real axis. In case $\underline{H}$ is not bounded from above, we have to further assume this asymptotic behaviour of $G_{ss}(Z)$. Finally $\underline{G}(Z) = G^{\dagger}(Z)$. All these properties define a 'Herglotz' function.

In some representation $\{|s\rangle\}$ the Green function is given by,

$$G_{ss}(Z) = \langle s|(Z\underline{I}-\underline{H})^{-1}|s\rangle \qquad (B\text{-}2)$$

$$= \sum_{n} \frac{\langle s|n\rangle \langle n|s\rangle}{Z - E_n}$$

where $\{|n\rangle\}$ is the complete set of eigen-states of $\underline{H}$ corresponding to the eigenvalues $\{E_N\}$, normalized to unity. Then the trace of the Green function matrix in this representation

$$\text{Tr } G_{ss}(Z) = \sum_{s} \sum_{i} \frac{\langle s|n\rangle \langle n|s\rangle}{Z - E_n}$$

$$= \sum_{n} \frac{1}{Z-E_n}$$

where the completeness of the basis set $\{|s\rangle\}$ is used. In case of tight-binding basis in a crystal, all diagonal matrix elements are identical and we can write

$$g(Z) = \frac{1}{N} \text{ Tr } G_{ss}(Z) = \frac{1}{N} \sum_{n} \frac{1}{Z-E_n}$$

Since the eigenvalues are all real, the $g(Z)$ is defined along the real axis in the limit that the imaginary part of Z becomes very small i.e.

$$\lim_{n \to 0^+} g(E+in) = \lim_{n \to 0^+} \frac{1}{E+in-E_n}$$

$$= \frac{1}{N} \sum_n \left[\mathcal{P} \frac{1}{E-E_n} - i\pi \delta (E-E_n) \right]$$

E being real and $\mathcal{P}$ represents the principal part so that

$$-\frac{1}{\pi} \lim_{n \to 0^+} \operatorname{Im} g(E+in) = \frac{1}{N} \sum_n (E-E_n)$$

$$= n(E)$$

where $n(E)$ is the density of states per site. This relation is very useful because knowing $n(E)$, the complete Green function at any value Z can be obtained from Krammer's-Kronig relation

$$g(Z) = -\frac{1}{\pi} \int_{-\infty}^{\infty} \frac{\operatorname{Im} g(E + i0^+)}{Z - E} \, dE$$

$$= \int_{-\infty}^{\infty} \frac{n(E)}{Z-E} \, dE.$$

This relation is a consequence of the Hergolotzicity of $g(Z)$.